Chlamydia infection impairs host cell motility via CPAF-mediated Golgi fragmentation

D I S S E R T A T I O N

zur Erlangung des akademischen Grades

Dr. rer. nat.
im Fach Biologie

eingereicht an der
Mathematisch-Naturwissenschaftlichen Fakultät I
der Humboldt-Universität zu Berlin

von
Dipl.-Biol. Julia Heymann

Präsident der der Humboldt-Universität zu Berlin:
Prof. Dr. Jan-Hendrik Olbertz

Dekan der Mathematisch-Naturwissenschaftlichen Fakultät I:
Prof. Dr. Andreas Herrmann

Gutachter:
1. Prof. Dr. Thomas F. Meyer
2. Prof. Dr. Andreas Herrmann
3. Prof. Dr. Kai Matuschewski

eingereicht am: 17.01.2012
Tag der mündlichen Prüfung: 18.06.2012

"We have a hunger of the mind
which asks for knowledge of all around us,
and the more we gain, the more is our desire;
the more we see, the more we are capable of seeing."
Maria Mitchell, Astronomer (1818-1889)

Zusammenfassung

Chlamydien sind obligat intrazelluläre Bakterien, die sich in einem membranumschlossenen Kompartiment namens Inklusion vermehren. Nach Infektion fragmentiert der Golgi-Apparat der Wirtszelle in kleine Membranstapel. Dies verbessert die Aufnahme von Sphingolipiden und ist deshalb für die chlamydiale Vermehrung essentiell.

Die infektionsinduzierte Golgi-Fragmentierung geschieht nach Spaltung des Golgi-Matrix-Proteins Golgin-84. In dieser Arbeit konnte, durch den Vergleich mit bekannten Substraten und Inhibitorstudien, die chlamydiale Protease CPAF (*Chlamydia protease-like activity factor*) als das Enzym identifiziert werden, das diese Spaltung induziert, abhängig von der Anwesenheit zweier Rab-Proteine, Rab6 und Rab11, die den zellulären Vesikeltransport kontrollieren und zur Inklusion rekrutiert werden. Die Fragmentierung des Golgi-Apparates verhinderte dessen Relokalisierung während der Zellpolarisierung nach Einbringen eines migratorischen Stimulus. Sowohl infizierte als auch Golgin-84-depletierte Zellen migrierten langsamer und randomisiert in einem Motilitätsassay. Die Relokalisierung des Golgi-Apparates konnte durch seine Stabilisierung mittels WEHD oder Rab-Depletion wieder gewonnen werden, was die Zellmotilität teilweise wieder herstellte. Darüber hinaus konnte gezeigt werden, dass die Infektion außer der Golgi-Reorientierung die Signaltransduktion durch GTPasen beeinflusst. Die Aktivität von Cdc42 in infizierten Zellen war erhöht und die Interaktionen mit vielen ihrer Effektoren laut quantitativer Massenspektrometrie stark verändert.

Die Ergebnisse dieser Arbeit zeigen, dass CPAF die für Chlamydien lebenswichtige Golgin-84 Prozessierung und Fragmentierung des Golgi-Apparates auslöst. Dies verringert die Mobilität der Wirtszelle, vor allem da der Golgi-Apparat während der Polarisierung nicht mehr ausgerichtet werden kann, des Weiteren durch Modulierung der Protein-Protein-Interaktionen von Cdc42.

Abstract

Chlamydia are obligate intracellular human pathogens that proliferate inside a membrane-bound compartment called the inclusion. In infected cells, the Golgi apparatus is fragmented into small ministacks that are aligned around the inclusion. This facilitates uptake of host cell sphingolipids and is essential for chlamydial development.

Infection-induced Golgi fragmentation happens after processing of the Golgi matrix protein golgin-84. This work could, via comparison with well-known substrates and inhibitor studies, identify the chlamydial protease CPAF (Chlamydia protease-like activity factor) as the enzyme accountable for this cleavage. Golgi Fragmentation depended on two Rab proteins, Rab6 and Rab11, which control vesicle transport and are recruited to the *Chlamydia* inclusion. As a consequence of Golgi fragmentation, cells lost the capacity to reorient the Golgi apparatus during polarization after a migratory stimulus. Both infected and golgin-84 depleted cells with a permanently fragmented Golgi apparatus displayed decelerated and furthermore randomized migration in a motility assay. Relocalization of the Golgi apparatus could be restored via stabilizing WEHD treatment or Rab depletion which partly rescued cell motility. Moreover, it could be shown that migration signaling via small GTPases was influenced by *Chlamydia* infection. Infected cells exhibited activation of the small polarity GTPase Cdc42. Numerous interactions with downstream effectors were strongly altered in infected cells according to quantitative mass spectrometry. Particularly, the binding of Cdc42 to migration-associated effectors was decreased.

The results of this work show that CPAF, by processing of golgin-84, induces Golgi fragmentation which is vitally important for *Chlamydia*. This disturbs host cell motility because the Golgi apparatus cannot be reoriented during polarization and, additionally, via the modulation of protein-protein-interactions of Cdc42.

Contents

Parts of this work have been published in the following article:

Targeting of a chlamydial protease impedes intracellular bacterial growth
Jan G. Christian* and Julia Heymann*, Stefan A. Paschen, Juliane Vier, Linda Schauenburg, Jan Rupp, Thomas F. Meyer, Georg Häcker and Dagmar Heuer
PLoS Pathogens, 2011 September; 7(9)
* equal contribution

1 Introduction

1.1 The pathogen *Chlamydia*

Chlamydiae are obligate intracellular pathogens infecting humans and animals alike. The gram-negative bacteria survive and procreate inside a membrane-bound vacuole called the inclusion, and are known to cause a variety of diseases. *Chlamydia* infections in humans were described as early as 1500 BC, in the Ebers papyrus, one of the oldest medical texts preserved unto this day (Ebers, 1875 (1987).

In 1907, following the investigation of the eye infection trachoma, the German scientists Halberstädter and von Prowazek were the first to identify a relationship between *Chlamydia* and disease (Halberstaedter and von Prowazek, 1907). Working in Java, the two researchers discovered inclusion bodies in the conjunctiva of orang-utans after inoculating them with trachomal tissue scrapings. Using Giemsa staining, they noted intracellular particle-containing vacuoles and determined them to be the causative agent of trachoma. In humans, trachoma manifests itself in recurring inflammation of the conjunctiva, swelling of the upper eyelid and ultimately, blindness (Burton, 2007).

The name *Chlamydia* is derived from the Greek word $\chi\lambda\alpha\mu\upsilon\delta\alpha$, meaning "cloak", and refers to the inclusion's enveloped appearance as microscopically observed by the scientists. Until the 1960s, *Chlamydia* were mistaken for viruses because of their small size and intracellular way of life (Wang, 1999). It was only with the advancement of tissue culture and electron microscopy techniques, that these particles were identified to be bacteria.

Chlamydia are among the most common sexually transmitted bacterial pathogens worldwide, with 90 million new infections occurring every year (WHO, 2001). The first of altogether 28 complete genome sequences were published in 1998 (Griffiths et al., 2006). However, the understanding of this organism and related pathologies is currently less advanced than that of other bacterial human pathogens. Not least due to a missing feasible genetic system, *Chlamydia* still guards many secrets and is the subject of important ongoing research.

1.1.1 Taxonomy of *Chlamydiae*

Within the previous ten years, the classification of *Chlamydia* species has undergone two major revisions. In 2001, Bush and Everett subgrouped the family of *Chlamydiaceae* into two distinct genera, *Chlamydia* and *Chlamydophila*, based on the analysis of the 16S rRNA (Figure 1.1, Everett et al., 1999; Bush and Everett, 2001).

This organization, although rejected by parts of the community (Schachter et al., 2001), was set until 2009 when Stephens *et al.* proposed to reunite the genera (Stephens et al., 2009). The authors argued that the relatively small differences of ribosomal genes (accounting to 3 %) did not justify separation of the species because it could easily have arisen from geographic isolation. *Chlamydiae* of different regional islands had evolved in the same ecological niche - the intracellular inclusion - which prevented, for example, gene transfer from other microbes. Furthermore, they shared the same fundamental phenotypic characteristics. Accordingly, all mentioned species had to belong to the single genus *Chlamydia* (Figure 1.2).

However, researchers have not yet agreed on either one of the classifications as the ultimate system and both ways of notation are presently used in publications. This thesis adheres to the taxonomy according to Stephens *et al.* (Figure 1.2).

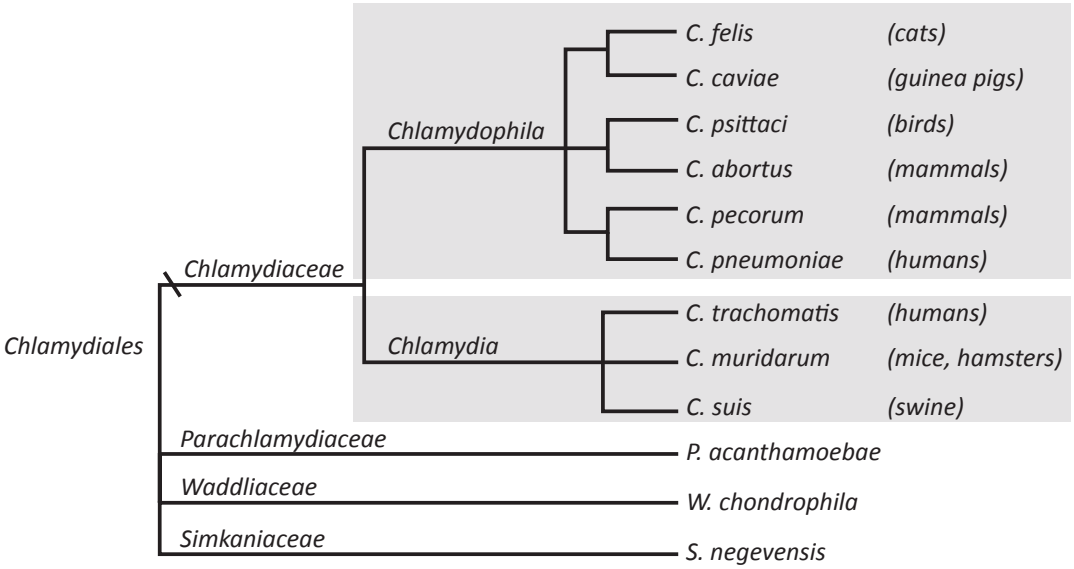

Figure 1.1: Taxonomy of *Chlamydia* after Bush and Everett. Two separate genera are distinguished. The genus *Chlamydiae* contains the species *C. trachomatis*, *C. suis* and *C. muridarum*, while others belong to the *Chlamydophilae*. *Parachlamydiaceae*, *Waddliaceae* and *Simkaniaceae* are related to *Chlamydiaceae* and can be found in free-living amoebae or cause aborts in cattle. Modified from Bush and Everett, 2001, distances arbitrary.

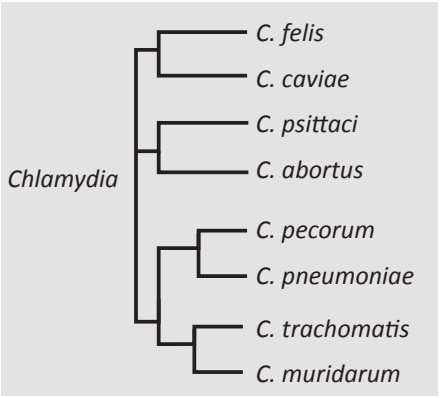

Figure 1.2: Taxonomy of *Chlamydia* after Stephens *et al.* In this system, all species are united in the genus *Chlamydiae*, considering the lack of major biological differences between them. Modified from Stephens et al., 2009, distances arbitrary.

1.1.2 The developmental cycle of *Chlamydia*

Chlamydia possess a unique biphasic life cycle that alternates between two morphologically distinct forms (Figure 1.3). The initial infection is mediated by the environmentally stable elementary body (EB) which is infectious but metabolically inactive. This particle, approximately 0.3 μm in size, is internalized by the host cell via endocytosis. Several bacterial factors and host cell receptors have been suggested to mediate the initial attachment, including heparin and heparan sulphate (Zhang and Stephens, 1992; Wehrl et al., 2004), but the exact mechanisms of adhesion and uptake remain elusive. Invasion strategies can vary, depending on *Chlamydia* species and host cell types. Different routes mediated by clathrin, caveolin or lipid rafts have been described (Dautry-Varsat et al., 2005).

Evidentially, entry requires actin remodeling at attachment sites controlled by the small GTPase Rac1 (Ras-related C3 botulinum toxin substrate 1, Carabeo et al., 2004). Rac1 activation is induced by the chlamydial effector, tarp (translocated actin-recruiting phosphoprotein), which is inserted into the host cell by the chlamydial type three secretion system (TTS, Lane et al., 2008; Jewett et al., 2010). This multi-protein complex acts as a molecular syringe and punctures the plasma membrane to secrete tarp into the host cytoplasm (Hsia et al., 1997). At later stages, more effector proteins are translocated across the inclusion membrane into the host cytosol.

Once the EB has been taken up, it transforms into the larger (1-1.5 μm) reticulate body (RB) that is no longer infectious and replicates by binary fission. Transcription of the first bacterial proteins starts as early as 15 minutes post infection (Plaunt and Hatch, 1988). How this EB-to-

RB transition is initiated is still unknown. The *Chlamydia*-containing endosomal compartment then develops into the inclusion, a protective intracellular niche which evades the lysosomal pathway. If more than one EB is internalized, endosomes containing *C. trachomatis* fuse homotypically with each other using host cell cytoskeletal and motor proteins (Clausen et al., 1997).

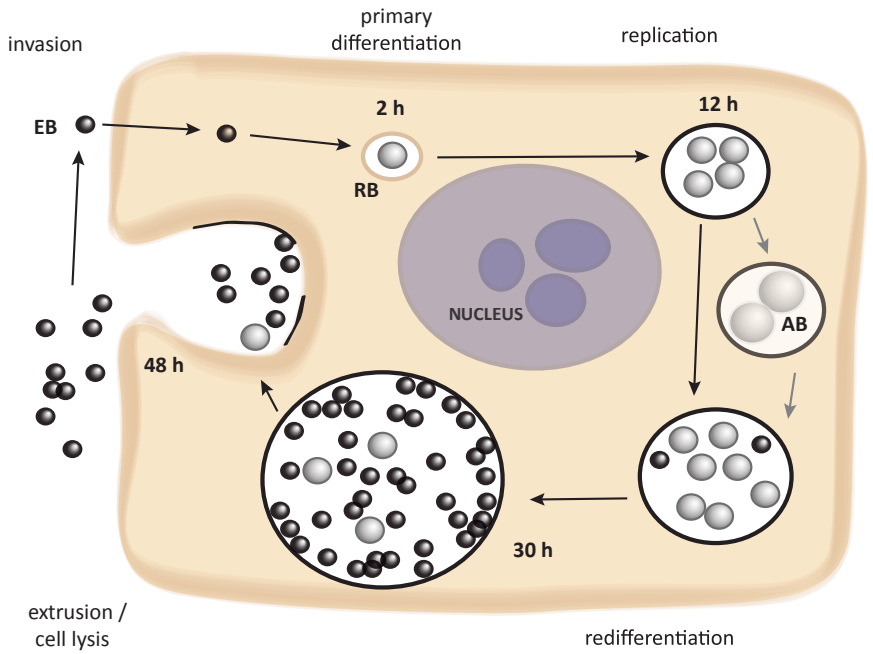

Figure 1.3: The developmental cycle of *Chlamydia trachomatis*. Infection of a host cell with *Chlamydia trachomatis* starts with the attachment and invasion of an elementary body (EB). Inside the cell, it differentiates into the metabolically active, replicating reticulate body (RB). After a sufficient number of bacteria is produced, the RBs re-differentiate into new EBs that are released after about 48 h to start a new infectious cycle. Exit can happen via cell lysis or extrusion of the inclusion. Poor growth conditions induce reversible persistency whereupon *Chlamydia* transforms into aberrant bodies (ABs).

The maturing inclusion membrane is heavily modified and ultimately consists of an unknown combination of bacterial and host cell proteins. It is directed away from the endocytic towards the exocytic pathway to escape degradation (Scidmore et al., 2003). Additionally, it mimics specific host cell membrane characteristics to intercept trafficking routes and acquire nutrients including sphingolipids and cholesterol (Wylie et al., 1997; Hackstadt et al., 1996). Newly inserted bacterial Inc (inclusion-) proteins enable capturing of cargo vesicles (Delevoye et al., 2008). They recruit Rab (Ras-related in brain) GTPases (Rzomp et al., 2006; Rejman Lipinski et al., 2009) that regulate many steps of membrane traffic, including vesicle formation, transport and fusion (Zerial and McBride, 2001). Rab proteins are anchored to membranes via prenyl

groups and switch between an active and inactive state by the binding of either GDP (guanosine diphosphate) or GTP (guanosine triphosphate). Activation leads to the interaction with effectors and subsequent regulation of membrane targeting. Inc proteins can also exert functions resembling SNARE (soluble NSF attachment protein receptor) proteins that mediate vesicle tethering and membrane fusion by mutual interaction of their coiled-coil domains (Delevoye et al., 2008).

After 20 to 48 hours, depending on *Chlamydia* species, re-differentiation into new infectious EBs begins. Altered gene expression towards EB development possibly depends on nutrient exhaustion. The inclusion meanwhile grows exceptionally large, taking up most of the cytoplasmic space. The bacteria recruit not only host cell lipids, but also iron, nucleotides and ATP (adenosine triphosphate, McClarty and Fan, 1993; McClarty and Qin, 1993; Tipples and McClarty, 1993). Conditions such as nutrient starvation or antibiotic treatment trigger differentiation into aberrant bodies (AB), a latent, persistent form insensitive to clinical treatment. Yet this state is reversible upon the improvement of growth conditions (Wyrick, 2010; Al-Younes et al., 2001; Raulston, 1997).

How the eventual release of the newly developed EBs is induced is not yet known. In most cases, membranes of both inclusion and the cell disintegrate and the cell ruptures, releasing the EBs which then start a new infection cycle. An alternate mechanism, called extrusion, has been described during which a part of the inclusion is pinched off and ejected while cell is left intact (Hybiske and Stephens, 2007).

The developmental cycle of *Chlamydia* is unique within the bacterial world and many open questions remain. Discovering solutions would assist in counteracting clinical pathogenesis and possibly contribute to the understanding of general aspects of cellular biology including membrane composition, vesicle trafficking or endocytosis.

1.1.3 Human diseases caused by *Chlamydia*

Of the different *Chlamydia* species, three are capable of causing diseases in humans, namely *C. pneumoniae*, *C. psittaci* and *C. trachomatis*. Infection with the airborne pathogen *C. pneumoniae* results in respiratory diseases and are a major cause of community-acquired pneumonias (Wreghitt, 1993). *C. psittaci*, a bird-pathogenic species, can be zoonotically transmitted and cause human ornithosis which may progress towards severe and even fatal systemic infections (Beeckman and Vanrompay, 2009).

C. trachomatis, the third human pathogenic species, encompasses several serologically detectable subspecies. These so-called serovars provoke different clinical outcomes after invading mucosal epithelial cells. Serovars A to C cause trachoma, a serious eye infection and the primary cause for preventable blindness worldwide and is mostly found endemically in developing countries (Gambhir et al., 2007). *C. trachomatis* D to K are responsible for genital tract

infections and represent the most common cause of sexually transmitted bacterial diseases. These infections are generally curable with microbicidal treatment (tetracyclines, macrolides and quinolones) but often remain asymptomatic and therefore go unnoticed and untreated. In females, these chronic and recurring infections result in severe pathologies like ectopic pregnancies, tubal occlusion and infertility (Faro, 1985). Lastly, *C. trachomatis* L serovars give rise to lymphogranuloma venerum (LGV), an infection invading the lymphatics and lymph nodes after genital or rectal contagion.

Interestingly, both genital and ocular *Chlamydia* infections are accompanied by characteristic scarring of epithelia and suboptimal wound healing (Van Voorhis et al., 1997; Abu el Asrar et al., 1998). Female infertility is directly caused by fibrosis and subsequent occlusion of the fallopian tubes. Blindness of trachoma patients arises from scarring of the cornea caused by scratching of the eyelashes after the swollen upper eyelid turns inward.

1.1.4 The lack of a genetic system

In contrast to *Neisseria*, *Helicobacter*, *Salmonella* or other bacterial pathogens which invade the human host, there is no genetic system available for *Chlamydia*. This makes it difficult to assign functions to specific bacterial gene products by classical genetic methods and complicates understanding the biology of this pathogen. Genetic manipulation has been pursued but was never successful enough to be applied as a standard technique (Tam et al., 1994; Binet and Maurelli, 2009).

There are several reasons why *Chlamydiae* are resistant to genetic manipulations (Heuer et al., 2007). (1) The EB is a spore-like transport form surrounded by heavily cross-linked proteins and very hard to permeabilize for gene uptake. Highly condensed DNA packing furthermore hinders integration of genetic material. (2) The RB is less inert but resides inside the intracytosolic inclusion, meaning that introduced DNA will have to cross at least four membranes, greatly decreasing efficiency. (3) The obligate intracellular lifestyle and easily induced persistency make it virtually impossible to select for transformants.

The methodology concerning this problem is nevertheless advancing. A tryptophane synthesis null mutant has been generated by chemical mutagenesis but so far, the technique is disproportionally laborious and mutation cannot be site-directed (Kari et al., 2011). Recently, Wang and colleagues successfully transformed *Chlamydia trachomatis* with a GFP-encoding plasmid, employing β-lactamase expression and several rounds of penicillin selection (Wang et al., 2011). This enables the prospective introduction of external genetic material but a technique to generate deletion mutants is still missing. Therefore, research on *Chlamydia* greatly relies on inhibitors or circumvents the problem by manipulating host cell factors.

1.2 The secreted chlamydial protease CPAF

The *Chlamydia* protease-like activity factor (CPAF) is so far the only known virulence factor of *Chlamydia* that is not transported via the TTS (Zhong et al., 2001). The serine protease is conserved among chlamydial species and is initially secreted into the inclusion lumen before being translocated into the host cell cytoplasm. CPAF contains an N-terminal signal sequence that suggests translocation into the periplasmic region via sec-dependent secretion pathway (Chen et al., 2010b). From there, it is proposed to enter the inclusion lumen via outer membrane vesicles (OMV) budding from the RBs which possibly fuse with the inclusion membrane and are emptied into the cytosol (Jorgensen and Valdivia, 2008; Giles et al., 2006).

CPAF is initially synthesized as an inactive zymogen of 70 kDa (Huang et al., 2008). To convert the zymogen into the proteolytically active enzyme, it needs to be processed into two parts of ∼35 kDa ($CPAF_c$) and ∼29 kDa ($CPAF_n$). The inhibitory segment (IS) in between is removed by three autocatalytic cleavage events whereafter the segments are joined (Figure 2.2). This promotes homodimerization, conformational changes and assembly of the catalytic triad in the mature molecule (Figure 1.4, Chen et al., 2010a). CPAF is primarily secreted in acute compared to persistent infection and has been used as a candidate antigen for vaccination studies in mice where immunization led to reduced infertility in female animals (Heuer et al., 2003; Murthy et al., 2011).

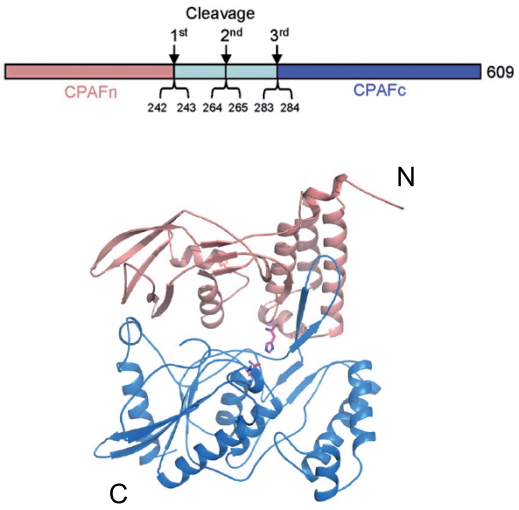

Figure 1.4: Crystal structure of chlamydial CPAF. Illustration of CPAF segments and the crystallographically resolved structure of a mature CPAF monomer. Modified from (Huang et al., 2008). N: $CPAF_n$ (residues 25–239); C: $CPAF_c$ (residues 284–601); magenta: catalytic residues.

1.2.1 Proteolysis of host cell substrates

CPAF processes numerous host cell substrates and influences several essential cellular pathways in favor of *Chlamydia*. For example, it cleaves the transcription factors RFX5 (regulatory factor X, 5) and USF1 (upstream stimulatory factor 1) functioning in antigen presentation via the major histocompatibility complex (MHC). It also degrades the pro-apoptotic proteins Puma (p53 upregulated modulator of apoptosis) and Bim (Bcl-2 interacting mediator of cell death) to counteract cell death and it can process the NFκB (nuclear factor κB) subunit p65 which is involved in inflammation-related gene transcription (Zhong et al., 2001; Pirbhai et al., 2006; Christian et al., 2010). In addition, cleavage of cell cycle regulators and DNA damage mediators has been observed (Yu et al., 2010; Paschen et al., 2008). Furthermore, it was proposed that CPAF remodels intermediate filaments to mechanically stabilize the inclusion (Dong et al., 2004; Kumar and Valdivia, 2008a).

This multitude of substrates and missing specific inhibitors have thus far complicated determining the significance of CPAF-mediated proteolysis in infection. CPAF is highly conserved among species and can even be found in environmental *Chlamydia* found in amoeba (Collingro et al., 2011). Antigen presentation or apoptosis inhibition play no role in this type of infection model. Therefore, CPAF could also act in more essential ways, especially since modification of host cell processes by proteases is often critical for the survival of intracellular pathogens (Huston, 2010).

1.3 Interaction of *Chlamydia* with the host cell Golgi apparatus

The Golgi apparatus is the center of protein maturation and distribution in a eukaryotic cell. It consists of flattened and stacked membrane cisternae and is a highly dynamic organelle with constant membrane turnover. Proteins and lipids synthesized in the endoplasmic reticulum (ER) arrive at the *cis*-region and are posttranslationally modified and sorted. From the *trans*-region at the other side of the organelle, they are distributed to their target destination in the cell or secreted into the extracellular space. Meanwhile, endocytic vesicles arrive at the *trans*-Golgi from the plasma membrane (Jackson, 2009). Generally, cargo containing vesicles as well as nonvesicular transport mediate the traffic to and from the Golgi apparatus (Hanada et al., 2009).

Intracellular bacterial pathogens heavily depend on host cell nutrients. They have been shown to manipulate cellular trafficking at different stages of the secretory pathway to divert nutrients for their own needs and protect themselves from degradation (Salcedo and Holden, 2005). Hence, the Golgi apparatus is not only the central logistic hub of the cell but also a highly important resource for the survival of parasitic bacteria like *Chlamydia*.

1.3.1 The mammalian Golgi ribbon

In mammalian cells, the individual cisternae of the Golgi apparatus are laterally linked to form the so-called Golgi ribbon (Wei and Seemann, 2010). This interconnected higher order organization facilitates diffusion of processing enzymes and directed secretion and therefore is thought to increase the efficiency of protein processing (Puthenveedu et al., 2006).

The structure of the Golgi apparatus is built and maintained by resident Golgi proteins and small G proteins which are found in the Golgi matrix (Short et al., 2005). This definition describes a protein scaffold that is resistant to detergents. Part of the matrix is built by the family of golgins, coiled-coil proteins that are anchored to the Golgi membrane in three possible ways. Some are transmembrane proteins, others are bound via adapter proteins called GRASPs (Golgi reassembly stacking proteins) and many are recruited by Golgi-localized GTPases (Figure 1.5). Other than building the Golgi stack, some of them have been described as tethering factors for membranes, vesicles and microtubule motor proteins (Shorter et al., 2002; Nakamura et al., 1997; Sönnichsen et al., 1998; Hoogenraad et al., 2001).

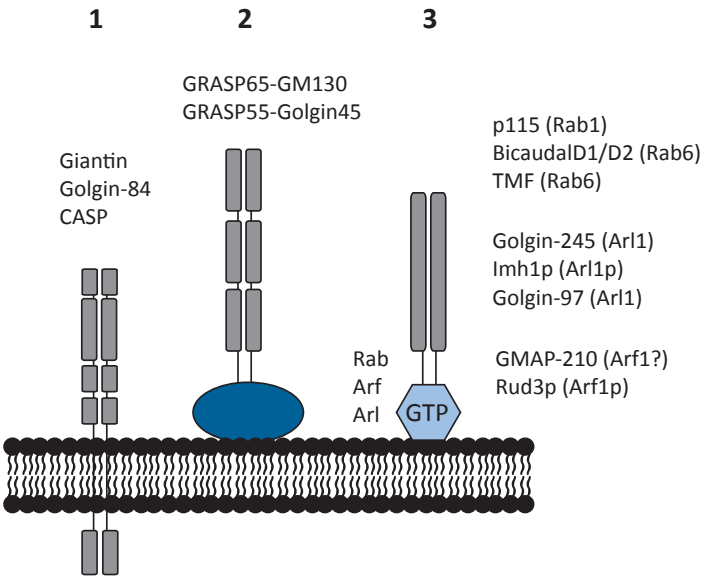

Figure 1.5: Association of golgins with the Golgi matrix. Proteins of the golgin family share coiled-coil domains (grey squares) and are found at the Golgi membrane (modified from Short et al., 2005). They can be attached in several ways: (1) Transmembrane golgins possess a C-terminal transmembrane domain and are inserted into the lipid bilayer. (2) Peripheral golgins are bound via the interaction with an adaptor protein of the GRASP family. (3) GTPases recruit golgins depending on their nucleotide triphosphate-status.

1.3.2 Golgi fragmentation by *Chlamydia*

Golgins are essential for Golgi ribbon integrity and depletion results in disruption of the linked structure into small ministacks (Short et al., 2005; Ramirez and Lowe, 2009). Golgi fragmentation is usually observed in apoptotic cells or during mitosis, when the stacks are distributed to the developing daughter cells. This large-scale reorganization of the Golgi apparatus is necessary for cell cycle progression but does not normally occur in the interphase cell. Golgi fragmentation in mitosis is achieved through phosphorylation of Golgi proteins including GRASP65 and GM130 by mitotically regulated kinases (Lowe et al., 1998; Wang et al., 2003). In apoptotic cells, the Golgi apparatus is fragmented because golgins are proteolyzed by apoptotic caspases (Mancini et al., 2000; Lane et al., 2002; Chiu et al., 2002).

Interestingly, this phenomenon is also observed upon infection with *Chlamydia*. The ribbon structure is dissolved into small ministacks after 16 h of infection (Heuer et al., 2009). Moreover, those fragments are recruited to the growing bacterial inclusion and aligned around the inclusion membrane (Figure 1.6). The ministacks are still functional concerning protein processing and secretion. It has been shown that fragmentation and relocalization of Golgi elements after infection is crucial for chlamydial development. It allows better bacterial uptake of host cell sphingolipids which are converted from precursors in the Golgi apparatus after being synthesized in the ER. Cholesterol, glycerophospholipids and glycerosphingolipids are usually produced only by eukaryotic cells, nevertheless, they are detected in the bacterial cell membranes of purified EBs (Hatch and McClarty, 1998). They are needed for the assembly of membranes including the growing inclusion membrane and those of developing EBs. If their incorporation is blocked by inhibitor treatment the production of infectious progeny dramatically decreases (Heuer et al., 2009).

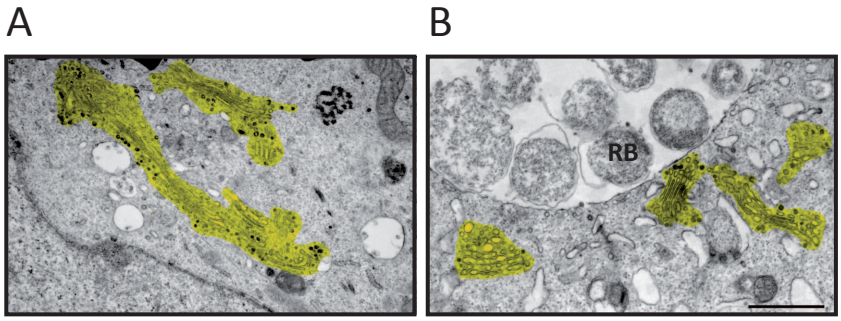

Figure 1.6: *Chlamydia*-induced Golgi fragmentation. Electron micrograph showing the Golgi apparatus highlighted in yellow (modified from Heuer et al., 2009). **A**. Cytoplasm of an uninfected cell with intact Golgi ribbon. **B**. Golgi fragments in an infected cell in close vicinity of the bacterial inclusion. RB: reticulate body. Scale bar: 1 μm

Chlamydia-induced Golgi fragmentation is triggered by processing of the Golgi matrix protein golgin-84. Golgin-84 has previously been described to be essential for the stability of the Golgi ribbon (Diao et al., 2003). It is an integral golgin with a 400-residue coiled-coil domain and anchored to Golgi membranes via a single C-terminal transmembrane domain (Figure 1.7, Bascom et al., 1999). It has been reported to form dimers and interact with Rab proteins (Diao et al., 2003). Golgin-84 is cleaved after about 16 hours of *Chlamydia* infection, resulting in two smaller fragments of ∼78 and ∼65 kDa (Heuer et al., 2009). One cleavage site was identified to be located at serine residue S157 (Heuer et al., 2009). Simultaneously with this processing, the Golgi ribbon starts to disintegrate.

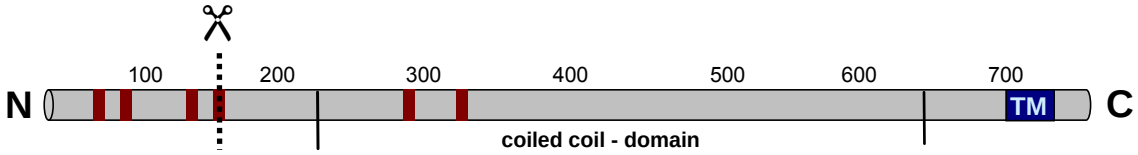

Figure 1.7: Protein structure of golgin-84. Schematic representation of golgin-84 protein structure. Golgin-84 is a transmembrane Golgi matrix protein, featuring a large coiled-coil domain mediating dimerization and interaction with Rab GTPases, one transmembrane domain (TM) and several FH (formin homology)-domains for possible protein-protein-interactions (red). One of two cleavage sites has been identified and is located at S157 (indicated by scissors, Heuer et al., 2009).

In addition to golgin-84, two Rab GTPases contribute to infection-mediated Golgi fragmentation. Rab6A (hereafter designated Rab6) is involved in retrograde intra-Golgi transport of vesicles and Rab11A (hereafter termed Rab11) in that of recycling endosomes (Martinez et al., 1994; Wilcke et al., 2000). Both GTPases are recruited to the inclusion by *Chlamydia* and are important for the formation of new infectious EBs (Rzomp et al., 2003). Interestingly, Golgi fragmentation in infected cells can be prevented by knockdown of these two proteins (Rejman Lipinski et al., 2009).

This leads to the conclusion that *Chlamydia* manipulates (1) the Golgi architecture by degradation of the Golgi matrix protein golgin-84 and (2) the trafficking of certain vesicles via Rab6 and Rab11 to have better access to nutrients. Both processes are vitally important for bacterial development and progression of the infection.

1.4 Eukaryotic cell motility

Directional migration of cells contributes to many fundamental biological processes. Starting with embryogenesis, during which whole cell sheets move to construct a multilayered organism or nerve tracts develop, to immune surveillance, wherein motile leucocytes defend the body against infections, to wound healing, whereupon a combination of fibroblasts, vascular endothelial cells and epithelial cells repairs all kinds of tissue damage (Gurtner et al., 2008). Dysfunctions in the migration process can result in severe pathologies, namely vascular disease, osteoporosis, chronic inflammatory diseases or mental retardation. In addition, the invasion of cancer cells into peripheral tissue is governed by transendothelial migration into blood vessels (Gaggioli et al., 2007).

There are more than one kind of cell migration. Cells can move individually or collectively and they can move in every direction of two or even three dimensions (Friedl and Gilmour, 2009). Depending on the cell type and the form of movement, different molecules contribute to the process in the form of stimuli, receptors or signal transducers. In all cases, the process is started by stimulus sensing at the plasma membrane and completed by the generation of mechanic force with the help of the cytoskeleton (Lauffenburger and Horwitz, 1996).

1.4.1 The migratory cycle

Cell movement repeatedly follows a series of integrated processes (Ridley et al., 2003; Lauffenburger and Horwitz, 1996). Perception of the usually extracellular trigger initiates the cycle. The cell responds by polarizing to define front and rear and starts membrane protrusion at the forward-oriented side (Condeelis, 1993). Attachment sites are established between the protrusions and the substratum and the cell body is translocated across. Finally, the membrane at the back is retracted (Kolega, 2003). All these actions are highly regulated by cellular adaptors and amplified by feedback loops to ensure efficient locomotion. However, the process as a whole is not completely understood.

The key players in migration are the three small Rho family GTPases Rac1, RhoA (ras homolog gene family, member A) and Cdc42 (cell division cycle 42, Ridley et al., 2003). Their activity is regulated by classical GTPase modulators: guanine nucleotide exchange factors (GEFs), GTPase activating proteins (GAPs) and guanine nucleotide dissociation inhibitors (GDIs), but they can also regulate one another. Cdc42 is the master regulator of cell polarity and contributes to most parts of the migration process (Etienne-Manneville, 2004). GTPases can in general exert multiple actions and the course of events happening in motile cells has not been wholly clarified. Their specific roles can vary depending on the cell type. The following description concentrates on the most relevant aspects for the twodimensional migration of cultured cells.

Stimulus sensing

A migratory stimulus can be a chemoattractive gradient, physical stress or the absence or presence of cell-cell-contacts (Etienne-Manneville, 2004). For example, if neighboring cells are removed because of tissue damage this is sensed by integrins on the cell surface. These transmembrane receptors usually mediate contact to the extracellular matrix (ECM) and cell-cell-adhesion. The latter involves further proteins such as adhesion proteins like nectins and E-cadherin (Takai et al., 2003). Integrins are heterodimeric proteins that possess one alpha- and one beta subunit. Each subunit consists of a large extracellular domain that is attached to the ECM (or to another cell) and an intracellular domain that is connected to the cytoskeleton via adaptor proteins (Banno and Ginsberg, 2008). Integrins can activate migration signaling through phosphorylation of small GTPases after conformational change which is induced after interaction of alpha and beta subunits upon binding or unbinding of ligands or ECM interaction (Geiger et al., 2001; Emsley et al., 2000). Whether the signal is coming from integrins or adhesion proteins, it is transmitted on to Cdc42 which then induces polarization (Etienne-Manneville and Hall, 2001; Arthur et al., 2002; Honda et al., 2003; Kawakatsu et al., 2002).

Polarization

After the cell has recognized the stimulus, it establishes an asymmetry between front and back. The frontal end is then called the leading edge (LE) and the cell rear, the trailing edge (TE). Cdc42 and Rac1 are locally activated at the LE via signaling coming from integrins or adhesion proteins (Itoh et al., 2002; del Pozo et al., 2000). The emerging gradient of GTP-bound Rac1 and Cdc42 restricts binding of specific effectors and downstream signaling to the cell front. This leads to localized activation of evolutionary conserved polarity proteins which regulate microtubule dynamics and control anchoring of microtubules to the cell cortex (Schlessinger et al., 2007).

While migration itself relies on actin reorganizations, its directionality is mediated by microtubules. Localized Cdc42-GTP activates a complex of atypical protein kinase C (aPKC) and the scaffolding protein Par6 (partitioning defective 6, Nobes and Hall, 1999; Gomes et al., 2005). The active aPKC/Par6 complex induces accumulation of the tumor suppressor protein adenomatous polyposis coli (APC) at microtubule plus-ends as well as Dlg (discs large) on the plasma membrane at the LE. This specific distribution is facilitated by the regulatory protein IQGAP (IQ motif containing GTPase activating protein) and is important for microtubule polarization and reorientation of centrosomes (Etienne-Manneville et al., 2005; Watanabe et al., 2004). The so-called Cdc42/Par6/aPKC pathway was first discovered in *C. elegans* and functions together with noncanonical Wnt signaling to provide cell polarity (Schlessinger et al., 2007).

In epithelial cells, RhoA activity is found predominantly in the cell body and at the rear where it is required for retraction (Worthylake et al., 2001). RhoA has therefore been suggested to be antagonistic to Rac1 and Cdc42 (Evers et al., 2000). This compartmentalization of GTPase activity is essential for migration. The timely overall concertation of GTPase activities has recently started to be understood (Etienne-Manneville and Hall, 2002; Machacek et al., 2009).

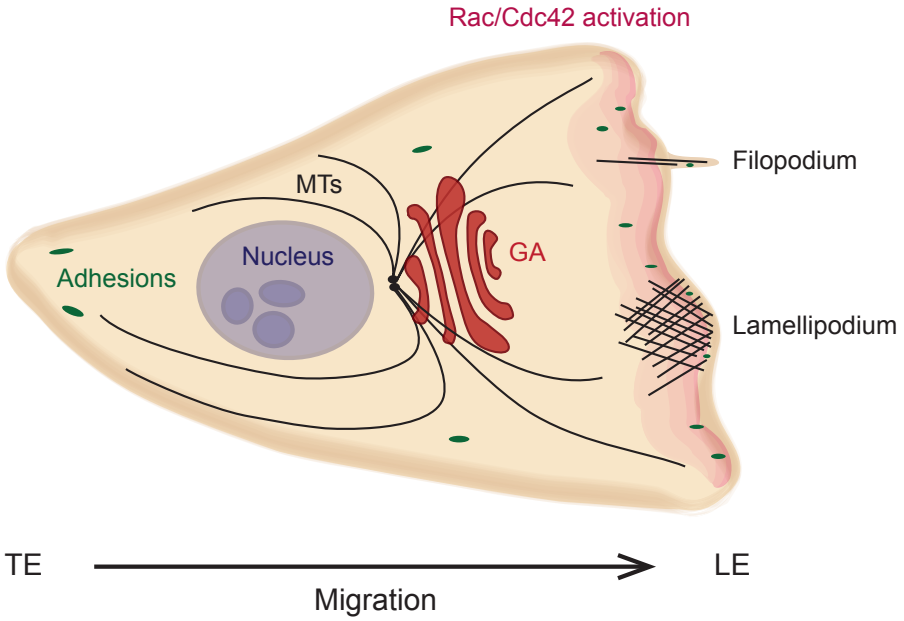

Figure 1.8: Polarization of a motile cell. Illustration of the polarized state that is established for migration. At the leading edge (LE), an activation gradient of GTP-bound Rac1 and Cdc42 promotes protrusion. Sheet-like lamellipodia are built from branched actin filaments while spike-shaped filopodia consist of parallel bundles. Adhesions form at the cell front and mature during translocation of the cytoplasm. The Golgi apparatus (GA) is aligned anterior to the nucleus. The centrosome is copositioned with the GA and secretion is directed along microtubules (MTs). At the trailing edge (TE), the membrane is retracted.

In the presence of a chemoattractant, PI3 kinase (PI3K) is activated at the LE which generates phosphatidylinositol (3,4,5)-trisphosphate, also called PI3 or PIP3 (Devreotes and Janetopoulos, 2003; Merlot and Firtel, 2003). The products of PI3K locally activate Rac1-activating GEFs and initiate chemotactic migration (Welch et al., 2003). Meanwhile, the corresponding phosphatase PTEN (phosphatase and tensin homologue) is active at the TE.

The alignment of cellular organelles is crucial for directional migration (Figure 1.8). Via Cdc42, the Golgi apparatus and microtubule organizing center (MTOC) are positioned in front

of the nucleus facing the migration direction (Kupfer et al., 1982; Etienne-Manneville and Hall, 2001; Sütterlin and Colanzi, 2010; Palazzo et al., 2001). This promotes microtubule growth into the protrusions as well as directed vesicle trafficking to the LE. Golgi orientation heavily depends on golgin-provided Golgi structure and microtubules originating from the Golgi apparatus itself are required (Bisel et al., 2008; Miller et al., 2009).

The position of the Golgi apparatus is essential for motility. Disturbance of Golgi architecture has been shown to inhibit the migration response (Yadav et al., 2009). This makes the Golgi apparatus an important component of the polarization process and indicates that changes inflicted on this organelle are likely to affect cell movement.

Protrusion

To manifest migratory signals into mechanical force, major reorganization of the actin cytoskeleton is induced (Coates et al., 1992). Local polymerization of actin filaments occurs at the LE after local Rac1- and Cdc42-activation and results in two types of protrusions: sheet-like lamellipodia are made of branched actin polymerizing from barbed ends while needle-shaped filopodia consist of bundled actin stemming from pointed ends (Ridley et al., 1992).

Both are initiated by the WASP/WAVE (Wiskott-Aldrich syndrome protein / WASP-family verprolin-homologous protein) family which controls the Arp 2/3 (Actin-related protein 2/3) complex mediating actin polymerization (Pollard and Borisy, 2003). The WASP/WAVE proteins are again regulated by Rac1 and Cdc42 (Eden et al., 2002; Le Clainche et al., 2007). One model proposes that this actin polymerization generates the mechanical force that pushes the membrane along. Recently, membrane blebbing has been identified as another form of protrusion that promotes migration which uses hydrostatic pressure to drive the membrane forward (Fackler and Grosse, 2008).

Adhesion

Protrusions are stabilized by the formation of adhesions to the substratum. Those are the sites where traction forces are highest and are made of activated integrins clustering at the LE and other proteins, depending on their maturation state (Kiosses et al., 2001). The formation of adhesions is Rac1-, RhoA- and Cdc42-dependent and the turnover is regulated by focal adhesion kinase (FAK, Nobes and Hall, 1995). They stay in place and mature while the cell body is moved forward across them. Early adhesions that are formed at the front are termed focal complexes. Apart from integrins, they contain vinculin, paxilin, alpha-actinin and Arp2/3. Classical focal adhesions are found in the cell periphery and also include zyxin (Zaidel-Bar et al., 2003).

Retraction

Retraction of the cell rear and adhesion disassembly is controlled by multiple signaling pathways, including RhoA GTPase and FAK. Contractile forces are generated with aid of myosin-II. Adhesions can be disconnected by physical tension while the integrins remain on the substratum as "footprints" or disassembled via calpain-mediated proteolysis (Regen and Horwitz, 1992; Franco and Huttenlocher, 2005).

Although the processes of cell migration remain partly unclear, it is certain that the Golgi complex is a main part of the cell's motility response. Golgi apparatus positioning and integrity are essential for polarization and therefore also for directional movement.

1.5 Aims of this thesis

Chlamydia infection induces fragmentation of the host cell Golgi apparatus via cleavage of golgin-84. The Golgi apparatus is dispersed into small ministacks that align around the inclusion upon *Chlamydia* infection. This is vitally important for bacterial growth and reinfection and promotes lipid uptake by *Chlamydia*. It is not known which bacterial factor induces this process and which protease executes golgin-84 processing. The chlamydial protease CPAF could be a candidate because it is secreted simultaneously with the onset of Golgi fragmentation and cleaves numerous host cell substrates.

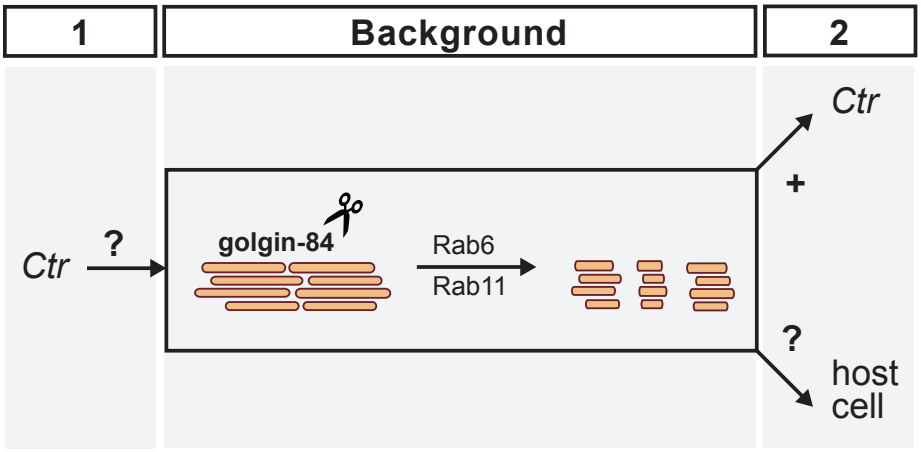

Figure 1.9: Investigative approach of the thesis. Illustration of known details of *Chlamydia trachomatis* (*Ctr*)-induced Golgi fragmentation (Heuer et al., 2009; Rejman Lipinski et al., 2009) and of issues addressed in this thesis. (1) Disruption into ministacks occurs after fragmentation of golgin-84 and is Rab6- and Rab11-dependent. Which bacterial enzyme or factor is involved is not known. (2) Golgi fragmentation promotes chlamydial development but the consequences for superordinate host cell functions have not been investigated.

In this thesis, two main questions and one accessory approach were addressed (Figure 1.9). Firstly, closer investigation of golgin-84 cleavage and its relevance for infection, as well as defining a potential involvement of CPAF in this process intended to clarify the mechanisms that precede *Chlamydia*-induced Golgi fragmentation. This was addressed by inhibition experiments and ectopic expression of CPAF in uninfected cells. Since golgin-84 dependent Golgi fragmentation was shown to be Rab6- and Rab11 dependent, a potential contribution of Rab6 and Rab11 was tested via siRNA-mediated knockdown of these two GTPases.

Secondly, the consequences of Golgi fragmentation on the infected cell were assessed. Since Golgi structure is important for cell polarization and thereby is a prerequisite of directional migration, disruption of Golgi structure in infected cells likely has an impact on cell motility. The migratory response was determined via motility and polarization assays in infected cells as well as uninfected cells with a disrupted Golgi apparatus after knockdown of golgin-84. Furthermore, cytoskeletal elements of protrusion and the activity of the polarity regulator Cdc42 were investigated after infection.

Finally, the interaction profile of Cdc42 was characterized in a proteomics approach to investigate whether the binding to downstream effectors was altered. This could reveal an influence of infection on other migration-associated pathways.

2 Materials and Methods

2.1 Materials

2.1.1 Organisms

Cell lines

Name (collection no.)	Origin	Source
HeLa2000 (C-0272)	human cervix carcinoma	ATCC: CCL-2
HeLa2000 sh luciferase (C-0276)	human cervix carcinoma	Heuer et al., 2009
HeLa2000 sh golgin-84 (C-0279)	human cervix carcinoma	Heuer et al., 2009
HeLa2000 sh Rab6 (C-0291)	human cervix carcinoma	Rejman Lipinski et al., 2009
HeLa2000 sh Rab11 (C-0147)	human cervix carcinoma	Rejman Lipinski et al., 2009
T-REx-293 (C-0102)	human embryonic kidney	Invitrogen: R710-07
T-REx-293-gyrB-CPAF (C-0103)	human embryonic kidney	Paschen et al., 2008

Bacteria

Species	Serovar	Origin	Source
Chlamydia trachomatis (batch AG 2008-08-13)	L2	lymphatic isolate	ATCC: VR-902B

2.1.2 Nucleic Acids

Expression Plasmids

Name (collection no.)	Expressed insert	Source
pcDNA4-gyrB-CPAF (H4032)	CPAF-gyrB (*C. trachomatis*)	Paschen et al., 2008
peGFP-N1 (H4030)	eGFP (*A. victoria*)	Invitrogen
peGFP-N1-Cdc42 (L183)	Cdc42-eGFP (human)	Churin et al., 2001

Small interfering RNAs (5' to 3')

Target	Sequence	Source
Luciferase	AACUUACGCUGAGUACUUCGA	Qiagen
Golgin-84	CTGAGTTTAGTGGTCCTAATA	Qiagen
Rab6	CAGATTCATGTATGACAGTTT	Qiagen
Rab11	AAGAGUAAUCUCCUGUCUCGA	Qiagen

2.1.3 Media and Solutions

Cell Culture Media

Application	Composition	Source
Cell growth	DMEM, 10 % FCS h.i.	Gibco, Biochrom
	100 mM sodium pyruvate	Gibco
	200 mM L-glutamine	Gibco
Infection	DMEM, 5 % FCS h.i.	Gibco, Biochrom
	100 mM sodium pyruvate	Gibco
	200 mM L-glutamine	Gibco
Transfection	OptiMEM	Gibco
Selection	Growth / infection medium,	Gibco
	350 μg/ml Zeocin^{TM}, 5 μg/ml Blasticidin	Invitrogen, Merck
SILAC "light"	Growth / infection medium, no amino acid labeling	Gibco
SILAC "heavy"	Growth / infection medium,	Gibco
	$^{13}C_6$ $^{15}N_4$ L-arginine, $^{13}C_6$ $^{15}N_2$ L-lysine	Cambridge Isotope Laboratories

Buffers

Buffer	Composition
PBS	137 mM NaCl, 2.7 mM KCl, 10 mM Na_2HPO_4 + 2 H_2O, 1.76 mM KH_2PO_4
TBS	137 mM NaCl, 10 mM Tris/HCl
TBST	TBS, 0.05 % Tween 20
Stacking SDS-gel buffer	1 M Tris/HCl pH 6.8
Separating SDS-gel buffer	1 M Tris/HCl pH 9.0
RIPA lysis buffer	20 mM Tris/HCl pH 7.5, 150 mM NaCl, 0.5 % NP-40, 0.5 % Triton X-100
SDS loading buffer	63 mM Tris/HCl, 10 % glycerol, 2 % SDS, 0.0025 % Bromophenol blue
SDS running buffer	25 mM Tris/HCl, 192 mM glycine, 0.1 % SDS
Transfer buffer	25 mM Tris/HCl, 192 mM glycine, 20 % methanol
Blocking buffer	TBST, 3 % powdered milk
Stripping buffer	62.5 mM Tris/HCl, 100 mM β-mercaptoethanol, 2 % SDS
Permeabilization buffer	PBS, 0.2 % BSA, 0.2 % Triton X-100
SPG buffer	PBS, 0.25 M saccharose

Selfmade Solutions

Solution	Composition
PFA	PBS, 2 % PFA, 2 % Saccharose
Mowiol	2.4 g Mowiol 4-88, 6 g glycerol, 6 ml H_2O, 12 ml 0.2 M Tris pH 8.5
Antibody diluent	PBS, 0.2 % BSA

Readymade Solutions

Solution	Source
ECL Solution	Roche
Trypsin-EDTA	Gibco

2.1.4 Reagents

Chemicals

Standard compounds and liquids were obtained from Merck, Sigma and Roth.

Inhibitors

Name	Source
DEVD-fmk, LEHD-fmk, WEHD-fmk, VEID-fmk	R&D
Mitomycin C	AppliChem
PhosSTOP Phosphatase Inhibitor Mix	Roche
Complete™ Protease Inhibitor Mix	Roche

Transfection Reagents

Name	Source
Lipofectamine 2000™	Invitrogen
RNAiFect	Qiagen

Fluorescent Markers

Name	Source
DRAQ5™	Biostatus
Alexa Fluor® 647-phalloidine	Invitrogen

Protein Marker

Name	Source
PageRuler™ Prestained Protein Ladder	Fermentas

Others

Name	Source
EGF (human)	Sigma
AHT	IBA
Coumermycin	Sigma
Zeocin™	Invitrogen
Blasticidin	PAA
Mowiol 4-88®	Roth
Glycoblue™	Ambion

Antibodies

Primary antibodies

Antigen	Species	Source
β-actin	mouse	Sigma
Cdc42	rabbit	Cell Signaling
Giantin	rabbit	Covance
Golgin-84	mouse	BD
GPP130	rabbit	BD
Hsp60	mouse	Alexis
MOMP	mouse	Gurumurthy et al., 2010
Pericentrin	rabbit	Abcam
Rab6	rabbit	Calbiochem
Rab11	mouse	BD
β-tubulin	mouse	Sigma
Vimentin	mouse	Sigma

Secondary antibodies

Conjugate	Source
IgG-Horseradish peroxidase	Amersham
IgG-Cyanine dye	Dianova

2.1.5 Kits

Name	Source
RhoA/Rac1/Cdc42-Activation Assay Combo Kit	Cell Biolabs
GFP-Trap®	Chromotek
BCA Protein Assay Reagent Kit	Pierce

2.1.6 Consumables

Material	Source
Cell culture flasks/dishes	TPP
Live cell dishes	Mattek, Ibidi
Cell culture inserts	Ibidi
Glass beads 2.2 mm	Roth
Cell scrapers	Biochrom
Reaction containers	Sarstedt
Microscopy slides	Roth
Glass cover slips	Marienfeld
PVDF membranes	Millipore
X-ray films	Kodak
Parafilm®	Pechiney

2.1.7 Equipment

Experiments were done using standard modern laboratory equipment.

Microscopes

Name	Configuration
Leica LSCM (TCS SP-1)	63x/1.32 NA HCX PL APO CS
Olympus IX81 live cell	10x/0.25 NA, live cell chamber (35 °C, 5 % CO_2), Hamamatsu C9100-02 CCD camera
Olympus IX81 inverted	UPlanS Apo 10x/0.40 NA, Hamamatsu C4742-80-12AG CCD camera, Scan^R system

2.1.8 Software

Name	Supplier
Confocal software	Leica
ImageJ	US National Institute of Health, Bethesda
MaxQuant	Max Planck Institute of Biochemistry, Martinsried
Metamorph	Molecular Devices
Photoshop	Adobe®
Illustrator	Adobe®
Excel	Microsoft
LaTeX	Public License

2.2 Methods

2.2.1 Cell culture

Since *Chlamydia* are intracellular bacteria, the quality of cell culture is vitally important for efficient infection and comparable experiments. Cell culture is generally performed in the absence of antibiotics which further increases the necessity for a careful culturing technique. All cell lines were propagated in DMEM growth medium with 10 % FCS in 75 cm^2 culture flasks. When reaching confluency (every 2-3 days), they were passaged into new flasks up to maximal 10 passages. The stable CPAF expression cell line (T-REx-293-gyrB-CPAF) was additionally kept under selection pressure with 350 μg/ml zeocin and 5 μg/ml blasticidin. For passaging, the cells they were rinsed with PBS and proteolytically detached with 1 ml trypsin-EDTA for 2-5 min at 37 °C. *Mycoplasma* contamination had been excluded by central laboratory quality management via PCR. Cells were seeded with a density of 1.5-2 $*$ 10^5 cells/ml into appropriate culture volumes, including 6-, 12- and 24-well plates, and kept in a culture volume of 2 ml medium per 10^6 cells in a humidified incubator providing 5 % CO_2 and 37 °C.

For the Golgi orientation assay (2.2.12), cells were grown in special silicone culture chambers to obtain defined cell layer borders (Figure 2.1). One chamber contains about 120.000 cells when confluent, in a culture volume of 70 μl.

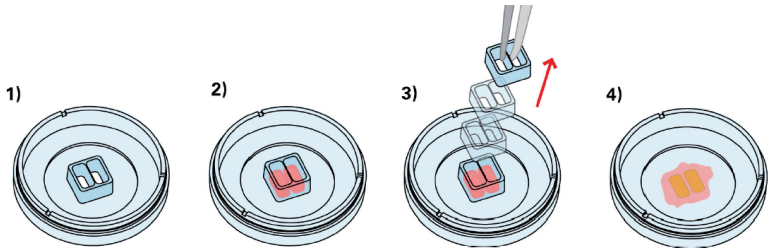

Figure 2.1: Culture chamber seeding for Golgi orientation assay. Illustration of seeding procedure for cell culture in two opposing chambers. 1: The self-adhesive silicone insert is placed in the culture dish, optionally containing a cover slip for later immunostaining. 2: 70 μl cell suspension is seeded into the two chambers and grown as needed. 3: The insert is removed with sterile forceps and two defined populated areas divided by a 500 μm gap remain. 4: The two cell patches are covered with medium. Modified from www.ibidi.com.

2.2.2 Transfection

Expression plasmids

For the ectopic expression of a specific protein, HeLa cells were seeded into 12-wells and grown to 70 % confluency. 1 μg plasmid DNA per well were mixed with 100 μl OptiMEM transfection medium. Of the transfection reagent Lipofectamine 2000, 2 μl per well were mixed with 100 μl OptiMEM. After 5 min incubation at RT, the two mixes were pooled and kept at RT for 20 min to allow complex formation. Cells were washed with PBS and 200 μl transfection mixture per well were added together with 400 μl growth medium. and the cells were incubated for 24 h.

Small interfering RNAs

In order to downregulate host cell proteins, HeLa cells were transfected with a siRNA specifically recognizing the desired mRNA. Cells were grown in 12-wells to around 70 % confluency. 1 μg of siRNA per well were diluted in 100 μl OptiMEM and 6 μl of the transfection reagent RNAiFect were added to the dilution. For double knockdown, 0.5 μg of each siRNA were introduced into the mixture. Liposome formation occurred during subsequent incubation for 20 min at RT. The medium was aspirated from the wells and 600 μl fresh growth medium were added. 100 μl of the transfection solution were added dropwise to each well. Cells were incubated for 24 h before they were split into appropriate culture formats. 72 h post transfection, the subsequent experiment was started. Protein levels were monitored via Western Blot analysis (see 2.2.11).

2.2.3 Activation of chlamydial CPAF in human cells

Ectopic expression of the bacterial protease CPAF in human cells requires particular experimental conditions (Paschen et al., 2008). CPAF is initially produced as an inactive zymogen (Figure 2.2). Activation of the enzyme at a certain time point is possible due to an inserted upstream bacterial gyrase domain. Gyrase is a natural dimerizer and induces CPAF homodimers upon addition of coumermycin (CM, 1 μM). Homodimerization enables autocatalytic excision of the inhibitory segment and activation of the protease. Three subsequent cleavage events and conformational changes release an amino acid triad in the catalytic center (His105, Ser499, Glu558) and render the enzyme active. Moreover, CPAF displays autoactivity when overexpressed. This requires an additional transcriptional control given by an integrated tet repressor. Transcription is induced by addition of 5 ng/μl anhydrotetracycline (AHT). Depending on the experiment, CPAF is expressed in HeLa cells after transfection of an expression plasmid (pcDNA4-gyrb-CPAF) or in a stably transfected cell line (T-REx-293-gyrB-CPAF).

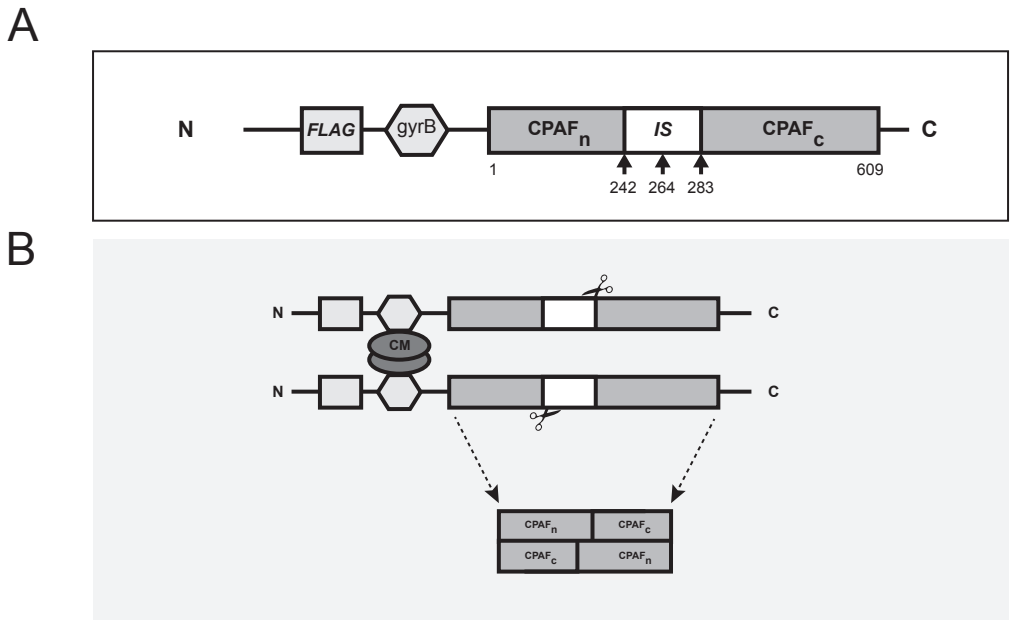

Figure 2.2: The CPAF expression system. A. The catalytically inactive CPAF zymogen of 70 kDa consists of N-terminal and C-terminal parts separated by the inhibitory segment (IS). This segment includes three sites for autocatalytic cleavage (arrows). The construct furthermore harbors a FLAG tag and a bacterial gyrase domain (gyrB) for dimerization. **B**. Addition of coumermycin (CM) triggers transient dimerization of the monomers which induces self-cleavage events that remove the inhibitory segment and stabilize the homodimer. This process frees the catalytic triad in the active center and activates the enzyme.

2.2.4 Infection with *Chlamydia*

In this work, *Chlamydia trachomatis* serovar L2 was employed as infection model and is henceforth referred to as *Chlamydia*. HeLa cells were grown to 70-80 % confluency and infected 24 h after seeding in the appropriate volume. Cells were washed with DMEM infection medium containing 5 % FCS, the stock solution of EBs was diluted into infection medium to yield the appropriate MOI (multiplicity of infection, see 2.2.6) and the inoculum was added to the cells. Infection volume equaled 1 ml per 10^6 cells (half of the culture volume). After two hours, cells were washed and kept in infection medium (standard culture volume). Infected cells were grown in a humidified incubator providing 5 % CO_2 and 35 °C.

2.2.5 Preparation of *Chlamydia* stock solution

HeLa cells were cultured in 150 cm^2 flasks to 80 % confluency and several flasks were infected (MOI 3). After two days of incubation when new EBs had developed, infected cells were harvested with a cell scraper and collected in 50 ml plastic tubes containing sterile glass beads. To release infectious EBs, the cells were lysed mechanically by vortexing for 3 min. The lysate was cleared from cell debris via centrifugation (10 min, 500 g, 4 °C) and EBs were pelleted (60 min, 4800 g, 4 °C). After washing and resuspending the pellet in cold SPG buffer, the solution was homogenized by passing through a 26 G syringe. Small aliquots were kept at 4 °C for the first 3-4 h and then stored at -80 °C. For each infection, a fresh aliquot of EBs was thawed on ice.

2.2.6 Titer determination

HeLa cells were seeded into 24 well culture dishes containing glass cover slips and grown to 80 % confluency. Serial dilutions of the *Chlamydia* stock solution were titrated onto the cells. 24 h post infection, the cells were fixed with 2 % PFA for 30 min at RT. After immunostaining of chlamydial major outer membrane protein (MOMP), the developed inclusions were counted in 10 microscopic fields per dilution using 40 x magnification. The number of inclusion forming units (IFU) per ml was calculated with the following formula:

$$IFU/ml = \bar{x}\ inclusions\ per\ microscopic\ field \times 2975.2 \times dilution\ factor \times 4$$

In this equation, the factor 2975.2 corrects for the cell number visible in a microscopic section at 40x magnification compared to a whole 24well and the factor 4 corrects for the infection volume of 250 μl. While the unit IFU describes the absolute number of bacterial particles, the MOI (multiplicity of infection) is a term expressing the bacteria-to-cell ratio, taking into account how many cells are infected. Accordingly, 3 IFUs per cell equals MOI 3.

2.2.7 Reinfection assay

The reinfection assay is a standard method to compare the amount of infectious progeny that is produced by *Chlamydia* after a full developmental cycle. It can be used to compare bacterial development under different conditions, for example knockdown of host cell gene products or chemical treatment. The number of new infectious particles (EBs/IFU) after reinfection of naïve cells is quantified. Cells were infected with *C. trachomatis* L2 (MOI 3) after indicated time points. After 48 h of infection with equal infectious doses, the cells were lysed and the newly formed EBs were quantified. One portion was immunostained to assess primary infection. The rest of the cells were lysed with glass beads to release the infectious particles. The lysates were diluted serially and titrated onto fresh cells seeded onto glass cover slips. After 24 h of reinfection, they were fixed with 2 % PFA for 30 min at RT and inclusions were immunostained with an antibody against chlamydial MOMP. Quantification of newly developed EBs was performed as described in 2.2.6.

2.2.8 Immunostaining

Cells were cultured on cover slips inserted into 12-wells and staining was performed at 80-90 % confluency. Cells were washed with PBS and fixed for 30 min at RT with 2 % PFA. After simultaneous permeabilization and blocking in permeabilization buffer for 20-25 min at RT, 25 μl-droplets of the primary antibody dilution were placed on top of a sheet of parafilm and the cover slips were placed face down on the droplets. After incubation for 1 h at RT, the cover slips were placed back in the wells and washed with PBS for 30 min. The PBS was changed every 10 min. Cyanine-conjugated secondary antibody dilution was incubated 1h at RT with light protection to avoid fluorescent bleaching. After 30 min of washing, the cover slips were mounted on microscopy slides with mowiol, dried for 24 h at RT and stored in the dark.

2.2.9 Microscopy

Confocal microscopy

Fixed samples were analyzed with a Leica TCS SP-1 laser scanning confocal microscope (LSCM) equipped with Leica imaging software. Images were overlaid and processed with Adobe Photoshop CS3, applying the same corrections (brightness, contrast, channel intensity) to all images.

Live cell microscopy

To directly monitor the migration of cells, they were seeded into live cell dishes with glass bottoms containing silicone culture chambers (Figure 2.1). Cells were infected the next day with MOI 3 or left uninfected. After 48 h of culture (24 h post infection in infected samples), inserts were removed to allow cell migration into the gap between the two cell areas. Growth or infection medium was supplemented with 50 ng/ml EGF after insert removal to mildly accelerate motility and reduce the experiment's duration before infected cells started to lyse. Image stacks of 4 planes with 0.5 μm interspace were acquired every 4 min and processed using MetaMorph software.

Distances covered by individual cells (n $\geq$ 9) were determined with the manual tracking function of ImageJ that produces a track line from the x-y-position of the cell in each 4 min-frame and measures the total track length (l). The net displacement or vector length (d) was calculated from x- and y-axis displacements from start (t_0) to end (t_{16}).

$$d\,[\mu m] = \sqrt{(x_{t_{16}} - x_{t_0})^2 + (y_{t_{16}} - y_{t_0})^2}$$

To determine the directionality coefficient (D) describing the straightness of the track, the net displacement (d) was divided by the track length (l).

$$D = \frac{d}{l}$$

The most directed form of movement, a straight line, yields a directionality coefficient of 1, while a rectangular turn of direction would result in a value of 0.5. This means that the more directed the movement, the closer D approaches 1.

2.2.10 Western Blot analysis

About 10^6 cells per sample were harvested on ice by scraping in 1 ml cold PBS. After pelleting and decanting, cells were lysed for 30 min on ice in 100 μl cold RIPA buffer containing protease inhibitor mix while vortexing every 10 min. Lysates were cleared from cell debris by centrifugation for 30 min at 20.000 g and 4 °C and pellets were discarded. Protein concentrations were determined colorimetrically using a BCA Protein Assay Kit. SDS sample buffer was added to the lysates before heating them briefly at 95 °C. Equal protein amounts (10-20 μg) per lane were loaded onto denaturing 10 % SDS gels for electrophoretic separation (Sambrook et al., 1989). Afterwards, the proteins were transferred onto a PVDF membrane with a standard wet

blot apparatus. The membrane was incubated for 30 min at RT in blocking buffer and primary antibody diluted in blocking buffer was added to incubate over night at 4 °C with gentle shaking. After 3 times 10 min of washing with TBST, the HRP-conjugated secondary antibody diluted in TBST was incubated with the membrane for 1 h at RT. This was followed by another 30 min of washing and finally the chemiluminescent signal was detected after short incubation with ECL solution by exposure of X-ray films.

2.2.11 *In vitro* scratch assay

The in vitro scratch assay is used to compare the migration of cells on a two-dimensional surface (Liang et al., 2007). Cells were seeded into 6-wells and grown until 70 % confluency. After 48 h which, if applicable, included 24 h of infection with MOI 3, the cell monolayer was scratched multiple times vertically and horizontally with a sterile pipet tip. Detached cells were washed away with medium and cell migration into scratches was monitored for the next 24 h. At every time point, three scratches per condition were surveyed at two defined and unchanged positions per scratch. Images were acquired after 0, 8 and 24 h of migration and the scratch area was quantified using ImageJ. After thresholding the populated area, the remaining cell-free area was measured and normalized to t_0.

2.2.12 Golgi orientation assay

To determine the cells' ability to polarize along the anterior-posterior axis, the position of the Golgi apparatus was visualized after distinct time points. Cells were seeded into silicone cell culture chambers (Figure 2.1) on cover slips and the next day they were infected for 24 h with MOI 3 or left uninfected. After another 24 h, cell culture inserts were removed with sterile forceps to start polarization and the cells were covered with medium. After indicated time points, the cells were fixed for immunostaining with 2 % PFA for 30 min at RT. Inclusions and the Golgi apparatus were immunostained and the samples were analyzed via confocal microscopy. The number of polarized border cells was quantified as follows. Each cell was divided into three sections of 120 ° spanning from the nucleus, one section facing the cell border. A cell was scored as polarized if more than half of the visible Golgi signal localized within 120° section perpendicular to the border (Figure 2.3).

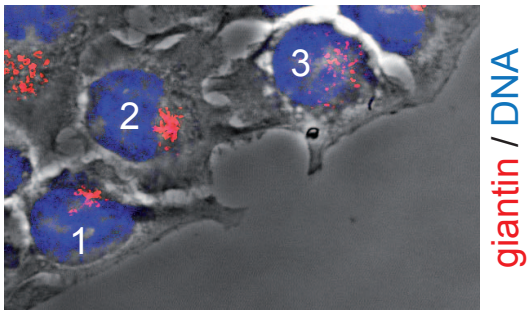

Figure 2.3: Quantification of cell polarization. Representative confocal microscopy image illustrating three scoring categories. A cell was defined as correctly polarized if the majority of the Golgi apparatus faced the cell border within 120 °, spanning from the nucleus. 1: Incorrect orientation. 2: Correct orientation. 3: Fragmentation without orientation. Red: giantin; blue: DRAQ5.

2.2.13 Precipitation of active Cdc42

To isolate the active, GTP-bound fraction of cellular Cdc42, it was precipitated with the help of bead-coupled Rac/Cdc42-binding (PBD) domain of PAK kinase provided with the Rac/Rho/Cdc42 Activation Assay Kit. Cells were seeded into 15 cm cell culture dishes and grown to 70 % confluency. The infected samples were infected with MOI 3 for 24 h. The cell layer was scratched 20 times horizontally, vertically and diagonally to induce migration. After washing with medium, the cells were allowed to migrate for 90 min at 35 °C and 5 % CO_2.

Cell lysis was performed in the culture dishes on ice. First, the cells were washed twice with cold PBS before 1 ml ice cold lysis buffer containing protease and phosphatase inhibitors was added and left on the cells for 10-20 min. Lysates were collected by scraping and passed through a 27 G syringe. They were cleared from cell debris by centrifugation (10 min, 14.000 g, 4 °C) and the pellets were discarded. Cleared lysates were incubated with 40 μl PAK-1 PDB agarose beads for 1 h at 4 °C. After washing with lysis buffer, GTP-bound proteins were eluted by boiling in SDS sample buffer and subjected to Western Blot analysis.

2.2.14 Quantitative interaction proteomics

To compare sets of interaction partners of a protein in two different conditions, mass spectrometry after differential stable amino acid isotope labeling (SILAC, stable isotope labeling with amino acids in cell culture) is a state-of-the-art method yielding quantitative binding ratios (Paul et al., 2011). The overall work flow is depicted in Figure 3.22.

Labeling

Cells were cultured with SILAC labeling medium containing amino acid isotopes for 8 cell divisions. Half of the flasks received "light" (unlabeled) medium, the other half "heavy" (labeled) medium to later distinguish proteins from two conditions in one sample. Additionally, each experiment was performed once more with swapped labeling (the first version is named the "straight" experiment, the swapped version the "cross" experiment). A list of the samples and different conditions is given in Table 2.1.

A

	infected	
	GFP	**Cdc42-GFP**
"straight"	light	heavy
"cross"	heavy	light

B

	Cdc42-GFP	
	uninfected	**infected**
"straight"	light	heavy
"cross"	heavy	light

Table 2.1: Experimental conditions for interaction proteomics. A. The interaction partners of Cdc42-GFP in infected cells were compared to GFP only. **B**. The binders of Cdc42-GFP were compared in uninfected and infected cells. Each experiment was performed twice with swapped labeling ("straight", "cross").

Coimmunoprecipitation

Labeled cells were seeded into 15 cm culture dishes and grown to 60 % confluency. Infected samples were infected with MOI 3 for 30 h. 8 h post infection, all samples were transfected with a plasmid coding for Cdc42-GFP or GFP only. Each 15 cm-dish received 40 μg DNA. Cdc42-GFP or GFP only were coprecipitated together with interacting proteins from the labeled cells via GFP-Trap employing magnetic beads coupled to a GFP-binding nanobody (a single-domain antibody). 22 h post transfection, the cells were washed twice with ice cold PBS and the samples were kept on ice for the rest of the experiment. 2×10^7 cells were harvested in 2-3 ml

PBS with a cell scraper and pelleted at 14.000 ×g. They were resuspended in 250 μl lysis buffer, passed through a 26 G syringe and lysed for 30 min. with extensive pipetting every 10 min. The lysate was cleared from cell debris by centrifugation (20.000 g, 10 min, 4 °C) and the pellet was discarded. GFP was bound to magnetic beads for 2 h with shaking at 4 °C. Beads were washed and the lysates of two corresponding conditions (light/heavy) were pooled. Proteins were eluted with 100 μl elution buffer after which the eluates were neutralized to pH 7.5 with 1 M Tris pH 9.0. Proteins were then precipitated with sodium acetate, glycoblue precipitation enhancer and ethanol over night. Proteins were pelleted at 20.000 g and air dried. Aliquots were taken at critical steps of the protocol and the precipitation efficiency was checked via Western Blot analysis.

Mass spectrometry

The quantitative mass spectrometry analysis was done in collaboration with Florian Paul, MDC Berlin as described in Paul et al., 2011. In addition to the human database, the spectrometry data was aligned to the chlamydial database "*Chlamydia_ trachomatis_* 434_ Bu". To include potential bacterial interaction partners.

Data analysis

First, proteins binding to Cdc42-GFP in infected cells were identified. Proteins binding to GFP alone were deducted and the list was thresholded to eliminate background. The cutoff excluded proteins with low abundance (peptide count ≤ 3) and proteins only found in one of the experiments ("straight" or "cross"). Proteins from this list appearing in the second experiment (Table 2.1 B) were declared as specific binders.

2.2.15 Statistical data analysis

All data was taken from at least three independent experiments except for the interaction proteomics approach (2 experiments) and the live cell monitoring (representative experiment). Technical replicates were included to correct for internal variations. Depicted in the diagrams are mean values with standard errors. Statistical significance was determined using Student's T-test ($*$: p-value< 0.05; $**$: p-value< 0.01; $***$: p-value< 0.005).

3 Results

3.1 Molecular basis of *Chlamydia*-induced Golgi fragmentation

3.1.1 Inhibition of *Chlamydia*-mediated golgin-84 processing

Proteolytic processing of the Golgi matrix protein golgin-84 in cell infected with *Chlamydia* can be blocked by the commercially available tetrapeptide inhibitor WEHD. This inhibition subsequently prevents Golgi fragmentation and dramatically reduces the production of infectious bacterial progeny (Heuer et al., 2009). WEHD encompasses the amino acid sequence *Trp-Glu-His-Asp*, a recognition motif originally designed to bind the active center of caspase-1 (Garcia-Calvo et al., 1998). Although caspase-1 is modulated in *Chlamydia* infection (Abdul-Sater et al., 2009), there was evidence for the involvement of other proteases in the execution of *Chlamydia*-mediated golgin-84 processing which are sensitive to WEHD. For example, another well-established caspase-1 inhibitor, YVAD (*Tyr-Val-Ala-Asp*), did not inhibit Golgi fragmentation. Neither did knockdown of caspase-1 itself (personal communication). Since *Chlamydia* actively secretes several proteases into the host cell cytosol where they cleave numerous eukaryotic substrates, the protease in question could likely be a bacterial factor (Zhong, 2009).

To narrow down the number of candidate enzymes which could be acting on golgin-84, the cleavage process was explored more closely[1]. The degradation kinetics were characterized in a time course experiment. Golgin-84 degradation in infected cells was monitored with and without WEHD treatment. Cell lysates were harvested at definite time points post infection and analyzed via immunoblotting. In addition to golgin-84, the lysates were probed for the intermediate filament vimentin, a well-characterized proteolytic substrate of CPAF (Paschen et al., 2008).

Without inhibitor treatment, golgin-84 was cleaved into its described fragments in infected cells (Figure 3.1). The first, larger fragment of $\sim$78 kDa had appeared 18 h post infection (*p.i.*). After 30 h, the smaller, $\sim$65 kDa-fragment had been produced and the full length golgin-84 had disappeared completely. WEHD treatment of infected cells conserved the full length golgin-84 and only a minimal signal was detected of the larger cleavage product.

[1] This experiment was designed and analyzed in collaboration with Prof. Dr. Georg Häcker (Uniklinik Freiburg) and performed by Jan Christian (Uniklinik Freiburg).

Apart from this, the analysis showed that vimentin was degraded simultaneously with golgin-84. A cleavage product was produced from 18-24 h post infection. WEHD addition completely abrogated vimentin processing synchronously with golgin-84 stabilization. Vimentin has been previously reported to be degraded by the *Chlamydia* protease-like activity factor CPAF which is secreted around mid-cycle, namely after about 16 h of infection (Savijoki et al., 2008; Paschen et al., 2008; Zhong et al., 2001). Furthermore, CPAF secretion is detected during the same time frame in which Golgi fragmentation is established (16-28 h *p.i.*).

In conclusion, golgin-84 cleavage in infected cells coincided with that of vimentin, a known CPAF substrate and the time of CPAF secretion as reported in the literature. Both reactions could be inhibited by WEHD treatment. This suggests that CPAF mediates golgin-84 processing in *Chlamydia*-infected cells.

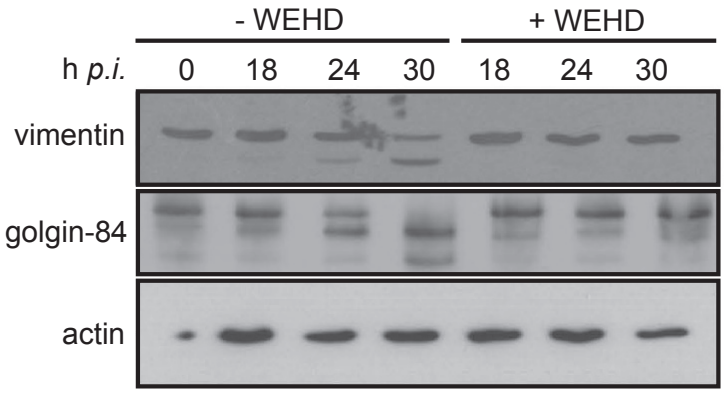

Figure 3.1: The influence of WEHD treatment on the proteolysis of golgin-84 and vimentin in infected cells. Western Blot analysis of cell lysates after different times of infection (h *p.i.*). 293T cells were infected (MOI 2) and WEHD (75 μM) was added 9 h *p.i.* Lysates were collected after indicated time points. Golgin-84 and vimentin were detected with specific antibodies. Generated in cooperation (see footnote 1) and modified from Christian et al., 2011.

3.1.2 Influence of caspase inhibitors on chlamydial development

The administration of WEHD not only inhibits golgin-84 processing but also severely hinders the development of *Chlamydia* (Heuer et al., 2009). To define the specificity of WEHD in this regard, its effect on the infection and reinfection capacity of *Chlamydia* was compared to three other caspase inhibitors (Figure 3.2).

The following tetrapeptides, designed to bind different kinds of caspases, were used in this experiment: WEHD particularly inhibits caspase-1, a member of the group I caspases that mediate inflammation processes by proteolytic activation of pro-inflammatory cytokines. Caspase-1 is

activated by signaling from the TNF (tumor necrosis factor) receptor. LEHD (*Leu-Glu-His-Asp*) specifically binds caspase-9, an apoptotic caspase of group III that is activated by cytochrome C release from mitochondria. Caspase-3 activity is blocked by DEVD (*Asp-Glu-Val-Asp*) and caspase-6 is inhibited by VEID (*Val-Glu-Ile-Asp*). Both are effector caspases that execute apoptosis by cleaving structural and homeostatic proteins. They are often activated via cleavage by other caspases (Garcia-Calvo et al., 1998; Thornberry, 1998).

The infection of HeLa cells with *Chlamydia* was compared in the presence of the four different inhibitors. Inclusions were visualized by immunostaining with an antibody raised against the chlamydial major outer membrane protein (MOMP). Both number and size of bacterial inclusions that had developed intracellularly at 24 h post infection was strongly reduced after WEHD treatment (Figure 3.2 A). The influence of VEID was less pronounced: VEID-treated cells contained smaller inclusions than untreated cells but the number of inclusions in this case remained comparable to that in untreated cells. Treatment with LEHD and DEVD had no effect on inclusion number or size.

A productive infection is defined by the production of new infectious EBs. The infectious bacterial progeny that was produced in HeLa cells after a complete developmental cycle (48 h) was determined per reinfection assay. After primary infection in the presence or absence of inhibitors, the *Chlamydia*-containing cells were lysed and titrated onto fresh, untreated cells. After another 24 h, the newly developed inclusions were immunostained and quantified. If WEHD or VEID had been added to the primary infection, only few inclusions were detected 24 h after reinfection (Figure 3.2 B). Namely, the relative infectivity was decreased to 3.5 % by WEHD and to 9.8 % by VEID. The other two peptides caused moderate reductions to 57 % (LEHD) and 62 % (DEVD).

In summary, these results confirm the inhibitory effect of the caspase-1 inhibitor WEHD on inclusion upgrowth and infectivity. When its impact was compared to that of other caspase inhibitors, only the caspase-6 inhibitor VEID induced a similar phenotype. The negative effect of VEID on chlamydial infectivity was similar to that of WEHD, while the reduction of the primary infection was less dramatic.

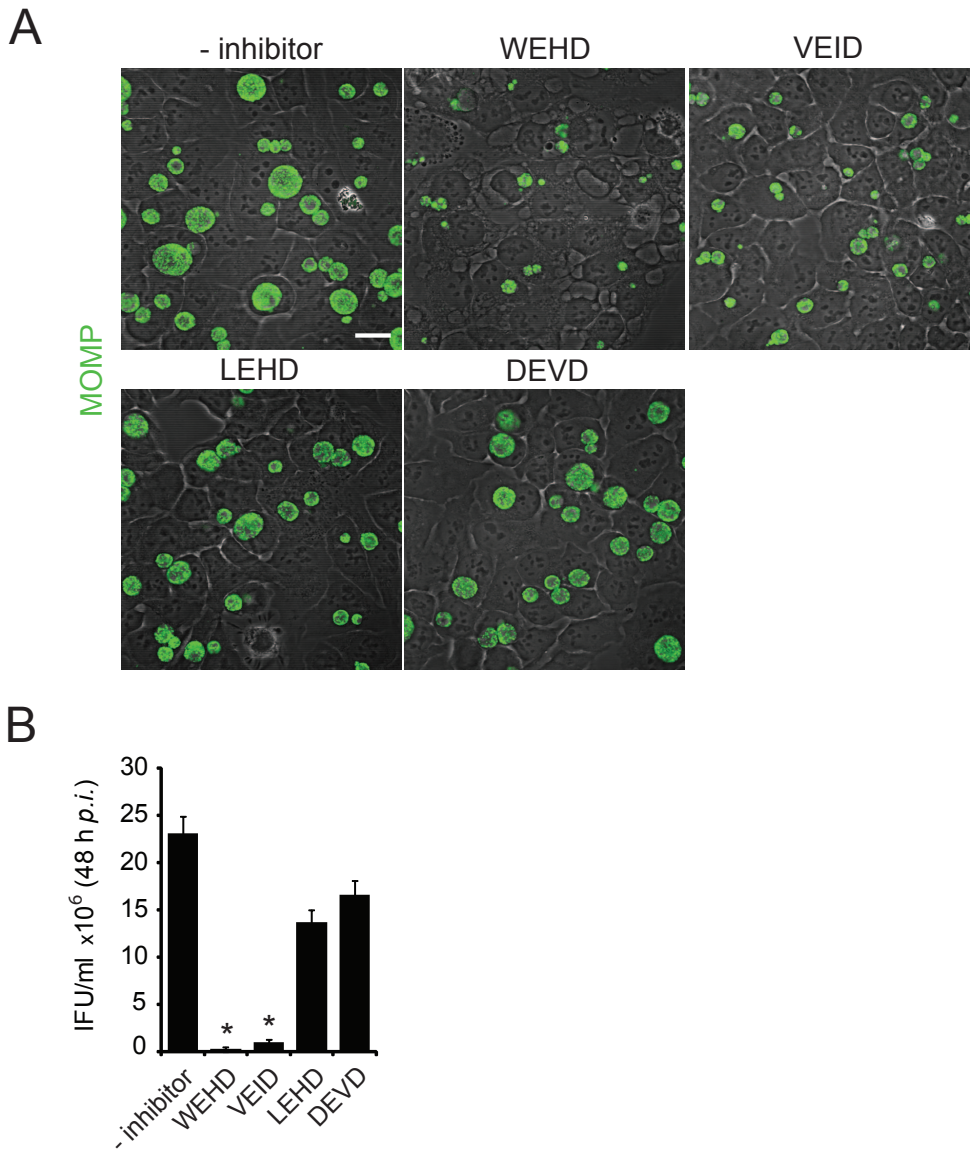

Figure 3.2: Effects of host cell caspase inhibition on *Chlamydia* development. **A**. Confocal microscopic images of infected HeLa cells. Cells were infected with a MOI of 3. Inhibitors (80 μM) were added 8 h later and cells were fixed 24 h post infection. Inclusions were immunostained with anti-MOMP antibody (false coloured green). Scale bar: 20 μm. **B**. Reinfection assay comparing the influence of caspase inhibitors on infectious bacterial progeny. HeLa cells were infected with a MOI of 3 and inhibitors (80 μM) were added after 8 h. Cells were harvested 48 h post infection, lysed mechanically with glass beads and titrated onto fresh, untreated HeLa cells. 24 h post re-infection, these cells were fixed and immunostained with anti-MOMP antibody. Inclusions of ten microscopic fields were counted to determine the number of inclusion forming units (IFU) per ml. Data taken from 3 independent experiments. Error bars: SEM.

3.1.3 Overexpression of chlamydial CPAF in uninfected cells

CPAF is a chlamydial protease that is translocated into the host cell and cleaves several host cell factors (Zhong et al., 2001; Pirbhai et al., 2006; Christian et al., 2010; Yu et al., 2010; Paschen et al., 2008; Dong et al., 2004; Kumar and Valdivia, 2008a). Its secretion temporally overlaps with Golgi fragmentation which suggests an involvement of CPAF in Golgi fragmentation. The question whether CPAF is directly involved in this process would usually be addressed by silencing the protein with an siRNA. But since no genetic system is available for *Chlamydia*, a knockdown of CPAF is not feasible and its relevance can not be defined by reverse genetics. To investigate if Golgi fragmentation directly depends on CPAF, it was ectopically expressed in uninfected cells from an inducible construct after transient or stable transfection. The effect of CPAF expression on Golgi structure was monitored by immunostaining of the Golgi markers GPP130 (Golgi phosphoprotein 130) or Giantin. Beforehand, an effect of the expression-inducing and activating agents had to be excluded.

Control treatment with anhydrotetracycline (AHT) and coumermycin (CM)

Prolonged expression of active CPAF has proven to be harmful for the cells which is why the transcription had to be controlled. The expression construct pcDNA4-gyrB-CPAF (Figure 2.2) contains a Tet repressor-controlled induction cassette to avoid undesired basal expression of CPAF (Paschen et al., 2008). Addition of AHT to the culture starts translation at defined time points. CPAF is synthesized as an inactive zymogen and is activated by dimerization. In the construct, this is controlled by a bacterial gyrase domain. Coumermycin supplementation initiates dimerization of CPAF via the gyrase domains and results in the active homodimer. Golgi morphology was assessed microscopically after addition of AHT and CM for 8 h (Figure 3.3). Treatment did not alter the structure of the Golgi apparatus. Therefore, these experimental conditions were applicable to investigate Golgi fragmentation.

Transient expression of chlamydial CPAF

To test whether ectopic CPAF expression can induce Golgi fragmentation in uninfected cells, pcDNA4-gyrB-CPAF was coexpressed with GFP (to identify transfected cells). In contrast to untreated cells, the Golgi apparatus was severely scattered in CPAF-expressing cells (Figure 3.4). This resembled the morphology observed after infection, where the Golgi ministacks are furthermore relocated around the inclusion (Figure 1.6, Heuer et al., 2009). In WEHD treated cells, the Golgi apparatus remained compact and stable despite CPAF expression.

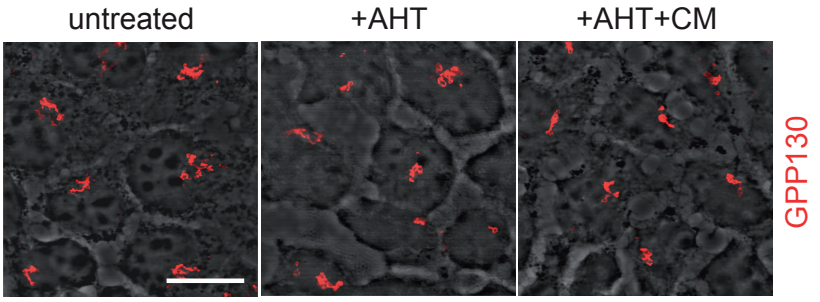

Figure 3.3: Golgi morphology after AHT and CM treatment. HeLa cells were treated with anhydrotetracycline (AHT, 5 ng/μl.) and coumermycin (CM, 1 μM.) for 8 h. Golgi structure was visualized by immunostaining of GPP130 (red). Scale bar: 20 μm. Images by Anja Greiser.

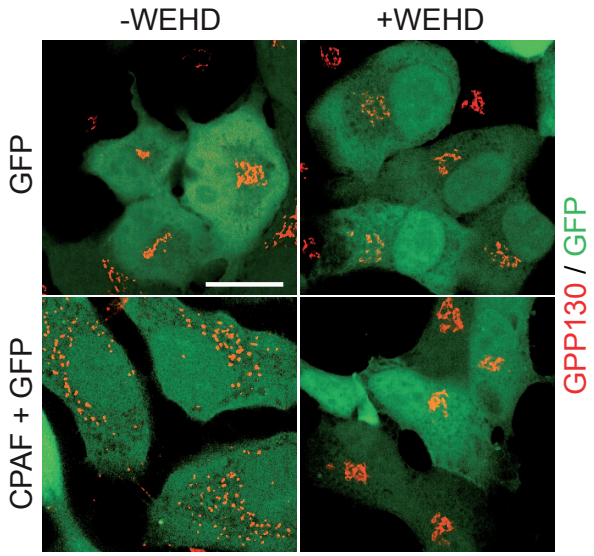

Figure 3.4: Golgi morphology after ectopic expression of active CPAF. Confocal images of HeLa cells transiently expressing CPAF. Cells were cotransfected with gyrB-CPAF and GFP or transfected with GFP only. CPAF was induced and activated 8 h post transfection by addition of 5 ng/μl AHT and 1 μM CM, WEHD treatment (80 μM) was started simultaneously. Morphology of the Golgi apparatus was visualized 48 h post induction by immunostaining of GPP130. Red: GPP130; green: GFP expression. Scale bar: 20 μm.

Stable expression of chlamydial CPAF

In addition to the transient expression of the bacterial protease described above, the analysis of Golgi architecture was repeated in an inducible cell line (T-REx-293-gyrB-CPAF) stably expressing CPAF (Figure 3.5). Once more in the absence of infection, induction and activation of CPAF led to a scattered Golgi appearance. WEHD treatment of these cells restored the compact Golgi morphology, resembling the structure present in control cells where the CPAF construct was present but protein expression had not been induced.

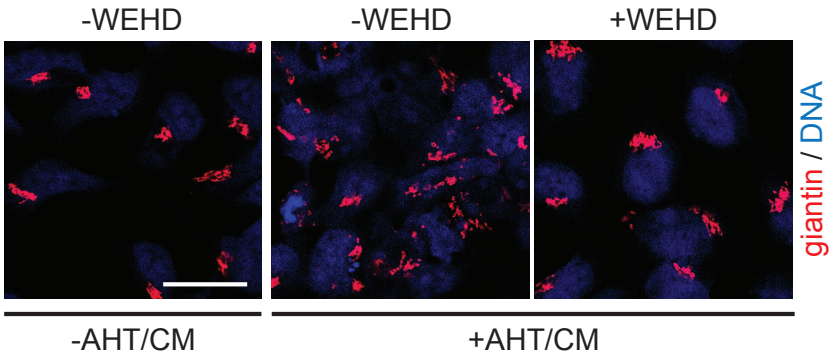

Figure 3.5: Golgi morphology in a CPAF expressing cell line. Confocal images of a 293T cell line expressing CPAF (T-REx-293-gyrB-CPAF). Expression and activation of CPAF were induced by addition of AHT and CM, WEHD was added simultaneously. After 5 h of induction, cells were fixed and immunostained to visualize the Golgi apparatus. Red: giantin; blue: DNA stain (DRAQ5). Scale bar: 20 μm.

Golgin-84 processing in CPAF expressing cells

To confirm whether golgin-84 and vimentin were processed in the CPAF expressing cell line, lysates of T-REx-293-gyrB-CPAF cells were harvested after different induction intervals and subjected to Western Blot analysis (Figure 3.6). After CPAF activation, processing of both proteins was detected, similar to what is observed in infected cells.

Taken together, the overexpression experiments demonstrate that the presence of active chlamydial CPAF alone, be it transient or stable, is able to cause fragmentation of the Golgi apparatus. WEHD addition prevented Golgi fragmentation in infected cells as well as in CPAF-expressing cells (stable and transient). In the CPAF expression cell line, golgin-84 and vimentin are cleaved in a similar manner compared to infected cells.

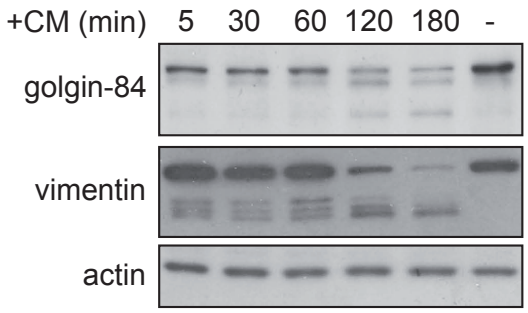

Figure 3.6: Proteolysis of golgin-84 and vimentin in CPAF expressing cells. Western Blot analysis of lysates from 293T cells expressing active CPAF. Expression was induced with AHT for 16 h. CPAF was activated by CM and cells were harvested at time points indicated. Golgin-84 and vimentin were detected via specific antibodies. Generated in cooperation (see footnote 1) and modified from Christian et al., 2011.

3.1.4 The role of Rab GTPases in CPAF-mediated Golgi fragmentation

Golgi fragmentation is a prominent characteristic of infected cells. It can be induced in uninfected cells by depletion of golgin-84 via RNA interference (Heuer et al., 2009). Recently, golgin-84 dependent Golgi fragmentation has been shown to involve two more host cell proteins: The small GTPases Rab6 and Rab11 (Rejman Lipinski et al., 2009). Rab6 controls retrograde vesicle transport from the Golgi to the ER, while Rab11 is found on recycling endosomes (White et al., 1999; Ullrich et al., 1996). In infected cells, Rab6- and Rab11- decorated vesicles are recruited to the bacterial inclusion and both Rab proteins are important for chlamydial propagation (Rzomp et al., 2003). Knockdown of either one prevents Golgi disruption caused by *Chlamydia* infection or golgin-84 depletion, presumably because they control membrane dynamics required for this reorganization (Rejman Lipinski et al., 2009).

To evaluate the role of Rab6 and Rab11 in CPAF-induced Golgi fragmentation, both Rab proteins were silenced in a siRNA approach and Golgi morphology was investigated after expression of active CPAF (Figure 3.7). Western Blot analysis confirmed decreased protein levels (Figure 3.7 A). The structure of the Golgi apparatus in CPAF expressing cells previously depleted for Rab6 or Rab11 was assayed microscopically after immunostaining. Extensive fragmentation was observed in control cells expressing active CPAF and transfected with a luciferase control siRNA (Figure 3.7 B). But after either Rab6 or Rab11 silencing, the organelle was stabilized despite the presence of active CPAF.

These findings indicate that Golgi fragmentation after CPAF expression is Rab6- and Rab11-dependent. Thus, CPAF-induced Golgi fragmentation does not only display an inhibitable phenotype highly similar to *Chlamydia*-caused Golgi fragmentation, it furthermore shares the same characteristic Rab dependency. Therefore, the two processes could be analogous or identical.

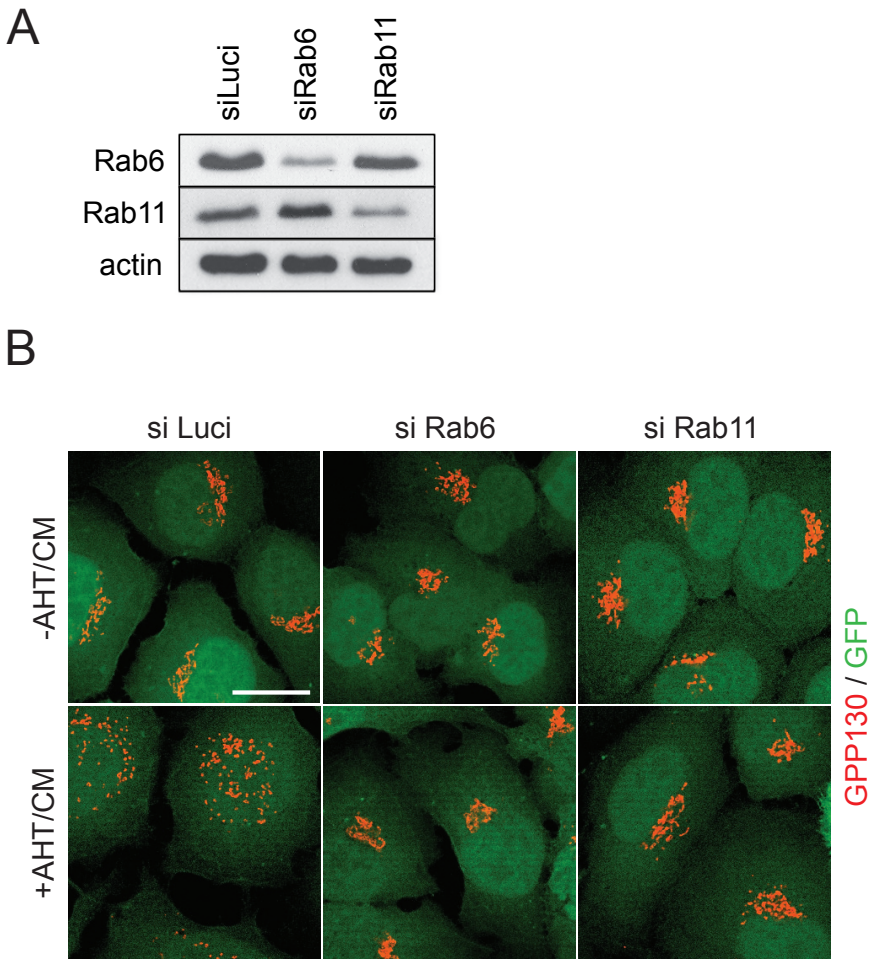

Figure 3.7: Golgi morphology after CPAF expression in Rab-depleted cells. A. Western Blot analysis of HeLa cells depleted for Rab6 or Rab11. Cells were transfected with specific siRNAs for Rab6, Rab11 or luciferase control siRNA and grown for 72 h. After lysis, equal amounts of total protein were blotted and probed with specific antibodies to compare protein levels. **B**. Confocal microscopic images of cells after knockdown of Rab6 or Rab11 and consecutive expression of active CPAF. HeLa cells were transfected with siRNAs specific for Rab6, Rab11 or luciferase. After 48 h, gyrB-CPAF was cotransfected with GFP to label transfected cells. CPAF was induced and activated by addition of AHT and CM 4 h post transfection. Cells were fixed 48 h post transfection (44 h post induction) and immunostained to visualize Golgi morphology. Red: GPP130; green: GFP. Scale bar: 20 μm.

3.2 Consequences of *Chlamydia*-induced Golgi fragmentation for higher-order cell functions

3.2.1 Anterior-posterior polarization of *Chlamydia*-infected cells

The determination of the preconditions for infection-mediated Golgi fragmentation raised the question about possible consequences for the host cell. The massive change of Golgi architecture inflicted by *Chlamydia* likely has a profound impact. The highly organized structure of the Golgi apparatus is important for its functions, for example cargo processing and directed secretion (Lowe, 2011). Moreover, alterations of Golgi architecture can affect superordinate cellular processes including cell polarization and migration on a planar surface. During the polarization of a cell, the Golgi apparatus and MTOC are placed anterior to the nucleus to allow directed secretion and efficient cell migration (Figure 1.8). Golgi fragmentation after depletion of golgins was recently reported to hinder polarization and directed cell movement (Yadav et al., 2009). This suggested inquiring the polarization ability of infected cells.

The reorientation of the Golgi apparatus towards a certain direction was monitored over time. HeLa cells were seeded into culture chambers which were later removed to allow migration (Figure 2.1). The average position of the Golgi apparatus was determined, whereby a cell was defined as properly polarized if the Golgi apparatus localized within an angle of 120° spanning from the nucleus and facing the cell border (Figure 2.3).

Immunostaining of the Golgi marker giantin and the chlamydial heat shock protein 60 (Hsp60) showed that in almost all uninfected cells, the Golgi apparatus had been relocated anterior to the nucleus facing the target direction after 4 to 6 hours of migration (Figure 3.8 A). In contrast, the fragments of the Golgi apparatus in infected cells associated to the bacterial inclusion and did not preferably orient towards one direction. After 6 hours, the polarization phase of the uninfected cells was completed and 80 % of the cells harbored a correctly oriented Golgi apparatus (Figure 3.8 B). The fraction of polarized infected cells meanwhile did not exceed 30 %, a value corresponding to the stochastic percentage of Golgi apparatuses oriented in migration direction at the beginning of the experiment (initially, the Golgi orientation is randomly distributed between the 360° of a roundish cell and one third of the cells already fulfill the criteria of a "correct orientation").

In summary, this result demonstrates that *Chlamydia* infection accompanied by Golgi fragmentation hinders reorientation of the Golgi apparatus after a migratory stimulus.

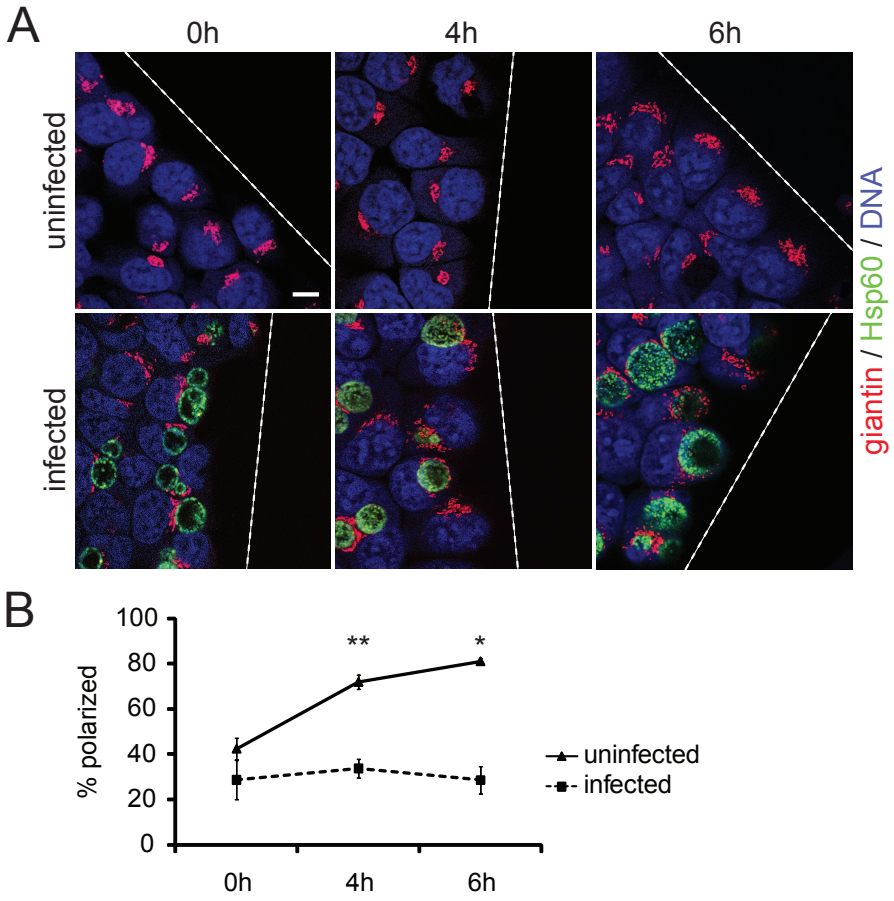

Figure 3.8: Polarization of uninfected and infected cells. A. Confocal images of polarizing HeLa cells. Cells were seeded into cell culture chambers and infected with a MOI of 3. 24 h post infection, chambers were removed and cells were allowed to polarize for times indicated. Cells were fixed and stained with specific antibodies against chlamydial Hsp60 and the Golgi matrix protein giantin to visualize the position of the Golgi apparatus. Red: giantin; green: Hsp60; blue: DRAQ5. Cell layer border indicated by a dashed line. Scale bar: 20 μm. **B**. Quantification of polarized uninfected or infected cells. Cells were scored as polarized if the Golgi apparatus localized within 120° perpendicular to the cell layer border. Data taken from three independent experiments. Error bars: SEM.

3.2.2 Polarization of infected cells after WEHD treatment

The fragmented Golgi apparatus of infected cells could not be reoriented in migration direction. Because the tetrapeptide WEHD can inhibit *Chlamydia*-induced golgin-84 processing and Golgi fragmentation, it was tested if treatment could improve polarization of *Chlamydia*-infected cells. Confocal images of migrating infected cells treated with WEHD, as expected, showed smaller inclusions and stable Golgi architecture (Figure 3.9 A). Moreover, the orientation of the Golgi apparatus, as measured in relation to the nucleus, was almost entirely restored (Figure 3.9 B). This shows that Golgi stabilization by WEHD treatment can rescue the polarization of infected cells.

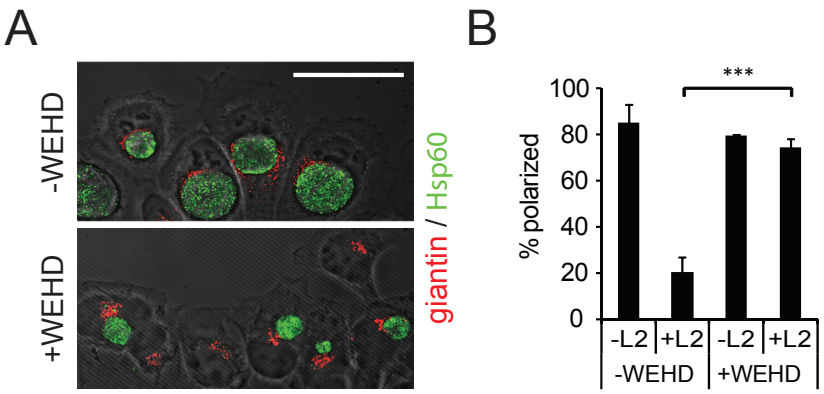

Figure 3.9: Polarization of infected cells after WEHD treatment. A. Confocal images of cells after 6 h of polarization. Cells were infected (+L2) with a MOI of 3 for 24 h. Inhibitor treatment was started 8 h post infection (+WEHD). 24 h post infection, culture inserts were removed. Cells were fixed and immunostained 6 h after removal to visualize the position of the Golgi apparatus. Red: giantin, green: Hsp60. Scale bar: 20 μm. **B**. Quantification of polarized cells. Cells were scored as polarized if the Golgi apparatus localized within 120° perpendicular to the cell border, spanning from the nucleus. Data taken from three independent experiments. Error bars: SEM.

3.2.3 Migration of *Chlamydia*-infected cells

Cell polarity, in this case the correct alignment of organelles towards the leading edge, is a prerequisite for directional cell movement (Kupfer et al., 1982). The incapacity for front-to-back polarization could therefore result in disturbed cell migration of infected cells. In order to assess the consequences of *Chlamydia* infection for host cell migration, infected and uninfected cells were compared in an *in vitro* scratch assay (Figure 3.10).

The ability of cells to close a scratch wound of the monolayer introduced by a sterile pipet tip was followed via time-lapse scratch area measurement. While uninfected cells completely

repopulated the cell-free area within a period of 24 h, the migration of infected cells was severely impaired (Figure 3.10 A). After application of low or moderate infectious doses (up to MOI 2), the scratch wound was partially closed by migration. In these samples, only uninfected cells migrated into the scratch area (Figure 3.10 B). At high infectious doses (MOI 3-5), hardly any migration into the original scratch was left. Quantification of this effect showed that the relative remaining cell-free area continuously correlated with the applied MOI (Figure 3.10 C).

This data shows that *Chlamydia* infection not only disturbs cell polarization but also consequently abrogates *in vitro* cell migration into an applied scratch wound in a MOI-dependent manner.

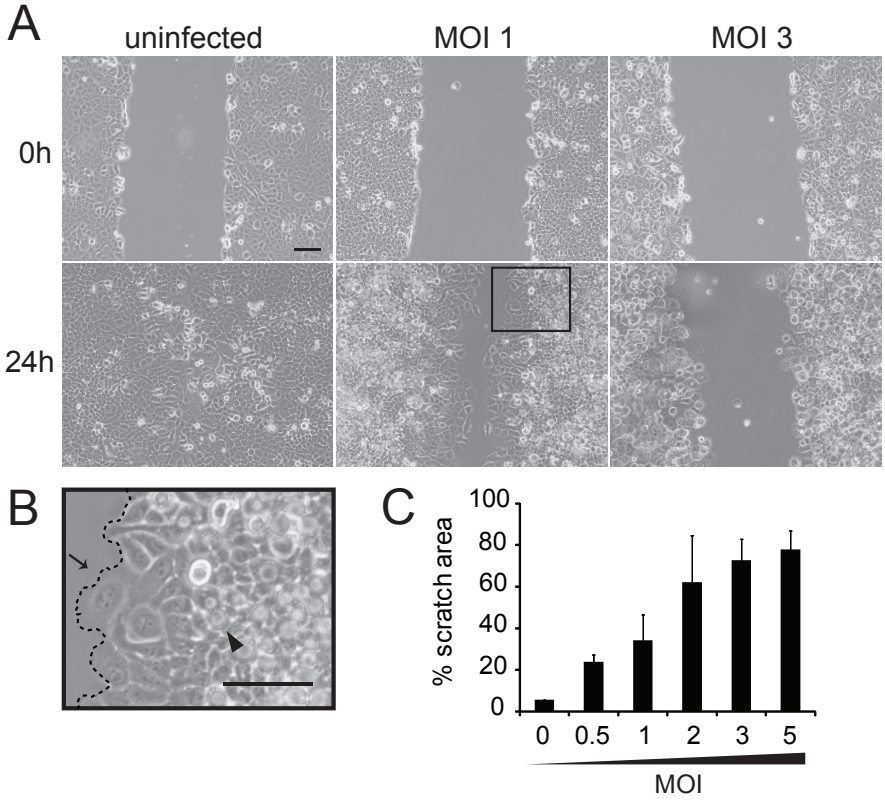

Figure 3.10: Cell migration after *Chlamydia* infection. **A**. *In vitro* scratch assay of uninfected and infected HeLa cells. Cells were treated with different infectious doses (MOI indicated) for 24 h before scratching the cell layer with a sterile pipet tip. Cells were allowed to migrate for 24 h. Scale bar: 100 μm. **B**. Enlargement of a section of A showing migrating border cells (border indicated by dashed line). Arrow: representative uninfected cell; arrowhead: representative inclusion. Scale bar: 100 μm. **C**. Quantification of remaining cell-free area after 24 h normalized to 0 h. Cells were infected with increasing MOIs for 24 h before scratching. Data taken from three independent experiments done in triplicate. Error bars: SEM.

3.2.4 Cell migration after WEHD treatment

Since Golgi stabilization with WEHD rescued polarization of infected cells (Figure 3.9), it was intended to investigate whether it could as well restore their migration. Beforehand, it was tested whether WEHD alone had an effect on cell motility.

WEHD treatment considerably slowed down migration of uninfected cells in a dose-dependent way (Figure 3.11). The scratch assay adds 24 h to all experimental procedures which results in an exceptionally long duration of inhibitor treatment (nearly 40 h compared to the usual 16 h). After this prolonged treatment, the cells furthermore exhibited signs of cellular stress. Thus, WEHD treatment would mask migration effects of infection and is not feasible in this long-term experimental setting. Therefore, the effect of CPAF inhibition by WEHD on the migration of infected cells could not be investigated.

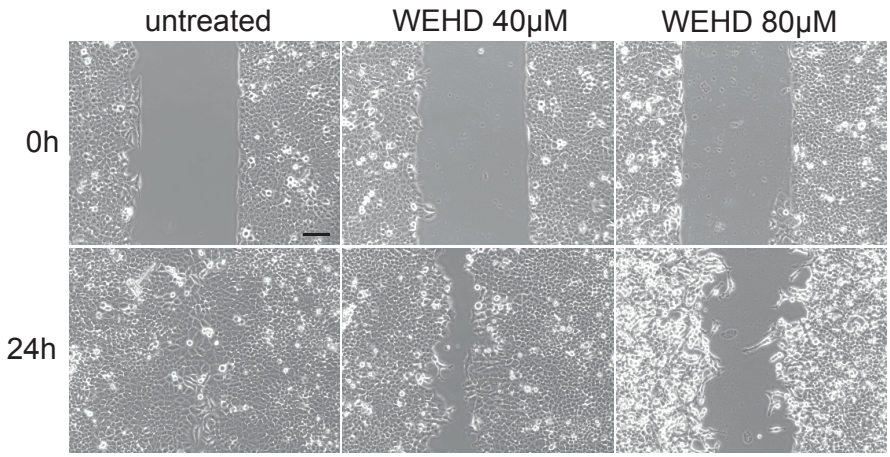

Figure 3.11: Cell migration after WEHD treatment. *In vitro* scratch assay with and without the CPAF inhibitor WEHD. Cells were mock-infected and WEHD was added 8 h later. After 24 h, the cells were scratched and allowed to migrate for 24 h. Scale bar: 100 μm.

3.2.5 Influence of proliferation on the *Chlamydia*-induced migration defect

The capability of cultured cells to close a scratch in the monolayer likely depends not only on migration but also on cell proliferation. To exclude the bias of varying proliferation rates, the *in vitro* scratch assay was performed in the presence or absence of the cytostatic agent mitomycin C. This reagent was shown to block cell proliferation but has no effect on cell viability or migration (Kanazawa et al., 2010).

The migration defect of infected cells showed no significant difference whether or not mitomycin C was present (Figure 3.12). The scratch was closed completely by treated and untreated uninfected cells alike. Infected cells repopulated 49.3 % of the scratch without inhibition and 61.7 % with inhibition of proliferation. This difference lay within the usual range of deviation and was therefore not significant. Thus, the influence of *Chlamydia* infection on cell motility in this model is not significantly influenced by cell proliferation.

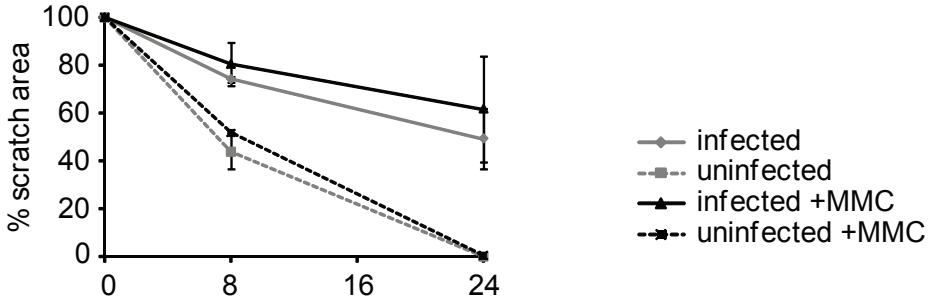

Figure 3.12: Migration of infected and uninfected cells after inhibition of proliferation. Quantification of relative remaining scratch area. HeLa cells were infected with a MOI of 3 for 24 h. 4 μg/ml of the cytostatic agent mitomycin C (MMC) was added 2 h post infection. Cells were scratched and after 24 h of migration, cell-free area was quantified from light microscopic images. Data taken from two independent experiments done in triplicate. Error bars: SEM.

3.3 Phenocopy of infection-induced effects by knockdown-stimulated Golgi fragmentation

3.3.1 Migration of golgin-84 depleted cells

After characterizing the disturbed cell polarity of infected cells, the role of Golgi fragmentation in migration was investigated more closely. For this purpose, a cell line stably depleted of golgin-84 was employed which features a permanently fragmented Golgi apparatus (Heuer et al., 2009). This made it possible to look at the consequences of Golgi disruption independently from infection.

The migration of golgin-84 depleted cells was compared to that of a control cell line in an *in vitro* scratch assay. Interestingly, knockdown-induced Golgi fragmentation provoked a similar migration phenotype to *Chlamydia* infection (Figure 3.13). Only 60 % of the original cell-free area was repopulated after 20 h while 92 % of the scratch area was closed by the control cells (Figure 3.13 A+B). This showed that cells with a fragmented Golgi apparatus have a migration defect, regardless whether the fragmentation is induced by golgin knockdown or infection. In quantitative terms, the extent of the defect after golgin-84 silencing was not as strong as in infected cells. It corresponded to that of moderately infected cells (MOI 1, see Figure 3.10).

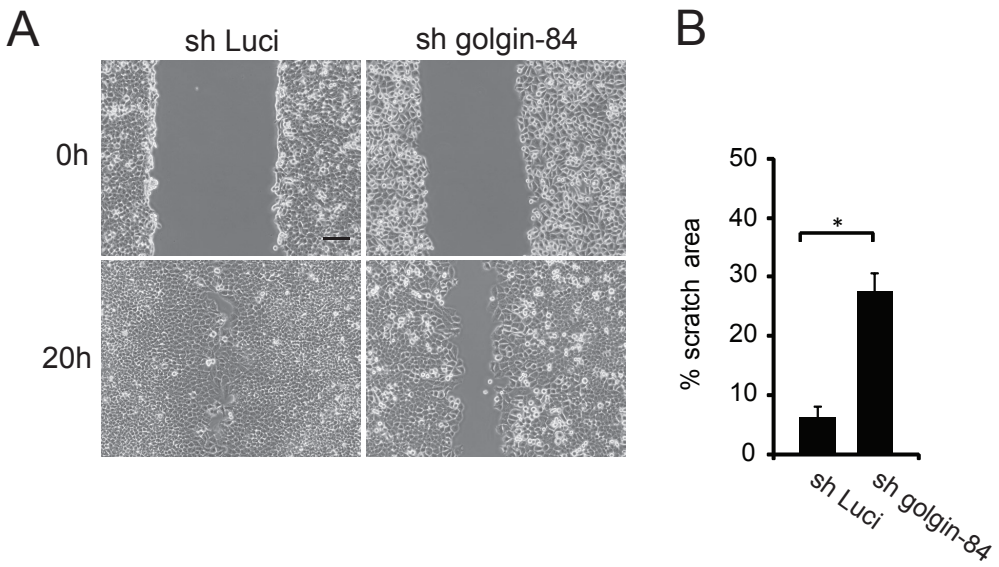

Figure 3.13: Migration of a golgin-84 depleted stable cell line. A. *In vitro* scratch assay comparing the migration of a HeLa cell line stably depleted for golgin-84 (sh golgin-84) to control cells (sh Luci). Cells were scratched and allowed to migrate for 20 h. Scale bar: 100 μm. **B**. Quantification of remaining scratch area after 20 h of migration. Data taken from three independent experiments done in triplicate. Error bars: SEM.

3.3.2 Polarization of golgin-84 depleted cells

The impact of golgin-84 dependent Golgi disruption on cell polarization was investigated in a Golgi reorientation assay and proved to be even more prominent than the influence on migration (Figure 3.14). In the stable knockdown cells, the Golgi apparatus was scattered and showed no tendency to align towards the leading edge. The fraction of polarized knockdown cells amounted to 39 % which was considerably less than in control cells (78.3 %). Together with the results from the *in vitro* scratch assay, this demonstrates that Golgi fragmentation by golgin-84 depletion phenocopies infection concerning its effects on cell polarization and, partly, migration.

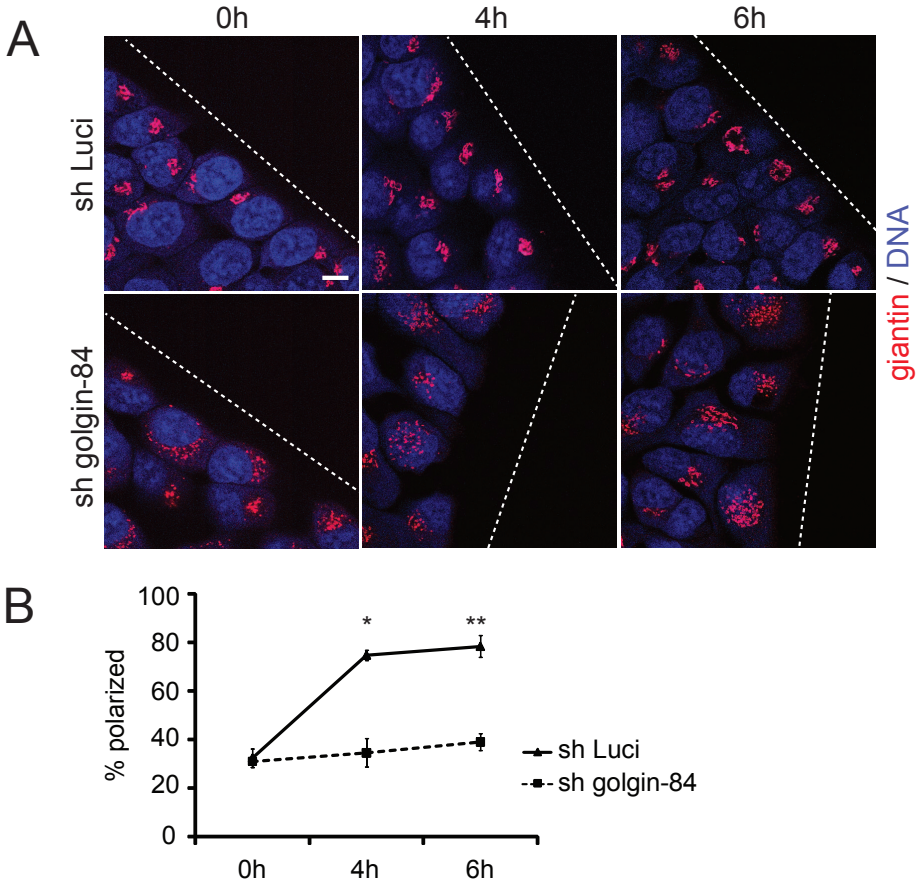

Figure 3.14: Polarization of a golgin-84 depleted stable cell line. A. Confocal images of cell lines stably depleted for golgin-84 (sh golgin-84) or control shRNA (sh Luci). Cells were seeded into culture chambers and migration was started by chamber removal. After times indicated, cells were fixed and immunostained to visualize the position of the Golgi apparatus. Red: Giantin; blue: DRAQ5. Scale bar: 20 μm. Cell layer border is indicated by a dashed line. **B**. Quantification of polarized cells. Cells were scored as polarized if the Golgi apparatus localized within 120° perpendicular to the cell border. Data taken from three independent experiments. Error bars: SEM.

3.3.3 Migration speed and efficiency of cells with a fragmented Golgi apparatus

Surveying migrating cells at discrete intervals might miss gradual progression of the phenotype in between time points. Cell movement is not always uniform and static images do not represent the manner of locomotion that leads to a certain displacement. To follow cell motion more precisely and along the entire experimental period, the cells were examined via live cell microscopy.

Figure 3.15 shows representative images taken from different live cell movies. Cells were monitored for 24 h, with single images acquired every 4 min. For standardization reasons, silicone chambers were used for cell culture. While processing the microscopic data, individual cells at the edge of the monolayer were marked and followed until the time point when the control cells had completed closing the gap (16 h). The coordinates were connected to result in a line-shaped track.

The tracks of uninfected control cells portray a directed movement in one direction, ending at the center of the gap, where both cell fronts meet after 16 h (Figure 3.15 A+B). At this time the cells had covered an average physical distance of 170.5 μm, while the infected cells had only moved about 22.7 μm. Also the golgin-84 knockdown cell line migrated significantly less that the control cells, although better than the infected cells (92.6 μm). Quantitation of mean velocities showed that control cells migrated 6.3 times faster (9.5 μm/h) than infected cells (1.5 μm/h) and 1.6 times as fast as golgin-84 silenced cells (5.9 μm/h).

Strikingly, the tracks of cells missing golgin-84 were not only shorter but also less linear than those of control cells. This means that these cells did not cover the total distance in the shortest possible way. This directionality of movement can be quantified by dividing the net displacement (vector length from starting point to end point) by the total track length (Lauffenburger and Horwitz, 1996). The more this coefficient approaches 1, the more does the route resemble a straight line. The result of this calculation shows, that both kinds of Golgi-fragmented cells migrated less efficient than control cells (Figure 3.15 C).

In total, the data indicates that cells with a fragmented Golgi apparatus migrate not only slower but also less directed than cells with a stable Golgi apparatus. Golgi fragmentation brought about by infection drastically reduces speed and directionality while knockdown of golgin-84 impairs directionality to a greater extent than migration velocity.

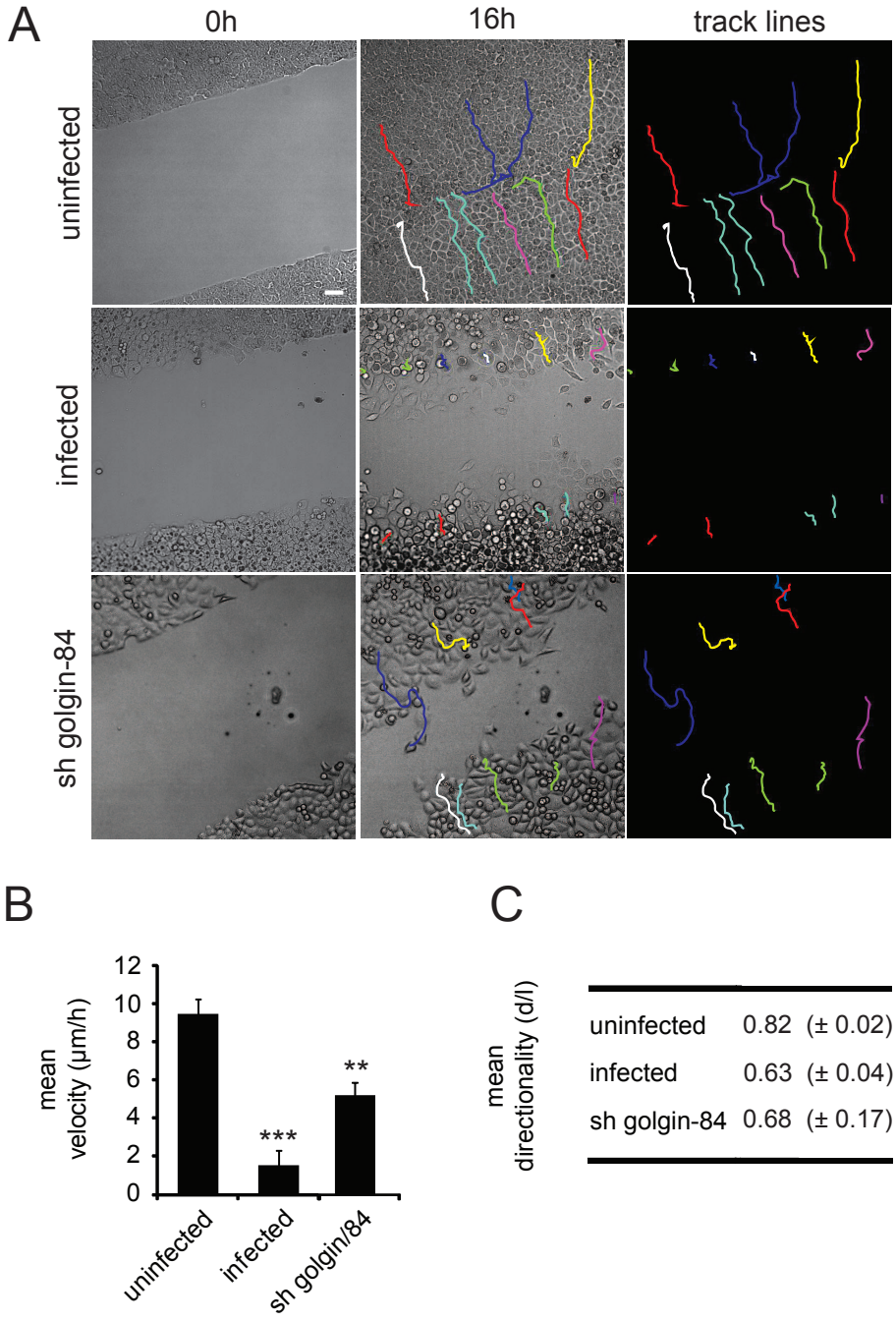

Figure 3.15: Live tracking of migration of cells after infection or golgin-84 depletion. A. Representative microscopic images from live cell movies. HeLa cells stably depleted for golgin-84 (sh golgin-84) and uninfected and infected control cells (sh Luci) were seeded into culture chambers. After chamber removal, 50 ng/ml EGF were added to globally accelerate migration. Images were acquired every 4 min for 16 h which equaled the closing time point of control cells. Movement of individual border cells was monitored and visualized as track lines. Scale bar: 50 μm. **B**. Quantification of mean migration velocity of individual cells analyzed by measuring the distance covered between time points. Data taken from at least 9 individual cells per movie. Error bars: SD. **C**. Directionality of cell movement. The efficiency of migration was calculated by dividing the net displacement from start to end (d) by the total track length (l), whereby a coefficient of 1 equals a straight line. Calculation represents the mean of all evaluated tracks.

3.3.4 Polarization of golgin-84 knockdown cells after silencing of Rab proteins

Chlamydia-induced Golgi fragmentation can be counteracted via depletion of Rab6 or Rab11 (Rejman Lipinski et al., 2009). Furthermore, fragmentation induced by expression of chlamydial CPAF in uninfected cells is also Rab6- and Rab11 dependent (Figure 3.7 B). This raised the question, whether stabilization of the host cell Golgi apparatus by Rab knockdown could improve its reorientation in golgin-84 depleted cells.

A polarization assay was performed testing Golgi reorientation after different combinations of golgin-84 and Rab knockdowns (Figure 3.16). Control transfected and golgin-84 depleted cells were used for negative and positive controls, respectively, and the reorientation of the Golgi apparatus was assessed. Depletion of Rab6, Rab11 or both stabilized the structure of the Golgi apparatus despite golgin-84 depletion and almost fully rescued orientation towards the leading edge, whereby Rab11 appeared to be slightly more effective (Figure 3.16 A+B).

3.3.5 Polarization of infected Rab-deficient cell lines

To transfer this investigation to the infection model, cell lines stably depleted for Rab6 or Rab11 were used in a Golgi reorientation assay. Polarization was partially improved in infected, stably Rab11-depleted cells. 57 % of the cells were able to orient their Golgi apparatus. Rab6 knockdown did not significantly improve reorientation and only led to 48.1 % polarization of infected cells (Figure 3.17 A). A transient double knockdown of both Rab proteins also resulted in partial rescue but the two siRNAs induced no additive effect (Figure 3.17 B).

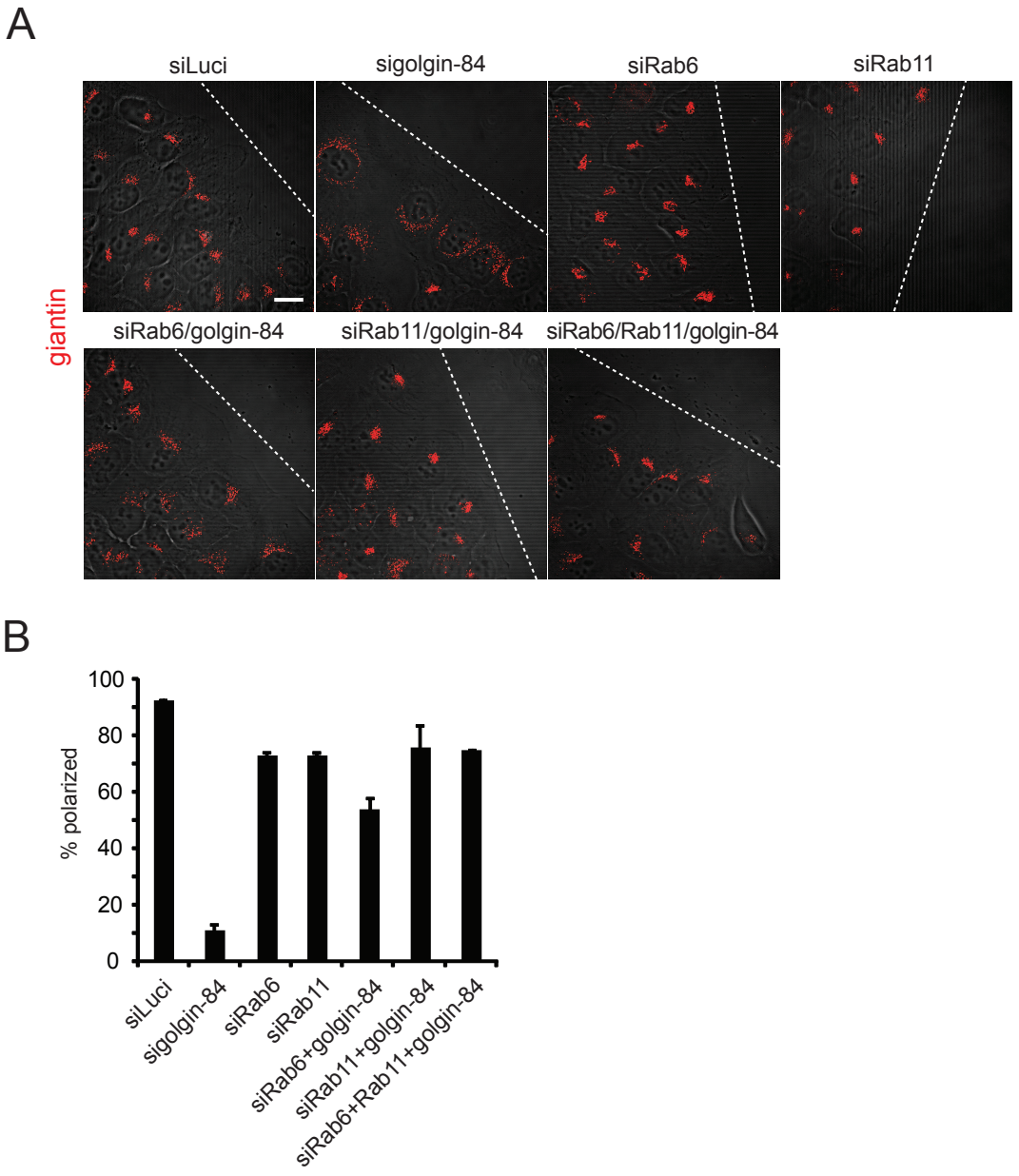

Figure 3.16: Golgi orientation after depletion of golgin-84 and Rab proteins. A. Confocal images of migrating HeLa cells deficient for golgin-84 and Rab GTPases. HeLa cells were transfected with specific siRNAs for Rab6, Rab11 or golgin-84, as well as combinations, or control luciferase siRNA. 72 h post transfection, cells were scratched and allowed to migrate for 6 h before fixing and immunostaining with a specific antibody against giantin (red). Scale bar: 20 μm. **B**. Quantitation of polarization in migrating knockdown cells. Cells with the Golgi apparatus distributed within a 120° angle perpendicular to the scratch were scored as polarized. Direction of migration: left to right. Data taken from three independent experiments. Error bars: SEM.

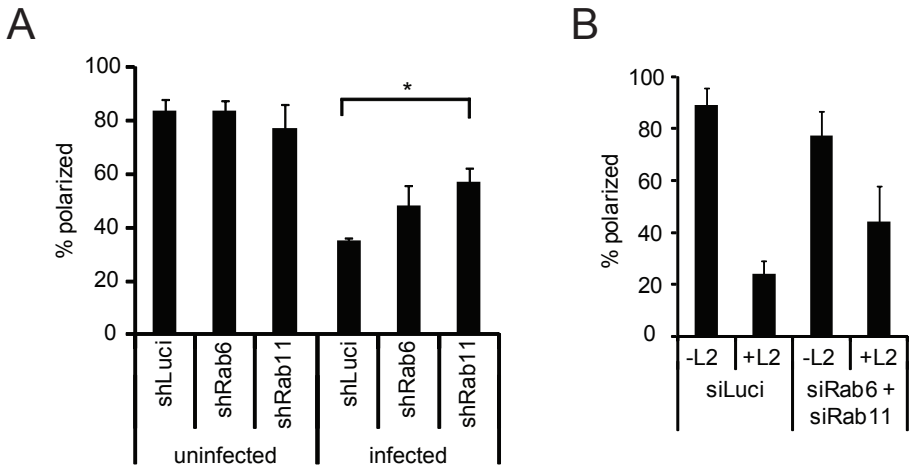

Figure 3.17: Polarization of infected Rab-deficient cell lines. A. Determination of polarization in infected Rab knockdown cell lines. HeLa cell lines, stably depleted for Rab6 (shRab6), Rab11 (shRab11) or luciferase (shLuci) were infected for 24 h (+L2) before scratching. Cells were fixed after 6 h of migration and immunostained to visualize the Golgi apparatus. Cells were scored as polarized if the Golgi apparatus located within a 120° angle facing the cell border. Data taken from 3 independent experiments. Error bars: SEM. **B**. Quantitation of the fraction of polarized cells after transient depletion of Rab6 and Rab11. HeLa cells were simultaneously depleted for both Rab proteins by transfection of two specific siRNAs (siRab6+siRab11) or transfected with a control siRNA (shLuci). After knockdown establishment, cells were infected with a MOI of 3 for 24 h before scratching. Data taken from 3 independent experiments. Error bars: SEM.

3.3.6 Cell migration after knockdown of Rab proteins

The polarization improvement after Rab knockdown in Golgi fragmented cells suggested monitoring migration of the shRab11 cell line after infection. In an *in vitro* scratch assay, infected cells lacking Rab11 migrated better than control cells. Only 20.2 % of the original scratch area was left after 24 h, compared to 70.6 % in infected control cells. The Rab11 knockdown itself had no significant effect on cell migration (Figure 3.18 A). Contrarily, when the Rab11 knockdown was achieved not by a stably integrated shRNA but by a transiently transfected siRNA, the migration of infected Rab11 knockdown cells was not improved (Figure 3.18 B). This was contradictory to the behavior of the stable cell line and not dependent on the amount of siRNA.

In summary, Golgi stabilization by depletion of either Rab6 or Rab11 rescued Golgi reorientation in uninfected golgin-84 knockdown cells. Polarization of infected cells could be significantly improved by Rab11 but not by Rab6 depletion and migration could be considerably improved in Rab11-depleted cells only after stable knockdown.

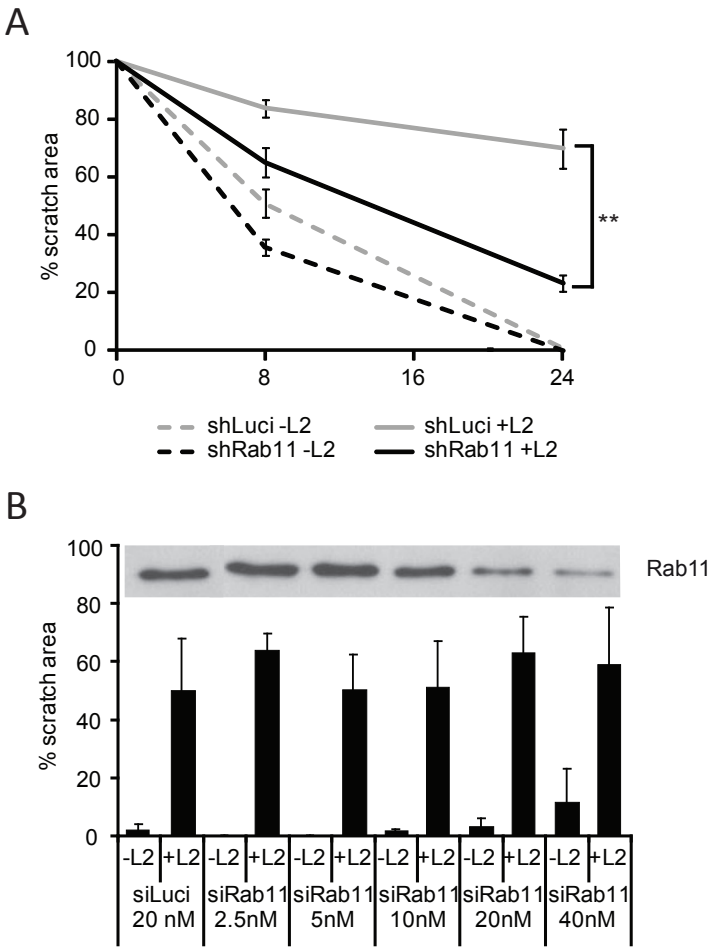

Figure 3.18: Migration of infected Rab11-deficient cells. A. Quantification of relative remaining scratch area. A HeLa cell line stably depleted for Rab11 (shRab11) or luciferase control cells (shLuci) were infected with a MOI of 3 (+L2) or left uninfected (-L2) for 24 h before migration was started. Scratch area was quantified from light microscopic images. Data taken from three independent experiments done in triplicate. Error bars: SEM. **B**. Quantification of remaining scratch area after transient knockdown of Rab11 via siRNA. Increasing amounts of siRNA were transfected and Rab11 protein levels were monitored by Western Blot analysis. Error bars: SEM.

3.4 Investigation of additional migration factors

3.4.1 Cytoskeletal elements of migration

Stabilization of the Golgi apparatus could restore the polarization of infected cells, meaning that the position of the organelle depends on its integrity. However, the migration behavior of stable golgin-84 knockdown cells and Golgi-stabilized Rab11 knockdown cells suggested that the *Chlamydia*-induced migration defect probably is of multifactorial nature. Golgi repositioning seems to be necessary but not sufficient for efficient cell migration. For this reason, other components of cell migration were studied to detect possible modifications caused by infection.

The most important aspects controlling cell movement are cytoskeletal rearrangement and protrusion formation. Massive reorganization of the host cell cytoskeleton by *Chlamydia* is likely to have consequences for cell motility (Kumar and Valdivia, 2008a). Microscopic monitoring of membrane protrusion assembly and immunostaining of cytoskeletal proteins in infected cells were done to gain insight about possible alterations in infected migrating cells (Figure 3.19).

In phase contrast images, migratory protrusions in the form of lamellipodia could be equally detected at the cell front of uninfected and infected cells (Figure 3.19 A). Staining of actin with a fluorescent version of the actin-binding toxin phalloidin illustrated polymerized actin typically observed at the cell front. This feature generally defines the leading edge of a migrating cell. Whether uninfected or infected, the cells possessed leading edges in equal abundance (Figure 3.19 A+B).

Another essential process is the transport of cargo to the leading edge along microtubules. To detect and compare tubulin structure, the cells were subjected to staining with an anti-tubulin antibody. The overall signal pattern in infected cells did not differ markedly, neither did the association of the microtubules to the MTOC which was visualized by pericentrin-specific immunostaining (Figure 3.19 A). Closer examination revealed association of microtubules to the bacterial inclusion. Also, the arrangement of the filaments appeared less organized and often did not reach to the very end of the lamellum, though the latter observation much depends on the microscopic plane of acquisition. All in all, infected and uninfected cells were equally able to form protrusions and a leading edge, contained a slightly modified microtubule network and normal MTOC.

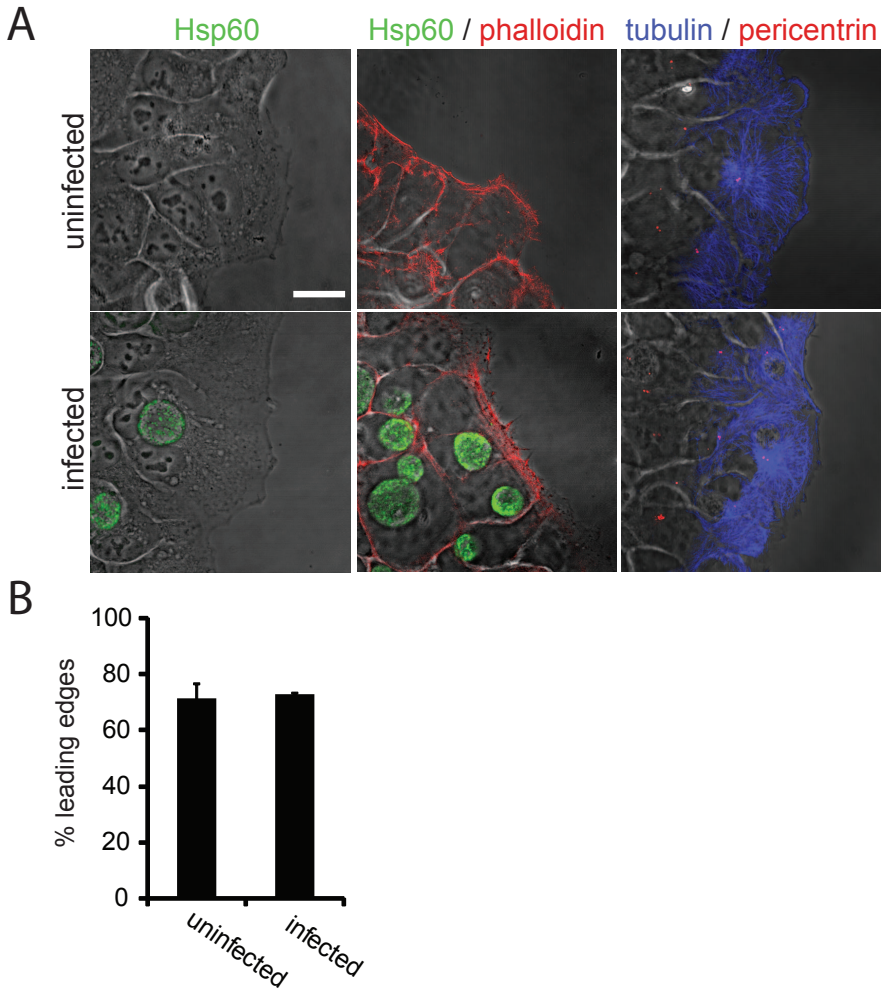

Figure 3.19: Cytoskeletal elements in uninfected and infected cells during migration. A. Confocal microscopic images of HeLa cells immunostained for several cytoskeletal components required for migration. Cells were infected with a MOI of 3 for 24 h before migration was started. After 6 h of migration, cells were fixed and immunostained with specific antibodies or fluorescent phalloidin (colour coding indicated). Scale bar: 20 μm. **B**. Quantification of formed leading edges at the anterior part of the cell membrane. Cells in confocal images were scored if they showed marked actin polymerization at the leading edge. Data taken from two independent experiments (n=100). Error bars: SD.

3.4.2 Activity of Cdc42 in *Chlamydia*-infected cells

The migratory response is governed by lots of preceding signaling events. The master regulators of migration signaling are the small GTPases Rac1, Cdc42 and RhoA (Ridley et al., 2003). While Rac1 induces cytoskeletal rearrangements and RhoA is involved in retraction of the cell rear, Cdc42 directly controls Golgi apparatus positioning (Nobes and Hall, 1999; Hehnly et al., 2010). A block in Cdc42 activation would explain why the Golgi apparatus is not positioned in infected cells.

To estimate the activity status of Cdc42, the GTP-bound fraction was isolated from cell lysates after induction of migration by scratch via precipitation with beads coupled to the PBD domain of PAK1. Western Blot analysis revealed more GTP-bound Cdc42 present in the infected samples (Figure 3.20). This shows that activation by GTP binding of Cdc42 is not blocked but, in fact, increased in infected cells.

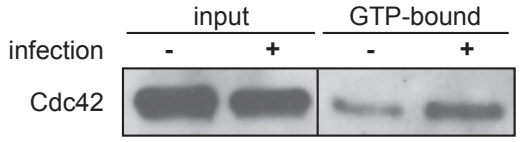

Figure 3.20: Amount of GTP-bound Cdc42 in uninfected and infected cells. Western Blot analysis after precipitation of GTP-bound Cdc42. HeLa cells were infected with a MOI of 3 for 24 h. After lysis, active Cdc42 was precipitated with PAK1-PBD agarose beads. Eluates were blotted and probed with a specific antibody.

3.4.3 Localization of Cdc42-GFP in in *Chlamydia*-infected cells

The dynamics of cellular GTPase are tightly regulated. Rho GTPases can be differentially recruited to specific subcellular locations and their spatial and temporal activation pattern determines the particular outcome (Spiering and Hodgson, 2011). This means that a measurement of the overall activity of a GTPase does not indicate where it is effective. Therefore, the localization of Cdc42 was followed via overexpression of a GFP fusion protein to compare its localization and look for changes after infection.

In migrating cells, active Cdc42 usually accumulates at the leading edge and the protein is generally also found at the Golgi apparatus (Machacek et al., 2009; Zhang, 1996). In transfected uninfected cells, Cdc42-GFP was present at the plasma membrane and leading edge as well as in the Golgi-associated region (Figure 3.21). In infected cells, the GTPase was additionally found in close proximity to the bacterial inclusion.

In conclusion, Cdc42- apart from being generally active - is furthermore not mislocalized after infection with *Chlamydia*. Furthermore, it can additionally be found in close proximity to the chlamydial inclusion.

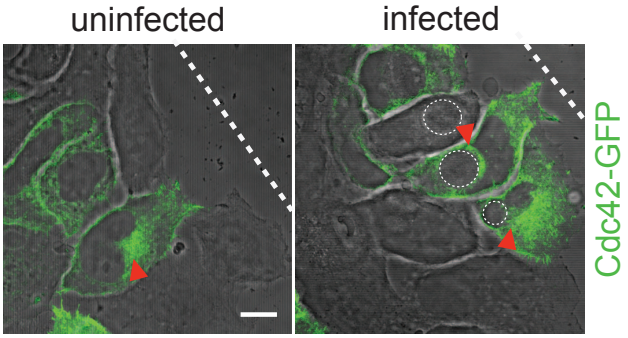

Figure 3.21: Localization of Cdc42-GFP in uninfected and infected cells. Confocal images of HeLa cells after expression of Cdc42-GFP. Cells were infected and transfected with Cdc42-GFP 8 h post infection. 24 h post infection, cells were scratched and allowed to migrate for 6 h before fixing. Cell layer border indicated by a dashed line. Circles: Inclusions; red arrowheads: approximate Golgi apparatus location (dispersed in infected cells). Direction of migration: left to right. Green: GFP-Cdc42. Scale bar = 20 μm.

3.5 Global protein-protein interaction profile of Cdc42 in *Chlamydia*-infected cells

3.5.1 Quantitative interaction proteomics of Cdc42

It has so far become clear that the master regulator of Golgi repositioning, Cdc42, is present and active in infected cells and can be found at the inclusion. Rho GTPases mediate signaling through recruitment of more than 50 known effector proteins with innumerable possible downstream outcomes. To identify interaction partners whose binding to Cdc42 is altered upon *Chlamydia* infection, the two conditions were compared in a quantitative interaction proteomics approach[2] as described in Paul et al., 2011.

The entirety of proteins in uninfected and infected cells was labeled differentially ("heavy" and "light") with stable amino acid isotopes (SILAC labeling), so proteins from the two conditions could be distinguished by their respective labeling state. Cdc42-GFP was transfected, expressed and coprecipitated together with its interaction partners from the labeled cell lysates via magnetic beads coupled to an anti-GFP-nanobody (GFP-Trap). The corresponding protein precipitates were pooled. Via quantitative mass spectrometry, the amount of each interaction partner found in infected cells was compared to that in uninfected cells. To exclude unspecific binders, the experiment was repeated with swapped labeling which gives inverted protein ratios if the interaction is specific. The original configuration is hereby designated as the "straight" experiment, while the one with swapped labeling is termed the "cross" experiment. The standard work flow is depicted in Figure 3.22 A. To further exclude unspecific interactions depending on GFP a control experiment was added with the expression of GFP only. After exclusion of this background, the output was a list of proteins depicted schematically in Figure 3.22 B.

The measurements resulted in several protein sets (Tables 2, 3, see appendix). A general threshold was applied which excluded unspecific binders without inverted ratios and peptides which were found less than three times in both straight and cross experiments. Table 2 shows the interaction partners of Cdc42-GFP found in infected cells. Of those, only IQGAP1 has been published before (Erickson et al., 1997). Table 3 contains the detected proteins whose interaction with Cdc42 changed in infected cells. Overall, the majority of the interactions decreased after infection (Figure 3.22 B). The overlap with Table 2 has been highlighted in bold face. Those are the proteins that have been found to interact with higher specificity than GFP and display altered binding after infection.

[2]This experiment was designed in collaboration with Prof. Dr. Matthias Selbach (MDC Berlin). The mass spectrometry measurement and primary data processing were performed by Florian Paul (MDC Berlin).

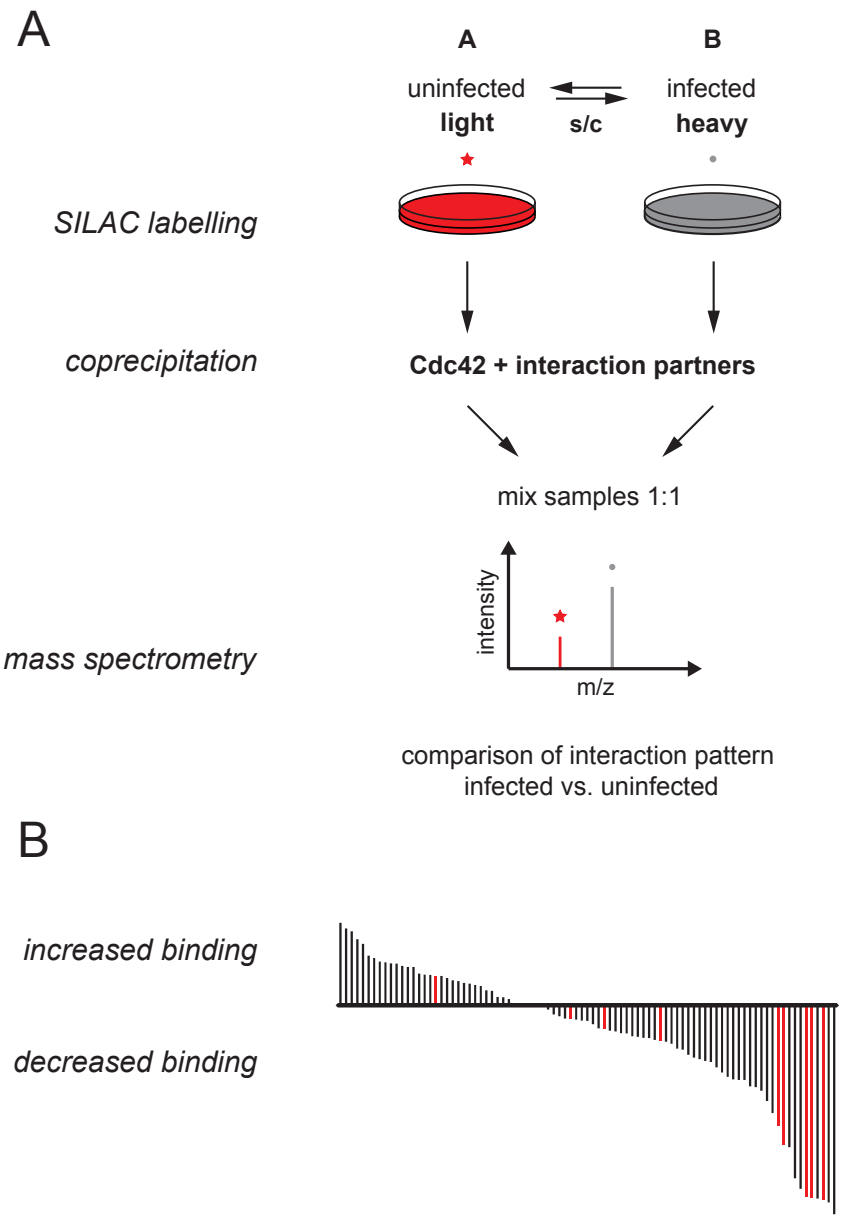

Figure 3.22: Mass spectrometry of Cdc42 interactions in infected cells. A. Experimental work flow for quantitative interaction proteomics (modified from Paul et al., 2011). The proteins present in infected and uninfected HeLa cells were labeled with stable amino acid isotopes (light or heavy). After coprecipitation, the samples were combined and subjected to mass spectrometry (LC-MS/MS) to determine the ratio of protein present in the heavy compared to the light sample. Each experiment was performed twice: once with original labeling (straight, s) and once with swapped labeling (cross, c). Specific interaction partners are characterized by high heavy-to-light ratios in the straight and low heavy-to-light-ratios in the cross experiment, in contrast to non-specific binders display a 1:1 heavy-to-light ratio in both experiments. **B**. Schematic representation of the Cdc42 protein-protein interaction profile in infected HeLa cells, normalized to uninfected cells. Red bars depict proteins that have been previously associated to the process of cell migration.

Literature mining narrowed this list down to nine top candidates (Figure 3.23). These are proteins that have been previously associated to migration in any way. They belong to various functional classes: IQGAP is a GTPase-activating protein, EEF1A1 (eukaryotic translation elongation factor 1 alpha 1) is required for protein synthesis and Hsc70 is a heat shock protein acting as a chaperone. Keratin 8 and 18 are cytoskeletal proteins that exist in the cell as a heterodimer (Mataraza, 2003; Noritake et al., 2005; Zhong et al., 2009; Grifoni et al., 2008; Bordeleau et al., 2010). The other candidates, PTBP1 (polypyrimidine tract binding protein 1), caprin1, G3BP1 (GTPase activating protein (SH3 domain) binding protein 1) and Sam68 (Src-associated substrate during mitosis of 68 kDa), are involved in RNA metabolism (Cheung et al., 2009; Solomon et al., 2007; Huot et al., 2009). G3BP1 and caprin were furthermore found to colocalize in RNA granules. Eight of those nine proteins bind to Cdc42 with lesser affinity (-0.3- to -4.9-fold) in infected cells. Only binding of Sam68 is slightly (0.76-fold) stabilized.

This indicates that *Chlamydia* infection drastically changes the interaction of Cdc42 with its effectors, particularly decreasing binding to motility-related interaction partners.

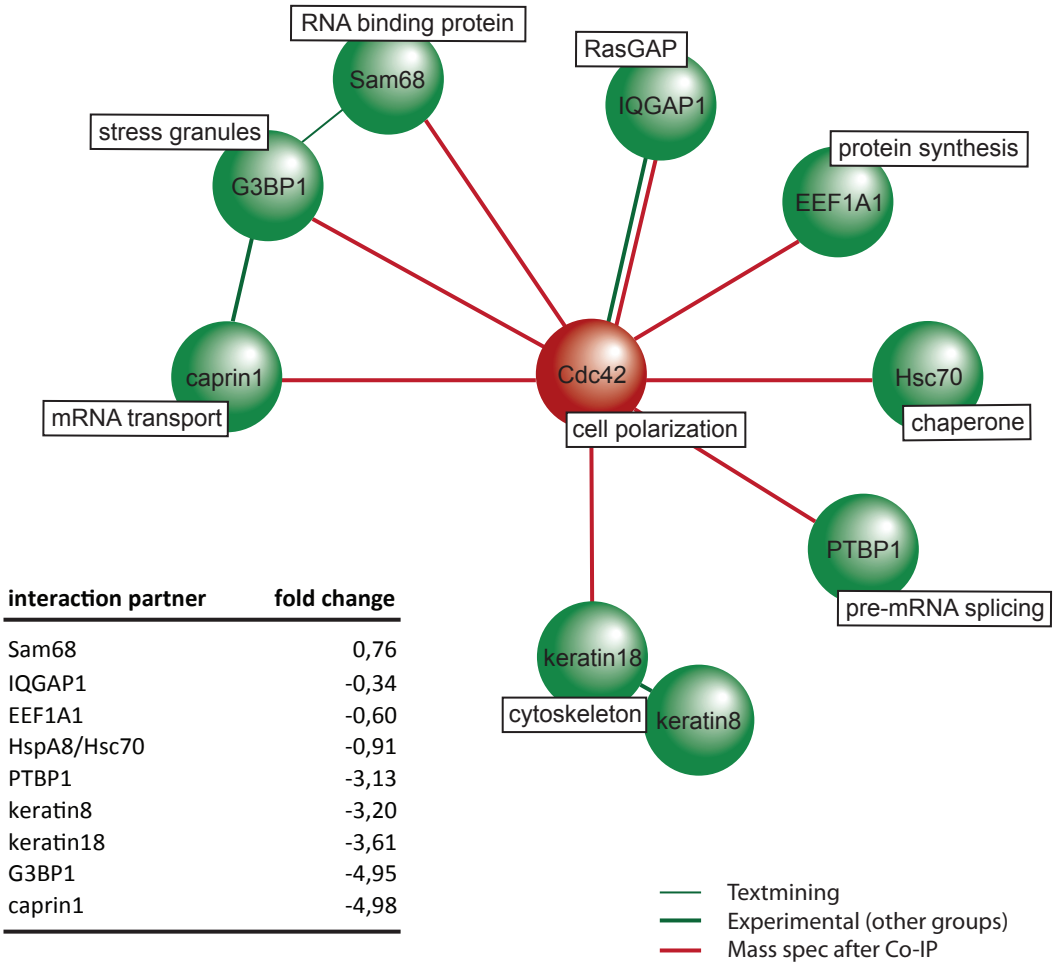

interaction partner	fold change
Sam68	0,76
IQGAP1	-0,34
EEF1A1	-0,60
HspA8/Hsc70	-0,91
PTBP1	-3,13
keratin8	-3,20
keratin18	-3,61
G3BP1	-4,95
caprin1	-4,98

Figure 3.23: Migration-associated interactions of Cdc42 that change upon *Chlamydia* infection. Schematic representation of the Cdc42 interaction partners found by quantitative mass spectrometry, that displayed modulated binding in infected cells and share a potential role in cell migration. Types of interactions are depicted by different connecting lines. Red: found experimentally in the described mass spectrometry approach, green: found by text mining, bold green: found experimentally and previously published by other groups. Position of proteins arbitrary.

4 Discussion

Chlamydia infection is characterized by the fundamental remodeling of host cell architecture. In particular, trafficking pathways are exploited by the bacteria to ensure their nutrient supply, going as far as the profound restructuring of an entire organelle. The process by which the the Golgi ribbon is broken down into small, inclusion-adjacent ministacks by *Chlamydia* and which are the responsible bacterial factors is not completely understood.

This work addressed the question of which factors induce golgin-84 processing and therefore Golgi fragmentation in infected cells. The chlamydial protease CPAF was proposed to be involved in golgin-84 processing after observation of simultaneous degradation of golgin-84 and the *bona fide* CPAF substrate vimentin. Ectopic CPAF expression caused golgin-84 processing and Golgi fragmentation in uninfected cells and confirmed the inducing role of CPAF. Inhibition of CPAF by the WEHD peptide reduced chlamydial development and infectivity which identifies CPAF as an essential bacterial factor.

The consequences of *Chlamydia*-induced Golgi fragmentation on cell mobility as a higher-order host cell function were determined. Infection disturbed Golgi repositioning towards the direction of migration, thereby rendering the cells less motile in a migration assay. Depletion of golgin-84 which is cleaved in infection phenocopied *Chlamydia*-induced motility effects. Golgi reorientation was disturbed while migration was only partly reduced. Stabilization of the Golgi ribbon by CPAF inhibition or Rab depletion restored polarization but whether this can improve the migration of infected cells could not be clarified.

The last two findings suggested that the migration defect of infected cells was not only determined by the loss of Golgi ribbon structure. Important cytoskeletal components remained largely intact, whereas GTP binding and localization of the most important polarity regulator Cdc42 were slightly modulated after infection. Interestingly, the protein-protein interaction profile of Cdc42 was considerably altered in infected cells, tending towards the decreased binding of migration-associated interaction partners.

These results provide an important insight into *Chlamydia*-induced restructuring of the Golgi apparatus and show how this influences basal cell functions including the capacity to move across a twodimensional surface. A model of the current view in analogy to the inital experimental approach (Figure 1.9) is given in Figure 4.1.

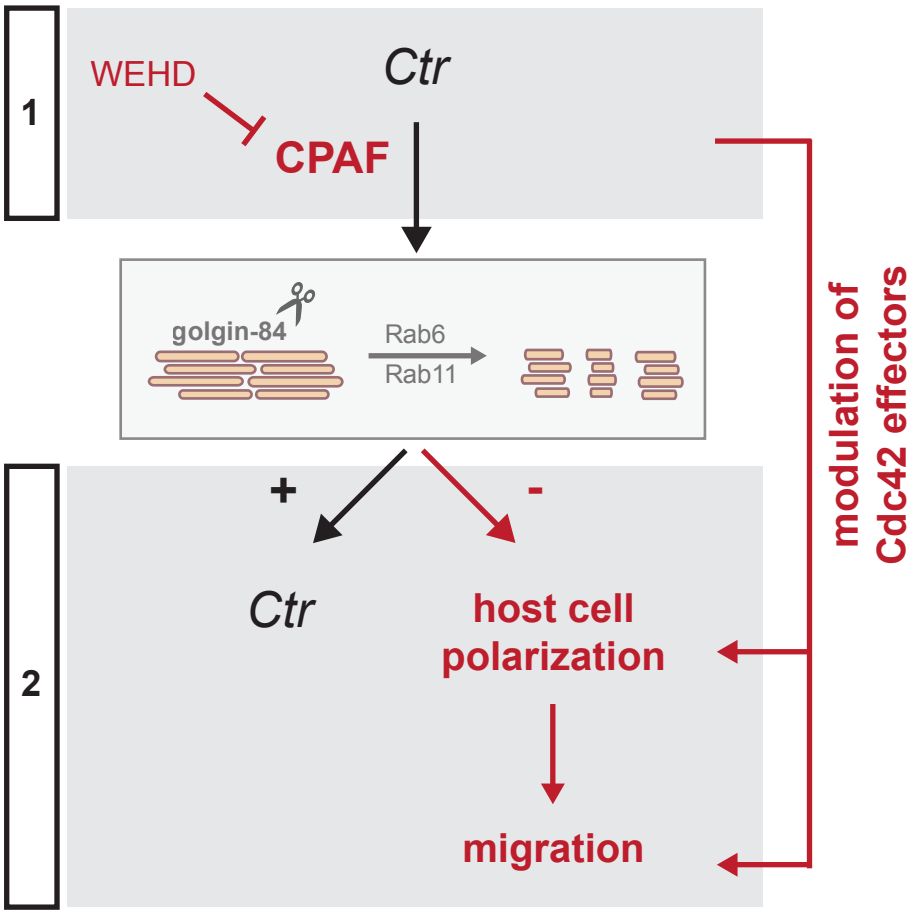

Figure 4.1: Summary of novel findings concerning the infection biology of *Chlamydia*. Schematic representation of the contributions of this work to what was previously described, in analogy to Figure 1.9. **(1)**: The *Chlamydia trachomatis* (*Ctr*)-mediated Golgi fragmentation depends on CPAF-induced processing of golgin-84. This can be inhibited by WEHD treatment. **(2)**: In addition to increased bacterial replication, Golgi fragmentation results in a block of host cell polarization and migration. Furthermore, migration is regulated in additional ways by modification of migration-related effectors of Cdc42. Red: novel findings of this thesis.

4.1 The role of CPAF in *Chlamydia*-mediated Golgi fragmentation

4.1.1 Pathogen-host interaction via CPAF

Intracellular pathogenic bacteria share a special requirement for survival-oriented interactions with their host cell. In order to propagate, they need to outlast a certain duration of residence inside the host cell. If, however, they survive the cell's defense mechanisms they gain access to an abundance of nutrients as well as protection from the immune system. A successful intracellular lifestyle ideally prevents antigen presentation, degradation in lysosomes and rapid cell death (Duclos and Desjardins, 2000; Finlay and Falkow, 1997; Sharma and Rudel, 2009). A productive and lasting infection therefore greatly depends on the ability of the pathogen to modulate host processes in its favor. Manipulation is achieved with the help of introduced effector proteins that can serve diverse functions in this tight pathogen-host interplay (Finlay, 1997).

CPAF is one of several effector proteins of *Chlamydia* (Valdivia, 2008; Betts et al., 2009). For example, tarp has been assigned to actin recruitment and signal transduction facilitating invasion (Clifton et al., 2004), Inc proteins are important for homotypic fusion of inclusions and membrane recruitment (Delevoye et al., 2008) while Lda (lipid droplet-associated) effectors have been proposed to recruit lipid droplets (Kumar et al., 2006). A predicted 5-8 % (Arnold et al., 2009) of the *Chlamydia* genome, including tarp (Clifton et al., 2004), are transferred into the host cytoplasm via the TTS. About 60 proposed Inc proteins remain on the interface of the inclusion membrane (Bannantine et al., 2000; Subtil et al., 2005). Other effectors, one of them CPAF, are transported in type three-independent ways (Chen et al., 2010b). Different sets of effectors are expressed and introduced during the progressing stages of infection to promote invasion, inclusion modification or nutrient acquisition (Valdivia, 2008). However, the identity and function of most remain unknown because genetic analysis is currently not possible.

CPAF is one of the better-characterized *Chlamydia* effectors and has been shown to act on several host proteins. It cleaves the transcription factors USF-1 and RFX5 required for expression of MHC antigen presentation molecules (Zhong et al., 2001). The proapoptotic proteins Puma and Bim as well as p65, a subunit of NFkB, are degraded by CPAF (Pirbhai et al., 2006; Zhong et al., 2001; Christian et al., 2010). Additional CPAF targets include the stress-response related factor HIF-1, PARP, which is involved in DNA repair, the cell cycle regulator CyclinB, the cytoskeletal proteins vimentin and keratin 8/18 as well as the cell surface proteins CD1d and nectin-1 (Rupp et al., 2007; Paschen et al., 2008; Kumar and Valdivia, 2008a; Kawana et al., 2007; Sun and Schoborg, 2009). Even chlamydial proteins are processed: CPAF can cleave tarp, presumably to block superinfection (Jorgensen et al., 2011). Considering the limited chlamydial genome (8 kb), this broad substrate specificity might well provide an efficiency advantage, given that CPAF could act as a "master regulator", remodeling various aspects at once.

4.1.2 Processing of host cell golgin-84 caused by chlamydial CPAF

Chlamydia-induced Golgi fragmentation is a critical precondition of intracellular development because it facilitates essential uptake of host cell sphingolipids. Processing of golgin-84 is required to disperse Golgi stacks and relocate them to the vicinity of the inclusion, presumably to increase membrane contact. Golgin-84 cleavage and Golgi fragmentation can be inhibited with the caspase inhibitor WEHD, subsequently diminishing bacterial development (Heuer et al., 2009).

Monitoring of golgin-84 processing in infected cells over time showed that it took place simultaneously with cleavage of vimentin, a *bona fide* CPAF substrate (Figure 3.1, Kumar and Valdivia, 2008a; Paschen et al., 2008). Both reactions coincided at times of CPAF secretion and Golgi fragmentation as previously described (16-28 hours). The peptide inhibitor WEHD that was shown to block golgin-84 processing also prevented vimentin cleavage at the same time. Therefore, *Chlamydia*-mediated golgin-84 cleavage likely has the same underlying mechanism as *Chlamydia*-induced vimentin cleavage which is known to be CPAF-mediated.

This experiment showed that golgin-84 cleavage happens in parallel and probably via the same enzyme as vimentin processing. However, it did not clarify whether processing is directly or indirectly CPAF-dependent. At this stage, it could not be excluded that golgin-84 processing involves an additional enzyme that is activated by *Chlamydia* and sensitive to WEHD. A possibility is caspase-1, which fulfills both criteria (Abdul-Sater et al., 2009; Garcia-Calvo et al., 1998). For this reason, CPAF function needed to be investigated separately and in the absence of other bacterial proteins. It was tested whether CPAF alone was able to induce golgin-84 degradation and Golgi fragmentation.

Ectopic expression, be it transient or stable, of chlamydial CPAF in uninfected cells was sufficient to induce strong Golgi dispersion (Figures 3.4, 3.5) similar to the morphology observed in infected cells, while the CPAF-inducing and activation agents alone had no effect on Golgi structure (Figure 3.3). Possible side effects of heterologous protein expression could be excluded by transfection of CPAF without subsequent induction. Furthermore, the sensitivity to an inhibitor made this possibility very unlikely. In agreement with what has been shown in the infection model, fragmentation could be prevented by WEHD treatment (Figures 3.4, 3.5, Heuer et al., 2009). Consistently, the stable CPAF-expressing cell line exhibited proteolysis of golgin-84 and vimentin shortly after CPAF induction (Figure 3.6).

These findings show that the effects of *Chlamydia*-infection on host cell golgin-84 and Golgi structure are caused by expression of active CPAF. They eliminate the potential involvement of another chlamydial effector during this process. Still, it can not be excluded that CPAF regulates an unidentified host cell factor that contributes to this process. So far, all experiments showing golgin-84 cleavage after CPAF expression have been done with whole cell lysates (Christian

et al., 2010). A direct interaction of CPAF with golgin-84 can only be proven by biochemical assays.

Indication for direct proteolytic cleavage could be identified by the presence of an adequate cleavage site. So far, no definite common motif of CPAF substrates has been postulated. The molecular basis for CPAF cleavage has been determined for keratin 8 and vimentin (Kumar and Valdivia, 2008a). Both proteins are cut at their N-terminal head domains which are followed by a rod domain and a tail domain. The motifs are of similar amino acid composition containing serine (S) and valine (V) residues. The most probable cleavage site found in golgin-84 has been predicted by mass spectrometry to be located at S157, between the C-terminal transmembrane domain and the cytoplasmic coiled-coil domain (Heuer et al., 2009; Bascom et al., 1999). The motif also contains the previously mentioned amino acids (Table 4.1). Even though the predicted CPAF-cleavage domains share no consensus sequence, the residues in the predicted cleavage motif of golgin-84 resemble those of vimentin and keratin 8.

vimentin:	VRLR**S**	**S**VPGV (S72)
keratin 8:	NQSL**L**	**S**PLVL (S73)
golgin-84:	SSQT**S**	**S**VSSV (S157)

Table 4.1: Cleavage sites of the known CPAF substrates vimentin and keratin 8 compared to golgin-84. CPAF cleaves vimentin and keratin 8 at serine residues in the head domain (indicated in bold, Kumar and Valdivia, 2008a). The predicted cleavage domain of golgin-84 is comprised of related residues (Heuer et al., 2009).

In *Chlamydia*-infected cells, Golgi fragmentation depends on the small GTPases Rab6 and Rab11. Rab6 usually mediates retrograde Golgi-to-ER and intra-Golgi transport and is found on Golgi-derived exocytotic vesicles (Martinez et al., 1997; Girod et al., 1999; White et al., 1999; Del Nery et al., 2006; Grigoriev et al., 2007) while Rab11 is found on recycling endosomes (Ullrich et al., 1996). Knockdown of either of the two Rab proteins stabilized the Golgi apparatus and reduced sphingolipid uptake by the bacteria, resulting in impaired development (Rejman Lipinski et al., 2009).

The two GTPases regulate vesicle formation and transport at the Golgi apparatus. This membrane turnover is proposed to contribute to the Golgi fragmentation observed in infected cells. *Chlamydia* disconnects Golgi cisternae by cleaving the matrix protein golgin-84 and intercepts Rab6- and Rab11-controlled vesicles. The vesicles are recruited to the inclusion to parasitize for Golgi-derived sphingolipids (Rzomp et al., 2003; Rejman Lipinski et al., 2009). If either of the GTPases are missing, presumably no more vesicles are formed and the Golgi stacks remain

stable, while the bacteria are no longer provided with sphingolipids. Golgi fragmentation after CPAF expression also proved to be strongly dependent on Rab6 and Rab11 (Figure 3.7). The two GTPases probably account for the dissolving of the ribbon structure in both fragmentation models after the stack interconnections have been dissected by golgin-84 degradation.

Because all the described aspects of *Chlamydia*-induced Golgi fragmentation could be reproduced independently with the help of ectopically expressed CPAF, it can be assumed that CPAF induces host cell Golgi fragmentation via golgin-84 degradation in a Rab6- and Rab11-dependent manner.

4.1.3 The significance of CPAF for bacterial development

Proteases can regulate pathways by degradation of functional proteins, activators or inhibitors. Conserved proteases of pathogens are often critical for survival and progression (Huston, 2010). The *Salmonella* Lon protease for example, is involved in invasion and regulation of pathogenicity islands (together with ClpXP, another protease) and is essential for bacterial survival (Boddicker and Jones, 2004). *Legionella* exports metalloproteases to cleave immune molecules and needs Pla protease to survive inside amobae (Moffat et al., 1994; Banerji et al., 2008). HtrA, a chaperone with proteolytic activity, is required for *Salmonella* and *Legionella* virulence (Lowe et al., 1999; Pedersen et al., 2001).

Inhibition of CPAF by WEHD dramatically reduced inclusion number and size in primary infection and drastically impaired reinfection of new cells after one developmental cycle (Figure 3.2). While definitely, a part of the latter observation directly results from the primary infection, the reduction of infectivity is stronger by several orders of magnitude. This indicates an additionally disturbed bacterial development inside the inclusion after inhibition of CPAF activity. Thus, CPAF is essential for the development and propagation of *Chlamydia*.

The effect of WEHD was compared to three other peptide inhibitors. In addition to WEHD, the caspase-6 inhibitor VEID reduced inclusion size and infectivity, but not the number of inclusions. This could indicate low inhibitor specificity which is a known drawback of inhibitors acting on host-pathogen interactions. Alternatively, the broad substrate range of CPAF might account for sensitivity to more than one peptide. Peptide inhibitors are very specific for their cognate caspase domains but the active center of CPAF may allow a larger variety of binding partners and this probably explains its sensitivity to caspase inhibitors.

The best characterized CPAF inhibitor so far has been lactacystein, which could be co-crystallized with CPAF monomers (Zhong et al., 2001; Huang et al., 2008). However, lactacystein not only also irreversibly inhibits the proteasome but has a detrimental effect on Golgi structure which is why it was not feasible for these experiments (Harada, 2003).

WEHD was originally developed as a caspase-1 inhibitor. The involvement of an additional

protease, perhaps a caspase which might be activated by CPAF (and is sensitive to WEHD treatment) cannot be excluded, especially since caspases are generally regulated by auto- and reciprocal cleavage. Furthermore, caspases control Golgi fragmentation during apoptosis (Lane et al., 2002). There is predominant evidence however, speaking against caspase-1 acting on golgin-84.

For one, infection of caspase-1 knockout MEFs (mouse embryonic fibroblasts) is principally possible and does not impede the course of infection (Cheng et al., 2008). Considering that Golgi fragmentation is essential for *Chlamydia* survival, caspase-1 knockdown would be expected to have a strong negative effect on infection if caspase-1 would execute *Chlamydia*-induced Golgi fragmentation. Additionally, shRNA mediated depletion of the inflammasome (which caspase-1 is a part of) only resulted in very moderate effects on bacterial development (Abdul-Sater et al., 2009). Recently, CPAF inhibition by another peptide led to an even higher and earlier activation of caspase-1 to suppress cell death, which argues against an indirect activation of caspase-1 via CPAF (Jorgensen et al., 2011). Lastly and most importantly, the caspase-1 inhibitor YVAD (*Tyr-Val-Ala-Asp*) and the pan-caspase inhibitor IV did not prevent golgin-84 cleavage (personal communication, Heuer et al., 2009). These findings together with the described experiments of this work indicate CPAF as the enyzme mediating golgin-84 cleavage and subsequent Golgi fragmentation.

CPAF is evolutionary conserved and can be found in all *Chlamydia* species including environmental *Chlamydiae* which are not adapted to vertebrates (Collingro et al., 2011; Capmany et al., 2011). Those species reside within free-living amobae and have no reason for immune evasion or anti-apoptosis promotion. This is why the original function of CPAF is probably more fundamental and its direct contribution to nutrient parasitism could be of vital importance for the bacteria. Golgi fragmentation is critical for chlamydial survival because it provides access to host cell sphingolipids.

CPAF is not the only protease secreted by *Chlamydia*. Intracellular pathogens possibly use this way of modulation because proteolysis is irreversible in contrast to regulation via phosphorylation status. The tail-specific protease (Tsp) has been proposed to be exported into the cytoplasm, although this has yet to be confirmed by immunostaining. It presumably cleaves the p65 subunit of NFκb to prevent activation of inflammatory genes (Lad et al., 2007b,a). The chlamydial periplasmic protein HtrA was detected in the host cell and the inclusion lumen (Zhong, 2011). It exists in eukaryotes and prokaryotes, has chaperone and proteolytic activity and is involved in the eukaryotic response to unfolded proteins (Clausen et al., 2002). In bacteria, it binds unfolded outer membrane proteins and induces activation of stress response genes (Walsh et al., 2003). Neither of these proteases are described as essential for infection or survival of *Chlamydia* and their roles in pathogenesis remain unidentified.

The described findings determine two characteristics for CPAF that were thus far unknown. (1) It induces proteolysis of the host cell substrate golgin-84. (2) It is essential for chlamydial development. These two aspects are functionally connected by the need for host cell lipids, which *Chlamydia* acquire from the Golgi apparatus via separation and recruitment of Golgi ministacks (Figure 4.2).

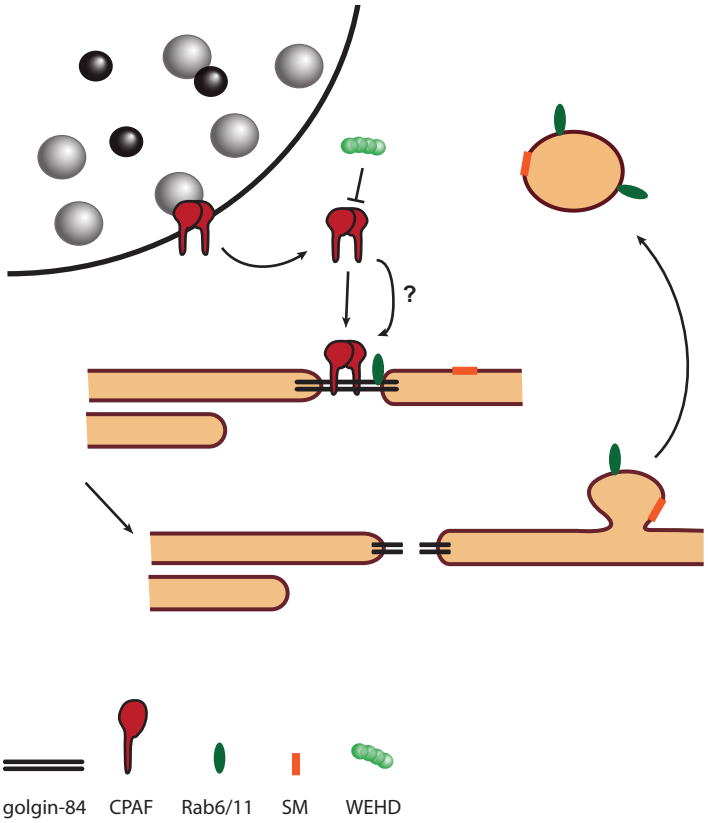

Figure 4.2: Initiation of Golgi fragmentation via CPAF. Schematic representation of the model proposed for *Chlamydia*-induced Golgi fragmentation. Secreted CPAF cleaves golgin-84, with or without the involvement of an additional, unknown host cell factor, thereby unlinking the Golgi stacks. The subsequent recruitment of Rab-controlled vesicles provides the bacteria with Golgi-derived sphingomyelin (SM) and leads to the membrane turnover that separates the Golgi stacks which are relocated to the inclusion. The whole process can be inhibited by WEHD whereafter *Chlamydia* are deprived of SM and cease to develop.

4.2 Consequences of *Chlamydia*-induced Golgi fragmentation for host cell motility

Structural disintegration of the Golgi apparatus has been shown to result in several cellular defects and pathologies. For example, it disrupts directed vesicle transport and secretion and hinders ciliogenesis (Stieber et al., 2004; Hurtado et al., 2011). In nerve cells, it perturbs neuronal outgrowth and has been observed in neurodegenerative diseases including Alzheimer's disease, Parkinson's disease, amyotropic lateral sclerosis and Creutzfeldt-Jakob disease (Gonatas et al., 2006). Inhibition of fragmentation on the other hand prevents cells from entering mitosis (Sütterlin et al., 2002; Colanzi et al., 2003).

An important underlying cellular response dependent on intact Golgi architecture and positioning, is front-to-back polarization in response to migration stimuli (Figure 1.8). During distinction of front and back the Golgi apparatus is positioned in a characteristic way, ending up anterior to the nucleus and facing the direction of migration (Kupfer et al., 1982). This is thought to enable directed secretion and promote compartmentalized signaling. If Golgi integrity is destroyed by knockdown of golgins, the dispersed Golgi elements can no longer reorientate. This is detrimental for directional cell migration (Yadav et al., 2009). Golgi fragmentation in *Chlamydia* infection is golgin-mediated which is why the consequences of infection for cell polarization and migration were determined.

4.2.1 Host cell polarization

Front-to-back polarization in *Chlamydia*-infected cells was monitored by determining the relocation of the Golgi apparatus in front of the nucleus, towards the cell border and in direction of migration. The cell culture method that was chosen for Golgi reorientation assays allowed monitoring the organelle distribution in border cells after the release of spatial restrictions without wounding the cell layer (Figure 2.1).

The experiments of this study focused on the first row of cells where polarization and migration are triggered initially through the absence of neighboring cells and interaction with the substratum. Usually, polarization happens in all cells at the front of the cell layer within 4-6 h after removal of spatial restrictions. Later, the migration response of collectively migrating cells is passed on to the following cells via mechanical force on adherence junctions while integrins of follower cells interact with the ECM left behind by the border cells (Friedl and Gilmour, 2009).

The reorientation of the Golgi apparatus was abrogated after infection with *Chlamydia* (Figure 3.8). In infected border cells, the dispersed Golgi apparatus was aligned around the inclusion and could not be repositioned to face the migration direction. If the Golgi was stabilized by the CPAF inhibiting peptide WEHD (which, as expected, affected chlamydial development

and resulted in smaller inclusions), reorientation was re-established (Figure 3.9). It is important to keep in mind that the angle of correct Golgi orientation extends from the nucleus and not from the inclusion. The data confirmed that *Chlamydia*-induced, golgin-84 dependent Golgi fragmentation renders border cells incapable of front-to-back polarization.

Rab11 knockdown rescued Golgi reorientation in infected cells more effectively than Rab6 silencing (Figure 3.17). Double knockdown did not achieve a synergistic effect, although both Rab6 and Rab11 knockdown have been shown to individually restore compact Golgi structure in infected cells (Rejman Lipinski et al., 2009). In contrast, in uninfected cells depleted for golgin-84, both Rab proteins reenabled Golgi reorientation (Figure 3.16). This suggests a Rab6-dependent process contributing to cell polarity of infected cells that does not exist in the same way in uninfected cells and is independent of Golgi element dispersion. The possibility exists that Rab6 mediates interaction of Golgi membranes with associated microtubules which are redistributed upon infection (Figure 3.19) and this eliminates mechanical guiding forces towards the migration direction that are exerted by the microtubules.

It seems obvious that the severe structural manipulation of the Golgi apparatus by *Chlamydia* is not without consequences for Golgi-dependent cell polarization. Yet, it was not completely clear how much of the reorientation incapacity was caused by unlinking of the Golgi ribbon. Further constraints of Golgi reorientation could well be affected by the bacteria.

For example, orientation could be hampered if the Golgi ministacks were mechanically attached to the inclusion, but there is no evidence thus far for colocalization of inclusion and Golgi membranes as has been observed for the ER (Derré et al., 2011). Furthermore, modulation of host cell signaling could interfere with polarization signaling. Golgi reorientation requires phosphorylation of GRASP65 by ERK, causing loss of GRASP65 oligomerization and temporary unstacking of cisternae, thereby freely allowing the Golgi to be dynamically reorganized (Bisel et al., 2008). However, *Chlamydia* infection generally leads to activation of ERK kinase which suggests that GRASP65 phosphorylation occurs (Gurumurthy et al., 2010). This would mean that Golgi orientation is not inhibited because the membranes are to static to react.

Rather, previous findings suggest that the interconnection of Golgi stacks, Golgi-derived microtubules and a compact structure provided by golgins is highly relevant for Golgi reorientation (Miller et al., 2009; Yadav et al., 2009). Knockdown of the golgins GMAP210 and golgin-160 had been shown to result in Golgi fragmentation and loss of reorientation in uninfected cells. This was confirmed by golgin-84 silencing in uninfected cells which was sufficient to disturb Golgi orientation in migrating cells (Figure 3.14). Moreover, inhibition of golgin-84 processing in infected cells by WEHD could again restore polarization (Figure 3.9).

This data indicates that, in both uninfected and infected cells, golgin-84 mediated Golgi fragmentation is sufficient to disable the reorientation of the Golgi apparatus. However, Golgi

fragmentation caused by infection and Golgi fragmentation caused by golgin-84 knockdown is not entirely the same. Although it leads to the same effect, is has to be considered that there could be differences. According to immunostaining, the Golgi apparatus of the golgin-84 knockdown cell line is fragmented but the ministacks still localize to the perinuclear region (Figure 3.14). In infected cells, they are displaced towards the inclusion which might have an implication on Golgi repositioning despite fragmentation (Figure 3.8). Perhaps one major overall direction of vesicle transport still dominates if the stacks are no more interlinked but also not completely dispersed throughout the cell.

4.2.2 Host cell migration

Previous studies have shown that Golgi polarization is essential for twodimensional migration (Yadav et al., 2009). The inability of infected cells to polarize indeed correlated with impaired cell migration. While uninfected cells fully closed a scratch wound of several hundred micrometers in 24 hours, this ability was lost with increasing infectious dose (Figure 3.10). At low-to-medium MOIs, the culture still contained uninfected cells that acted as pioneers and repopulated part of the cell-free area. This is in agreement with the MOI dependency that was observed for Golgi fragmentation (Heuer et al., 2009). Thus, a *Chlamydia*-infected cell which cannot reorient its Golgi apparatus loses its migration capability in addition.

The *in vitro* scratch assay is often used to assess changes in migration because it is a simple method to compare cell motility under different experimental conditions in parallel culture units (Liang et al., 2007). In contrast to culture in silicone chambers and subsequent removal of this barrier, scratching detaches and damages cells releasing cytoplasmic content. For comparability reasons, both techniques were initially applied for each assay to exclude any effects caused by cell damage. For confocal studies, the chamber culture was better suited because it yielded defined and straight cell borders.

The migration defect of infected cells could be phenocopied by Golgi fragmentation caused by golgin-84 knockdown in uninfected cells. Migration was reduced by about 20 % in golgin-84 depleted cells which is comparable to a rather mild infection (Figures 3.13, 3.10). One possible explanation for this partial effect might be that the cells at higher MOIs experience greater stress which is relevant during the migration assay because of the experiment being long term. Meanwhile, low infectious doses are definitely closer to physiological conditions. Apart from Golgi morphology, *Chlamydia* infection could modulate additional factors contributing to migration, including cytoskeletal organization, surface adhesion or regulation of these processes. For example, it is not yet known how extensive and how relevant the proposed actin or intermediate filament reorganization by *Chlamydia* is or if focal contact dynamics are modified (Kumar and Valdivia, 2008a). However, golgin-84 dependent Golgi fragmentation in uninfected cells

produces an effect similar to infection and this implies that the infection-induced motility loss can at least partially be attributed to Golgi structure disassembly.

Live cell microscopy revealed that infected cells, as well as golgin-84 knockdown cells, display diminished migration velocity (Figure 3.15 A+B). As previously discussed, the reduction was less prominent in golgin-84 knockdown cells. Beyond this, the directionality of the movement was lost (Figure 3.15 C). Usually, slower cells exhibit higher directional persistency (Laufenburger and Horwitz, 1996). Neither of the Golgi-fragmented cell types could maintain a constant direction during the course of the experiment. This could signify that Golgi fragmentation not only reduces the amount of forward secretion but that the entire secretion is directionally randomized. It remains unclear how this applies to the situation in an infected cell but it is assumed that numerous vesicles are rerouted to the inclusion and the fraction of transport that remains transported to the plasma membrane can probably not be targeted in one direction. But directional persistence requires constant polarity and site-directed secretion (Petrie et al., 2009). Whether infection beforehand changes local sensing of migration stimuli initiated by integrin signaling is an interesting question that could be addressed in single-cell migration experiments using a chemotactic stimulus gradient.

Chlamydia infection affects host cell apoptosis (Sharma and Rudel, 2009). Therefore, repopulation of a gap in the cell layer could be related to the proliferation rate. However, cell division was not relevant for the migration defect (Figure 3.12). Both infected and uninfected cells underwent comparable cell division which became especially clear during live cell microscopy.

Reduced migration after *Chlamydia* infection has recently been reported by another group (Kumar and Valdivia, 2008b). The authors showed a similar MOI dependency to the one observed in this work (Figure 3.10). The authors attributed the effect to the recruitment of actin and intermediate filaments to the inclusion in order to stabilize it mechanically. This would mean that actin-based membrane protrusion was decreased in infected cells.

On the contrary, microscopic analysis performed in this work showed that both uninfected and infected cells exhibit equal protrusion-forming ability. Six hours after migration induction, infected cells had formed lamellipodia and filopodia of similar morphology to that of uninfected cells (Figure 3.19 A). Furthermore, actin polymerization defining the leading edge occurred at the frontal plasma membrane of both uninfected and infected cells alike (Figure 3.19 A+B). Seemingly, cytoskeletal rearrangements still occur after infection but can not be transduced into locomotion.

The overall microtubule network appeared intact but slightly disorganized (Figure 3.19 A). Whether this is a cause or a consequence of the nonoriented Golgi has to be determined. It can not be excluded that it affects migration, particularly since it has been reported that a distinct microtubule population originating at the Golgi apparatus is important for polarization (Vino-

gradova et al., 2009). The applied staining method did not distinguish between microtubule subpopulations.

Subsequently, the results show that the polarization and migration defects of infected cells can be at least partly attributed to the disruption of Golgi structure, even if there might be additional effects of *Chlamydia* infection on cell migration.

Based on the observation that CPAF inhibition restores Golgi structure and reorientation in infected cells (Figure 3.9), it would be expected that treatment with WEHD would restore migration. Unfortunately, conducting the respective experiment was not feasible because long-term WEHD treatment itself has a negative effect on cell migration and would mask infection-induced effects (Figure 3.11). However, knockdown of Rab11 has been described as an additional tool to stabilize the Golgi apparatus of infected cells and improve polarization (Rejman Lipinski et al., 2009, Figure 3.17).

Stable depletion of Rab11 prominently restored the motility of infected cells (Figure 3.18 A). In contrast, when the knockdown was achieved transiently via siRNA, migration of infected cells was not improved, independent of knockdown efficiency (Figure 3.18 B). These findings do not allow an ultimate conclusion about the role of Rab11 in this process because the two methods of silencing did not yield the same result.

The reason for this discrepancy is most likely of technical nature because siRNA and shRNA-generated gene silencing follows different principles. A clonal cell line like the stable Rab11 knockdown cells are selected by single-cell sorting after transfection and integration of the shRNA via lentivirus. This is done to pick a single clone with sufficient knockdown according to the GFP expression from the lentiviral vector. The advantage compared to a non-sorted cell population is a better knockdown efficiency and stability, but also creates one drawback:

The lentiviral vector is integrated into random positions of the genome. This is usually not a problem unless it disrupts an open reading frame which is important for the investigated effect (Singh et al., 2011). If the respective cell is selected via cell sorting, it yields false positive observations. Although the possibility that the clonal cell line used in these experiments could display this kind of off-target effects is marginal, it is generally possible.

Transient knockdown suffers from even more off-target effects but leads to an inhomogeneous population of cells and therefore prevents a selection bias (Rao et al., 2009). However, this method does not rule out cytotoxic effects which are circumvented by propagation of a single clone. Neither method is entirely perfect to assess this question but the result of the shRNA cell line seems more reliable. An intermediate approach to silence a gene in a cell culture system would employ a stable cell line that has not been sorted. Then again, in this case the knockdown would supposedly be less strong and stable. A dominant-negative construct of Rab11 is another

possibility by which its relevance could be defined. Yet, the absence of a protein and the presence of a mutant are two different things. A permanently GDP-bound Rab11 for example might still be able to possess functions that are related to other characteristics that its GTP binding domain.

Depletion of Rab11 was previously shown to negatively affect the migration of neurons (Kawauchi et al., 2010). A comparable effect of Rab11 depletion was not observed during the experiments performed in this work. This could rely on cell type differences or knockdown conditions. Only after transfection of high amounts of siRNA, a slight motility reduction in uninfected cells was visible (Figure 3.18 B). Still, pleiotropic effect of Rab11 depletion at this stage cannot be separated from its Golgi stabilizing function.

Overall, the concluding effect of Rab11 depletion on the migration of *Chlamydia*-infected cells remains to be determined. Since Rab11 knockdown is also known to reduce sphingolipid uptake and chlamydial development, migration improvement might be an indirect consequence of the reduction of *Chlamydia* development.

4.3 Altered attributes of Cdc42 in *Chlamydia* infection

The migration of cells infected with *Chlamydia* was evidently dependent on Golgi structure. However, migration of the golgin-84 knockdown cell line and knockdown of Rab11 suggested that more aspects of motility could be modulated by the bacteria. While polarization is indispensable for directed migration, it is not the only key process involved. For instance, another essential aspect of migration is the preceding signal transduction via small GTPases.

A normally migrating cell exhibits an intact network of tubulin, spanning from the MTOC to the plasma membrane with the microtubule plus ends oriented towards the front. Increased actin polymerization which propels the membrane forward is found at the leading edge. These cytoskeletal rearrangements are primarily controlled by Rac and partly by Cdc42. Meanwhile, only Cdc42 provides the signaling cues for Golgi and MTOC reorientation. Cdc42 is locally activated by GTP binding and forms a gradient of GTP-bound Cdc42 which is highest at the leading edge. This gradient is crucial for migration and both dominant negative and constitutively active forms of Cdc42 hinder migration (Etienne-Manneville, 2004). Rho activation at the rear of the cell controls retraction of membranes and has recently been shown to induce Golgi fragmentation via the actin nucleator mDia (mammalian homologue of *Drosophila melanogaster* diaphanous, Zilberman et al., 2011).

Rho family GTPases hence are key regulators of cell polarity and are in dynamic contact with the Golgi apparatus, making them interesting targets in the context of *Chlamydia*-induced polarity loss. However, small GTPase regulation including recruitment, scaffolding proteins, GAPs and GEFs is a fine-tuned system which is not completely understood. The required form of a particular GTPase needed in a specific localization at a definite time is, in addition, not easy to experimentally dissect.

The previous experiments hinted at a modulation of Cdc42- rather than Rac activity because the cause of the migration defect of infected cells seemed to be related to the process of polarization and not to the protrusive machinery. Cdc42 localizes to the Golgi apparatus and the leading edge of migrating cells and is activated in a compartmentalized way (Etienne-Manneville, 2004). The localization of Cdc42 was determined after overexpression of a GFP fusion protein and the fraction of GTP-bound Cdc42 was examined after affinity precipitation and Western Blotting.

As expected, Cdc42 localized to the Golgi apparatus and the leading edge in uninfected cells and was additionally detected in these areas in infected cells (Figure 3.21). A fraction of the signal was furthermore observed in close proximity to the inclusion membrane. Meanwhile, the proportion of GTP-bound Cdc42 was increased in infected cells (Figure 3.20). This indicates that the lack of polarization is not caused by a block of Cdc42 activity. On the contrary, the activity in infected cell is increased.

Cdc42 is activated early during *Chlamydia* infection to promote actin assembly at entry sites (Subtil et al., 2004). Prolonged Cdc42 activation has so far not been investigated in this context. It can, in any case, influence cell polarization. Global GTPase activity is not necessarily beneficial for polarization, because a gradient needs to be established. The overall activation of Cdc42 destroys the gradient from front to back and the cell is no longer asymmetrical. The action pattern of a GTPase could only be grasped completely if localization and activity were traced simultaneously. An optimal experiment would compare the spacial and temporal distribution of active GTP-bound Cdc42 in infected and uninfected living cells. This has been performed with live cell imaging approaches employing biosensors, but only with single cells and not migrating cell sheets (Machacek et al., 2009).

Moreover, recent findings determined that Cdc42 is transported in vesicles and that disruption of Arf-dependent membrane trafficking inhibits polarization (Osmani et al., 2010). This means that the localization of Cdc42 depends directly on vesicle transport and Cdc42 activity can be influenced downstream of the Golgi apparatus. Infection-induced Golgi fragmentation might directly reduce Cdc42 transport. Although this is not confirmed by the localization experiment, it is neither excluded and more detailed microscopy of endogenous Cdc42 could show how much Cdc42 arrives at the plasma membrane in infected cells.

Binding of downstream effectors by GTPases is initiated by GTP binding. Activation and partial redistribution of Cdc42 could change the interaction with downstream effectors because the presence and amount of active and inactive forms are changed. The protein-protein interactions of Cdc42-GFP in uninfected and infected cells were compared by mass spectrometry after SILAC labeling (Paul et al., 2011).

Global assessment of this hit list showed that infection led to an overall reduction of interactions (Figure 3.22). A major change of total interactions was expected, considering how extensively *Chlamydiae* reorganize their intracellular niche and how many proteins are recruited away from their original locations to the inclusion.

Of the proteins highlighted in Table 3, nine candidates had been previously associated to cell migration or polarity in the literature. For this reason, those were particularly interesting (Figure 3.23). Except for one, the binding to Cdc42 decreases upon infection. The influence of some of those binding partners (IQGAP1, PTBP1, keratin 8/18) on migration is already well described.

The GTPase-activating protein IQGAP1 is already known to directly interact with active Cdc42 and is described as a key regulator of migration (Mataraza, 2003; Noritake et al., 2005). It localizes to the leading edge in migrating cells and to cell-cell contacts in stationary cells. Knockdown or dominant-negative expression reduces migration and cell adhesion. Vice versa, overexpression of dominant active mutants leads to multiple leading edges.

PTBP1 (polypyrimidine tract binding protein 1) is an RNA-binding splicing factor that can

form complexes with focal adhesion-encoding transcripts at the cell membrane. Its depletion increases adhesion and reduces migration of glioma cells (Cheung et al., 2009). Furthermore, PTBP1, which is also known as HNRNP1 (heterogeneous nuclear ribonucleoprotein 1), is found in so-called spreading initiation centers (SICs) that form during the early stages of cell spreading (de Hoog et al., 2004).

Keratin 8 and 18 are intermediate filaments of epithelial cells that form a heteropolymer. Keratin 8 knockout mouse and rat hepatocytes spread slower on fibronectin and stably depleted keratin 8 hepatoma cells migrate slower in the *in vitro* scratch assay (Bordeleau et al., 2010).

The three identified binding proteins EEF1A1, Hsc70 and caprin1 seem to contribute more indirectly to motility. The eukaryotic elongation factor EEF1A1 (eukaryotic translation elongation factor 1 alpha 1) has been reported to bind DLC1 (deleted in liver cancer 1), a RhoA GAP, and thereby decrease its migration inhibition (Zhong et al., 2009). The chaperone Hsc70 (heat shock cognate protein 70) interacts with ASIC2 (acid sensing ion channel 2) in muscle cells which also induces higher motility (Grifoni et al., 2008). The RNA binding proteins caprin1 and G3BP1 (GTPase activating protein (SH3 domain) binding protein 1) form a complex that colocalizes with cytoplasmic RNA granules accumulating at the leading edge of 293T cells (Solomon et al., 2007).

Migration-involved Cdc42 interactions seem to be modulated upon infection in a way that strongly disfavors migration. Only the interaction of Cdc42 with the RNA-binding protein Sam68 (KH domain-containing, RNA-binding, signal transduction-associated protein 1) was stabilized upon infection (Figure 3.23). Sam68, also called "Src-associated substrate during mitosis of 68 kDa", is a nuclear protein that is shuttled to the cytoplasm during mitosis where it acts as an adaptor of Src (sarcoma) family kinases (Lukong and Richard, 2003).

Sam68 has RNA binding activity and is thought to regulate transcription, alternative splicing and mRNA export (Babic et al., 2006; Cheng and Sharp, 2006; Coyle et al., 2003). During cell spreading, Sam68 localizes near the plasma membrane where it can regulate Src activity via phosphorylation (Huot et al., 2009; Taylor and Shalloway, 1994; Kaplan et al., 1994). Src kinases in turn associate with phosphorylated focal adhesion kinase (FAK) at focal adhesions and activate Rac by stimulating its GAPs (Schaller et al., 1994; Kawakatsu et al., 2005; Meng et al., 2004). Silencing of Sam68 reduces polarization and migration in knockout MEFs and HeLa cells (Huot et al., 2009).

Sam68 has been recently crystallized together with the tumor suppressor APC, one of the polarity proteins found at the leading edge and regulated by Cdc42 (Morishita et al., 2011; Näthke et al., 1996; Etienne-Manneville et al., 2005). APC stabilizes microtubule plus ends at the plasma membrane and loss of APC abrogates cell migration (Mogensen et al., 2002; Kroboth et al., 2007). If Cdc42 captures Sam68 to the inclusion, it could relocate APC and thereby disturb

microtubule polarization. Even though this is very speculative, there is a microtubule population around the inclusion (Figure 3.19) which could well be formed with the help of mislocalized polarity proteins (Figure 4.3).

A complex of IQGAP, activated Rac or Cdc42 and APC normally accumulates at the leading edge of migrating cells. It interacts with CLIP-170 (Cytoplasmic linker protein 170) complexes which are involved in microtubule capture at specific cortical regions (Fukata et al., 2002). This again speaks for a shift of microtubule polarity which is usually needed at the leading edge. Perhaps *Chlamydia* use redirected microtubules to maneuver vesicles towards the inclusion.

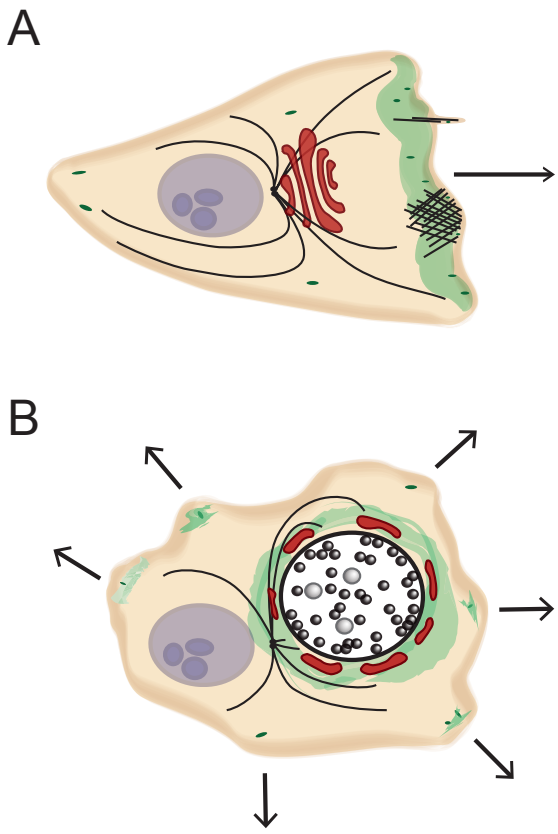

Figure 4.3: Possible background of the disruption of cell asymmetry after *Chlamydia* infection. A. In a normal migrating cell, the polarity proteins (green) accumulate at the leading edge inducing the necessary polarized alignment. Protrusion is restricted to one direction. **B**. If those proteins are redistributed by *Chlamydia*-induced recruiting processes or localized everywhere in equal amounts, due to overall Cdc42 activation, this asymmetry is annihilated and all possible directions are tantamount.

It was surprising that only very few bacterial proteins were coprecipitated together with Cdc42-GFP. Four chlamydial ribosomal proteins (two of the small and two of the large subunit) and one recombinase interacted with Cdc42-GFP (Table 3). Since they are not present in uninfected cells, they yielded the highest changing "ratios", which are in fact not to be understood as real ratios. One of the ribosomal proteins (CTL0774) and the recombinase (CTL0018) even bound with higher affinity to Cdc42-GFP than to GFP only. However, ribosomal proteins are common contaminants of mass spectrometry approaches (perhaps because they are still attached to nascent proteins), as are heat shock proteins, keratins (not including keratins 8 and 18) and tubulins (Keller et al., 2008). Recombinase A is involved in homologous recombination but also in stress response. Therefore, these bacterial interactions could result from non-specific binding. If, nevertheless, these binding changes were designated specific interactions, due to the missing connection of these proteins to migratory processes they were not considered as candidates.

The question emerged whether chlamydial proteins were sufficiently labeled during the preceding cell culture because the infection is introduced after most of the labeling is completed (the last 24 h of a two-week period). On the other hand, *Chlamydia* divide and grow very rapidly in the cells and produce a multiple of the original infectious dose in little time. During this development, they incorporate plenty of host cell amino acids (Moulder, 1991). Although different serovars show different amino acid requirements of the culture media and it is not yet clear which fraction is provided by the host cell, it is unlikely that the labeling was insufficient considering the high dependency of *Chlamydia* on host cell nutrients in combination with the high intracellular replication rate. It rather could indicate that Cdc42 regulation (redistribution and activation) is not achieved by direct binding but could happen via the modulation of host cell factors. Superordinate GAPs and GEFs might provide the level on which this is achieved.

In the future, the binding of candidates of this kind of interaction proteomics approach could be validated for example via coimmunoprecipitation. Increased or decreased binding of a certain protein could besides be a result of altered expression levels after infection. These could be checked by comparing the amounts of the respective protein in uninfected and infected lysates. A bias caused by overexpression is always possible and interactions would best be characterized in a reciprocal experiment where bait protein and interacting protein are swapped. Also, candidates could be computationally screened for the CRIB (Cdc42/Rac interactive binding) domain which is described as one structural motif mediating interactions of Cdc42 and Rac (Drechsel, 1995).

Taken together, many protein-protein interactions of Cdc42 were altered upon infection. This shows how fundamentally *Chlamydia* might manipulate individual protein functions of cellular

regulators. Migration-wise, almost all interactions found in this approach decreased after infection. The migration defect caused by infection is likely to be a multifactorial process and all candidates could contribute in their own way to the ultimate phenotype. The precise mechanism by which this occurs requires further investigation.

4.4 Conclusions and outlook

This work could show that the chlamydial protease CPAF induces Golgi fragmentation by processing of golgin-84. This ensures lipid supply and promotes reproduction of the bacteria inside their membrane-enclosed niche. Therefore, CPAF function is essential for *Chlamydia* infection. Whether golgin-84 processing is carried out in a direct or indirect mechanism remains to be determined.

Furthermore, the major consequence of Golgi fragmentation for the host cell could be characterized. Cells whose Golgi apparatus has been fragmented are incapable of migration because the Golgi apparatus cannot be reoriented to reach a polarized cell state. The effect is dependent on the infectious dose but not on proliferation. The defects of infected cells are phenocopied by uninfected cells with a fragmented Golgi after golgin-84 knockdown. Golgi stabilization via CPAF inhibition or knockdown of Rab11 can rescue polarization, but whether the possibility exists to restore migration remains unknown.

Lastly, it could be shown that *Chlamydia* can influence cell polarity on additional levels including Cdc42 redistribution and modulation of downstream effectors. Identifying which roles the individual effectors play in the migration of infected cells is a task that will be addressed in the future.

The identification of CPAF as an essential factor for *Chlamydia* survival could be of relevance for therapeutic treatment. If WEHD administration could be shown to arrest bacterial development and prevent propagation of the infection *in vivo*, it might be a suitable candidate for an anti-chlamydial drug.

An influence of intracellular infections on host cell motility has been described for other human pathogens and different biological consequences have been associated. *Helicobacter* infection reduces the number of focal adhesions and lamellipodia, impairing adhesion and migration, which is thought to promote gastric tissue damage and ulceration (Moese et al., 2007). *Toxoplasma* has been shown to inhibit polarization of MEFs by capturing organelles, including the centrosome, to the parasitophorous vacuole and causing a "frozen polarity" state that prevents migration (Wang et al., 2010). In dendritic cells and primary microglia, *Toxoplasma* induces transmigration and hypermobility to facilitate dissemination in the brain, presumably by a translocated parasitic effector (Lambert et al., 2006; Dellacasa-Lindberg et al., 2011). The *Salmonella* type three effector SseI is required for long-term systemic infections and inhibits migration of primary macrophages and dendritic cells, probably to promote immune evasion (McLaughlin et al., 2009).

In *Chlamydia* infection, defective migration could have serious consequences for the infected tissue because it is a part of the wound healing process. Inefficient epithelial healing is an

important hallmark of chlamydial pathology. An epithelial wound is not considered "healed" until it has been reepithelialized by motile cells (Gurtner et al., 2008). The two most severe disease outcomes are characterized by tissue scarring. Trachoma arises through wounding of the conjunctiva by the eyelashes and subsequent scarring (Burton, 2007) and tubal infertility in *Chlamydia*-infected women begins with damage of the inflamed tissue whereafter reinfections cause fibrosis and scarring, eventually leading to tubal occlusion (Van Voorhis et al., 1997). The quantitative involvement of these symptoms either directly or indirectly caused by impaired cell migration remains to be investigated. Consequently, the elucidation of migration inhibition by *Chlamydia* infection would surely be of therapeutical value. If scarring could be prevented in patients, the disease outcome would be greatly attenuated.

Novel findings have furthermore provided a connection between CPAF and host cell migration. CPAF was shown to cleave nectin-1, a protein found in cell-cell contacts (Sun and Schoborg, 2009). Collective migration is not possible without the connection of neighboring cells and therefore, CPAF activity could be part of the disturbed migration response. Hypothetically, the "frozen" state facilitates the complete conquest of the host cell by the bacteria and makes it easier for them to remodel and grow, converting it into a habitat that is forced to abandon its original purpose to meet the demands of the resident.

Appendix

Protein-protein interaction profile of Cdc42-GFP in infected compared to uninfected cells

Gene Name	Protein Description	Protein ID	Log2-fold interaction compared to GFP only
CDC42	Cell division control protein 42	B4E1U9	3,76
IQGAP1	Ras GTPase-activating-like protein IQGAP1	P46940	3,19
CTL0018	*Recombinase A (recA) {Chlamydia trachomatis 434/Bu}*		*2,62*
EFHD2	EF-hand domain-containing protein D2	Q96C19	2,50
ATP5A1	ATP synthase subunit alpha	P25705	2,46
CTL0774	*SSU ribosomal protein S5P (rpsE) {Chlamydia trachomatis 434/Bu}*		*1,99*
ACTA1	Actin, alpha skeletal muscle	P68133	1,93
ACTN4	Alpha-actinin-4	O43707	1,91
HNRNPC	Heterogeneous nuclear ribonucleoproteins C1/C2	P07910-1	1,80
ACTG1	Actin, cytoplasmic	P63261	1,78
LIMA1	LIM domain and actin-binding protein 1	Q53GG0	1,72
HNRNPAB	Heterogeneous nuclear ribonucleoprotein A/B	Q99729-2	1,65
SLC25A6	ADP/ATP translocase 3	P12236	1,60
PTBP1	Polypyrimidine tract-binding protein 1	Q9BUQ0	1,54
CORO1C	Coronin-1C	A7MAP0	1,40
CTL0574	*Translation elongation factor Tu (tufA) {Chlamydia trachomatis 434/Bu}*		*1,37*
TPM3	Tropomyosin alpha-3 chain	P06753-2	1,34
PABPC1	Isoform 1 of Polyadenylate-binding protein 1	P11940-1	1,31
HSP60	60 kDa heat shock protein	P10809	1,28
MYO1B	Myosin-Ib	O43795-1	1,23
CALM1	Calmodulin-1	A8K1M2	1,22
POLDIP3	Polymerase delta-interacting protein 3	B4E0L0	1,21
MYL6	Myosin light polypeptide 6	B7Z6Z4	1,20
ATP5B	ATP synthase subunit beta	P06576	1,14
MYH9	Myosin-9	P35579-1	1,11
DNAJA3	DnaJ homolog subfamily A member 3	Q96EY1-1	1,11
HNRNPA2B1	Heterogeneous nuclear ribonucleoproteins A2/B1	P22626-1	1,05
DNAJA1	DnaJ homolog subfamily A member 1	P31689	1,04
MYL12B	Myosin regulatory light chain 12B	Q53HL1	1,02
TUBA1B	Tubulin alpha-1B chain	P68363	0,98
HNRNPA1	Heterogeneous nuclear ribonucleoprotein A1	P09651-1	0,95
KRT8	Keratin, type II cytoskeletal 8	P05787	0,91
HNRNPD	Heterogeneous nuclear ribonucleoprotein D0	Q14103-1	0,88
TUFM	Tu translation elongation factor, mitochondrial precursor	P49411	0,87
RPS26	40S ribosomal protein S26	P62854	0,85
TUBB	Tubulin, beta	B4DQN9	0,84
CD109	CD109 antigen	Q6YHK3-1	0,83
HNRNPA3	Heterogeneous nuclear ribonucleoprotein A3	P51991-1	0,81
NCL	Nucleolin	P19338	0,81
CTL0566	*DNA-directed RNA polymerase beta-prime chain (rpoC) {Chlamydia trachomatis 434/Bu}*		*0,73*
EWSR1	Ewing sarcoma breakpoint region 1	Q96MX4	0,61
BCLAF1	Bcl-2-associated transcription factor 1	Q9NYF8-1	0,59
SFPQ	Splicing factor, proline- and glutamine-rich	P23246-1	0,54
RPS27	Ribosomal protein S27	Q5T4L4	0,52
SNRPD2	Small nuclear ribonucleoprotein Sm D2	P62316	0,52
FGF2	Heparin-binding growth factor 2	P09038-4	0,51
NONO	Non-POU domain-containing octamer-binding protein	Q15233	0,50

PRMT3	Protein arginine N-methyltransferase 3	Q8WUV3	0,49
DDX1	ATP-dependent RNA helicase DDX1	Q92499	0,47
TAF15	TATA-binding protein-associated factor 2N	Q92804-1	0,45
THRAP3	Thyroid hormone receptor-associated protein 3	Q9Y2W1	0,44
ERH	Enhancer of rudimentary homolog	P84090	0,44
PPP1CA	Serine/threonine-protein phosphatase PP1-alpha catalytic subunit	Q07161	0,41
C22orf28	UPF0027 protein C22orf28	Q9Y3I0	0,38
G3BP2	Ras GTPase-activating protein-binding protein 2	Q9UN86-1	0,36
MYH10	Myosin-10	P35580-3	0,34
UBAP2L	Isoform 2 of Ubiquitin-associated protein 2-like	Q14157-1	0,34
SNRPB	Small nuclear ribonucleoprotein-associated proteins B and B'	P14678-3	0,34
GAR1	H/ACA ribonucleoprotein complex subunit 1	Q9NY12-1	0,33
ZC3H4	Zinc finger CCCH domain-containing protein 4	Q9UPT8	0,33
RBM3	Putative RNA-binding protein 3	P98179	0,32
FAM98A	FAM98A	Q8NCA5	0,31
CTL0769	*DNA-directed RNA polymerase alpha chain (rpoA) {Chlamydia trachomatis 434/Bu}*		*0,31*
EEF1A1	Elongation factor 1-alpha **1**	P68104	0,30
G3BP1	Ras GTPase-activating protein-binding protein 1	Q13283	0,28
PSPC1	Paraspeckle component 1	Q8WXF1-1	0,26
XRCC6	X-ray repair cross-complementing protein 6	P12956	0,24
RPS8	40S ribosomal protein S8	P62241	0,23
CIRBP	Cold-inducible RNA-binding protein	B3KT17	0,22
RPS15A	40S ribosomal protein S15a	P62244	0,21
SNRPD3	Small nuclear ribonucleoprotein Sm D3	P62318	0,20
HSPA8	Heat shock cognate 71 kDa protein	P11142-1	0,20
RPS2	40S ribosomal protein S2	P15880	0,20
THOC4	THO complex subunit 4	Q86V81	0,19
HSPA5	HSPA5	P11021	0,19
SNRPG	Small nuclear ribonucleoprotein G-like protein	C9J303	0,15
CAPRIN1	Caprin-1	Q14444-1	0,14
HIST1H2BN	Histone H2B type 1-N	B4DR52	0,14
RPS3	40S ribosomal protein S3	P23396	0,11
FUS	Fus-like protein (Fragment)	P35637-1	0,09
RPL27A	60S ribosomal protein L27a	P46776	0,09
RPS14	40S ribosomal protein S14	P62263	0,08
SNRPD1	Small nuclear ribonucleoprotein Sm D1	P62314	0,07
SAM68	KH domain-containing, RNA-binding, signal transduction-associated protein 1	Q07666-1	0,06
PPP1R10	Serine/threonine-protein phosphatase 1 regulatory subunit 10	Q96QC0	0,06
ILF2	Interleukin enhancer-binding factor 2	Q12905	0,03
HNRNPU	Heterogeneous nuclear ribonucleoprotein U	Q00839-1	0,03
HNRNPK	Heterogeneous nuclear ribonucleoprotein K	P61978-2	0,03
GTPBP4	Nucleolar GTP-binding protein 1	Q9BZE4	0,00
RBM26	RNA-binding protein 26	Q5T8P6-1	0,00

Table 2: Interactions of Cdc42-GFP compared to GFP only in *Chlamydia*-infected cells. List of proteins coprecipitated with Cdc42 less unspecific binders. Values of the binding's fold change are denoted as log 2 in order to represent unchanged binding with a value of 0 instead of 1.

Gene Name	Protein Description	Protein ID	Log2-fold change of interaction upon infection
CTL0770	*SSU ribosomal protein S11P (rpsK) {Chlamydia trachomatis 434/Bu}*		*7,64*
CTL0774	***SSU ribosomal protein S5P (rpsE) {Chlamydia trachomatis 434/Bu}***		***6,97***
CTL0018	***Recombinase A (recA) {Chlamydia trachomatis 434/Bu}***		***6,66***
CTL0789	*LSU ribosomal protein L1E (rplD) {Chlamydia trachomatis 434/Bu}*		*6,52*
CTL0676	*LSU ribosomal protein L27P (rpmA) {Chlamydia trachomatis 434/Bu}*		*6,18*
HSP60	**60 kDa heat shock protein**	**P10809**	**2,29**
NAT10	N-acetyltransferase 10	Q9H0A0	2,12
PRPF19	Pre-mRNA-processing factor 19	Q9UMS4	1,87
SNRPD1	**Small nuclear ribonucleoprotein Sm D1**	**P62314**	**1,78**
KRT9	Keratin, type I cytoskeletal 9	P35527	1,76
SNRPD2	**Small nuclear ribonucleoprotein Sm D2**	**P62316**	**1,75**
HNRNPU	**Heterogeneous nuclear ribonucleoprotein U**	**Q00839-1**	**1,67**
THRAP3	**Thyroid hormone receptor-associated protein 3**	**Q9Y2W1**	**1,34**
PKM2	Pyruvate kinase isozymes M1/M2	P14618-1	1,32
HNRNPR	Heterogeneous nuclear ribonucleoprotein R	O43390-1	1,26
DDX18	ATP-dependent RNA helicase DDX18	Q9NVP1	1,07
HIST1H2BN	**Histone H2B type 1-N**	**B4DR52**	**1,05**
DDX17	probable ATP-dependent RNA helicase DDX17	Q59F66	1,03
BCLAF1	Isoform 1 of Bcl-2-associated transcription factor 1	Q9NYF8-1	0,99
SNRPD3	**Small nuclear ribonucleoprotein Sm D3**	**P62318**	**0,94**
SAM68	**KH domain-containing, RNA-binding, signal transduction-associated protein 1**	**Q07666-1**	**0,91**
FXR1	Fragile X mental retardation syndrome-related protein 1	P51114-1	0,85
RPL12	Isoform 1 of 60S ribosomal protein L12	P30050-1	0,82
CPSF1	Cleavage and polyadenylation specificity factor subunit 1	Q10570	0,77
CDC42	**Cell division control protein 42**	**B4E1U9**	**0,75**
DDX5	Probable ATP-dependent RNA helicase DDX5	P17844	0,64
ATP5A1	**ATP synthase subunit alpha**	**P25705**	**0,63**
DNAJA1	**DnaJ homolog subfamily A member 1**	**P31689**	**0,60**
RBMX	Heterogeneous nuclear ribonucleoprotein G	P38159	0,57
MYL6	**Myosin light polypeptide 6**	**B7Z6Z4**	**0,55**
TUFM	**Tu translation elongation factor, mitochondrial precursor**	**P49411**	**0,51**
FMR1	Fragile X mental retardation 1 protein	Q06787-1	0,30
THOC4	**THO complex subunit 4**	**Q86V81**	**0,27**
SYNCRIP	Heterogeneous nuclear ribonucleoprotein Q	O60506-3	0,23
ACTG1	**Actin, cytoplasmic 2**	**P63261**	**0,11**
FUS	**Fus-like protein (Fragment)**	**P35637-1**	**0,11**
SFPQ	**Splicing factor, proline- and glutamine-rich**	**P23246-1**	**0,09**
MYL12B	**Myosin regulatory light chain 12B**	**Q53HL1**	**0,07**
DNAJA3	**DnaJ homolog subfamily A member 3**	**Q96EY1-1**	**0,01**
TUBB	**Tubulin, beta**	**B4DQN9**	**-0,03**
HNRNPK	**Heterogeneous nuclear ribonucleoprotein K**	**P61978-2**	**-0,11**
RPS12	40S ribosomal protein S12	P25398	-0,12
RPL3	60S ribosomal protein L3	P39023	-0,22
FBL	rRNA 2'-O-methyltransferase fibrillarin	P22087	-0,29

IQGAP1	**Ras GTPase-activating-like protein IQGAP1**	**P46940**	**-0,35**
NONO	**Non-POU domain-containing octamer-binding protein**	**Q15233**	**-0,38**
RPL23	60S ribosomal protein L23	P62829	-0,43
ZC3H4	**Zinc finger CCCH domain-containing protein 4**	**Q9UPT8**	**-0,44**
RPS18	40S ribosomal protein S18	P62269	-0,45
TUBA1B	**Tubulin alpha-1B chain**	**P68363**	**-0,45**
MYH9	**Myosin-9**	**P35579-1**	**-0,46**
RPS16	40S ribosomal protein S16	P62249	-0,53
RPS3A	40S ribosomal protein S3a	P61247	-0,59
RPS4X	40S ribosomal protein S4	P62701	-0,61
CIRBP	**Cold-inducible RNA-binding protein**	**B3KT17**	**-0,66**
RPS2	**40S ribosomal protein S2**	**P15880**	**-0,71**
RPL9	60S ribosomal protein L9	P32969	-0,74
RPL17P34	60S ribosomal protein L17	A8MU02	-0,74
EEF1A1	**Elongation factor 1-alpha 1**	**P68104**	**-0,76**
PSPC1	**Paraspeckle component 1**	**Q8WXF1-1**	**-0,77**
RPL10	Ribosomal protein L10	Q5HY50	-0,77
HSPA8	**Heat shock cognate 71 kDa protein**	**P11142-1**	**-0,92**
WDR82	WD repeat-containing protein 82	Q6UXN9	-0,95
RPL22	60S ribosomal protein L22	P35268	-1,01
HSPA9	Stress-70 protein	P38646	-1,08
EWSR1	**Ewing sarcoma breakpoint region 1 isoform 1**	**Q96MX4**	**-1,13**
C14orf166	UPF0568 protein C14orf166	Q9Y224	-1,18
ILF3	Interleukin enhancer-binding factor 3	Q12906-4	-1,19
DDX1	**ATP-dependent RNA helicase DDX1**	**Q92499**	**-1,23**
C22orf28	**UPF0027 protein C22orf28**	**Q9Y3I0**	**-1,26**
RPS17	40S ribosomal protein S17	P08708	-1,29
RPS3	**40S ribosomal protein S3**	**P23396**	**-1,36**
DDX3X	ATP-dependent RNA helicase DDX3X	O00571	-1,54
HNRNPC	**Heterogeneous nuclear ribonucleoproteins C1/C2**	**P07910-1**	**-1,59**
RPS15A	**40S ribosomal protein S15a**	**P62244**	**-1,64**
RPS7	40S ribosomal protein S7	P62081	-1,69
UBAP2L	**Ubiquitin-associated protein 2-like**	**Q14157-1**	**-1,79**
FAM98A	**FAM98A**	**Q8NCA5**	**-1,87**
HNRNPA2B1	**Heterogeneous nuclear ribonucleoproteins A2/B1**	**P22626-1**	**-1,95**
HNRNPA1	**Heterogeneous nuclear ribonucleoprotein A1**	**P09651-1**	**-2,00**
POLDIP3	**Polymerase delta-interacting protein 3**	**B4E0L0**	**-2,19**
RBM3	Putative RNA-binding protein 3	P98179	-2,31
HNRNPA3	**Heterogeneous nuclear ribonucleoprotein A3**	**P51991-1**	**-2,34**
NCL	**Nucleolin**	**P19338**	**-2,61**
RBM14	RNA-binding protein 14	Q96PK6-1	-2,77
PTBP1	**Polypyrimidine tract-binding protein 1**	**Q9BUQ0**	**-2,91**
KRT8	**Keratin, type II cytoskeletal 8**	**P05787**	**-3,20**
HNRNPAB	**Heterogeneous nuclear ribonucleoprotein A/B**	**Q99729-2**	**-3,28**
YBX1	Nuclease-sensitive element-binding protein 1	P67809	-3,80
G3BP2	**Ras GTPase-activating protein-binding protein 2**	**Q9UN86-1**	**-4,44**
LSM12	LSM12	Q3MHD2-2	-4,47
NUFIP2	Nuclear fragile X mental retardation-interacting protein 2	Q7Z417	-4,57
VIM	Vimentin	P08670	-4,66
CAPRIN1	**Caprin-1**	**Q14444-1**	**-4,96**
G3BP1	**Ras GTPase-activating protein-binding protein 1**	**Q13283**	**-4,98**
PABPC1	**Polyadenylate-binding protein 1**	**P11940-1**	**-5,09**
PABPC4	Polyadenylate-binding protein 4	Q3B867	-5,11

Table 3: Interactions of Cdc42-GFP in *Chlamydia*-infected cells compared to uninfected cells. List of proteins coprecipitated with Cdc42-GFP in infected cells, normalized to uninfected cells. Values of the binding's fold change are denoted as log 2 in order to represent unchanged binding with a value of 0 instead of 1. The overlap with Table 2 is shown in bold face.

Abbreviations

AB	aberrant body
AHT	anhydrotetracycline
Arf	ADP-ribosylation factor
Arl	ADP-ribosylation factor-like
Arp	actin-related protein complex
ATCC	american tissue culture collection
ATP	adenosine triphosphate
BCA	bicinchoninic acid
Bim	Bcl-2-like protein 11 isoform
BSA	bovine serum albumin
CCD	charge-coupled device
Cdc42	cell division cycle 42
CLIP	cytoplasmic linker protein
CM	coumermycin
cm	centimeter
CO_2	carbon dioxide
CPAF	*Chlamydia* protease-like activity factor
CRIB	Cdc42/Rac interactive binding
Ctr	*Chlamydia trachomatis*
Dlg	discs large
DLC	deleted in liver cancer
DMEM	Dulbecco's modified Eagle medium
DNA	desoxyribonucleic acid
e.g.	*exempli gratia*
EB	elementary body
ECL	enhanced chemiluminescence
ECM	extracellular matrix
EDTA	ethylenediaminetetraacetic acid
EEF	eukaryotic elongation factor
EGF	epidermal growth factor
ER	endoplasmic reticulum

ERK	extracellular signal-regulated kinase
et al.	*et alii*
FAK	focal adhesion kinase
FCS	fetal calf serum
g	gram
g	times gravity
G	gauge
G3BP	GTPase activating protein binding protein
GA	Golgi apparatus
GAP	GTPase activating protein
GDI	guanosine nucleotide dissociation inhibitor
(e)GFP	(enhanced) green fluorescent protein
GM	Golgi matrix (protein)
GMAP	Golgi microtubule-associated protein
GPP	Golgi glycoprotein
°C	degrees Celsius
GRASP	Golgi reassembly stacking protein
GTP	guanosine triphosphate
gyrB	gyrase B
h	hour
h.i.	heat inactivated
H2O	water
HCl	hydrochloric acid
HNRNP	heterogeneous nuclear ribonucleoprotein
HRP	horseradish peroxidase
Hsc	heat shock cognate
Hsp	heat shock protein
HtrA	high temperature requirement factor A
ID	identification
IFU	inclusion forming units
IgG	immunoglobulin G
Inc	inclusion protein
IQGAP	IQ motif containing GTPase activating protein
IS	inhibitory segment
KCl	potassium chloride
kDa	kilodalton
KH domain	K homology domain

KH2PO4	potassium phosphate
l	liter
LC-MS/MS	liquid chromatography-tandem mass spectrometry
LE	leading edge
LGV	lymphogranuloma venereum
log	logarithm
LSCM	laser scanning confocal microscope
Luci	luciferase
M	molar
MDC	Max Delbrück Center
mg	milligram
MHC	major histocompatiblity complex
min	minute
ml	milliliter
mm	millimeter
mM	millimolar
MMC	mitomycin C
MOI	multiplicity of infection
MOMP	major outer membrane protein
mRNA	messenger RNA
MTOC	microtubule organizing center
μg	microgram
μl	microliter
μm	micrometer
μM	micromolar
NA	numeric aperture
Na2HPO4	disodium phosphate
NaCl	sodium chloride
NFκB	nuclear factor kappa-light-chain-enhancer of activated B cells
ng	nanogram
nm	nanometer
nM	nanomolar
NP-40	nonyl phenoxypolyethoxylethanol
p.i.	*post infectionem*
PAK	P21 protein (Cdc42/Rac)-activated kinase
PCR	polymerase chain reaction

PBD	protein binding domain
PBS	phosphate buffered saline
PFA	paraformaldehyde
PI3K	phosphoinositide-3-kinase
PIP	phosphoinositol phosphate
PTBP	polypyrimidine tract bindin protein
PTEN	phosphatase and tensin homolog
PVDF	polyvinylidene fluoride
Rab	member RAS oncogene family
Rac	Ras-related C3 botulinum toxin substrate
Ras	rat sarcoma oncogene
RFX	regulatory factor X
RB	reticulate body
Rho	Ras homolog
RIPA	radioimmunoprecipitation assay
RNA	ribonucleic acid
rRNA	ribosomal RNA
RT	room temperature
S	Svedberg
Sam	KH domain containing, RNA binding, signal transduction associated
SD	standard deviation
SDS	sodium dodecyl sulfate
SEM	standard error of the mean
SH domain	Src homology domain
shRNA	short hairpin RNA
SILAC	stable isotope labeling with amino acids in cell culture
siRNA	small interfering RNA
SM	sphingomyelin
SNARE	SNAP (Soluble NSF Attachment Protein) Receptor
sp.	species
SPG	accharose phosphate glutamic acid
Src	sarcoma
Tarp	translocated actin-recruiting phosphoprotein
TBS	Tris buffered saline
TBST	TBS with Tween 20

TE	trailing edge
Tet	tetracycline
Tsp	tail-specific protease
TTS	type three secretion system
t_x	time point
WASP/WAVE	Wiskott–Aldrich syndrome protein
WHO	world health organization

Bibliography

Abdul-Sater, A. a., Koo, E., Häcker, G., and Ojcius, D. M. Inflammasome-dependent caspase-1 activation in cervical epithelial cells stimulates growth of the intracellular pathogen Chlamydia trachomatis. *The Journal of biological chemistry*, 284 (39):26789–96, Sept. 2009. ISSN 1083-351X. doi: 10.1074/jbc.M109.026823. URL http://www.pubmedcentral.nih.gov/articlerender.fcgi?artid=2785367&tool=pmcentrez&rendertype=abstract.

Abu el Asrar, A. M., Geboes, K., Tabbara, K. F., Al-Kharashi, S. A., Missotten, L., and Desmet, V. Immunopathogenesis of conjunctival scarring in trachoma. *Eye (London, England)*, 12 (Pt 3a:453–60, Jan. 1998. ISSN 0950-222X. URL http://www.ncbi.nlm.nih.gov/pubmed/9775249.

Al-Younes, H. M., Rudel, T., Brinkmann, V., Szczepek, A. J., and Meyer, T. F. Low iron availability modulates the course of Chlamydia pneumoniae infection. *Cellular microbiology*, 3(6):427–37, June 2001. ISSN 1462-5814. URL http://www.ncbi.nlm.nih.gov/pubmed/11422085.

Arnold, R., Brandmaier, S., Kleine, F., Tischler, P., Heinz, E., Behrens, S., Niinikoski, A., Mewes, H.-W., Horn, M., and Rattei, T. Sequence-based prediction of type III secreted proteins. *PLoS pathogens*, 5(4):e1000376, Apr. 2009. ISSN 1553-7374. doi: 10.1371/journal.ppat.1000376. URL http://www.pubmedcentral.nih.gov/articlerender.fcgi?artid=2669295&tool=pmcentrez&rendertype=abstract.

Arthur, W. T., Noren, N. K., and Burridge, K. Regulation of Rho family GTPases by cell-cell and cell-matrix adhesion. *Biological research*, 35(2):239–46, Jan. 2002. ISSN 0716-9760. URL http://www.ncbi.nlm.nih.gov/pubmed/12415742.

Babic, I., Cherry, E., and Fujita, D. J. SUMO modification of Sam68 enhances its ability to repress cyclin D1 expression and inhibits its ability to induce apoptosis. *Oncogene*, 25(36): 4955–64, Aug. 2006. ISSN 0950-9232. doi: 10.1038/sj.onc.1209504. URL http://www.ncbi.nlm.nih.gov/pubmed/16568089.

Banerji, S., Aurass, P., and Flieger, A. The manifold phospholipases A of Legionella pneumophila - identification, export, regulation, and their link to bacterial virulence. *International journal of medical microbiology : IJMM*, 298(3-4):169–81, Apr. 2008. ISSN 1618-0607. doi: 10.1016/j.ijmm.2007.11.004. URL http://www.ncbi.nlm.nih.gov/pubmed/18178130.

Bannantine, J. P., Griffiths, R. S., Viratyosin, W., Brown, W. J., and Rockey, D. D. A secondary structure motif predictive of protein localization to the chlamydial inclusion membrane. *Cellular microbiology*, 2(1):35–47, Mar. 2000. ISSN 1462-5814. doi: 10.1046/j.1462-5822.2000.00029.x. URL http://doi.wiley.com/10.1046/j.1462-5822.2000.00029.xhttp://www.ncbi.nlm.nih.gov/pubmed/11207561.

Banno, A. and Ginsberg, M. H. Integrin activation. *Biochemical Society transactions*, 36(Pt 2):229–34, Apr. 2008. ISSN 0300-5127. doi: 10.1042/BST0360229. URL http://www.pubmedcentral.nih.gov/articlerender.fcgi?artid=2588347&tool=pmcentrez&rendertype=abstract.

Bascom, R. A., Srinivasan, S., and Nussbaum, R. L. Identification and characterization of golgin-84, a novel Golgi integral membrane protein with a cytoplasmic coiled-coil domain. *The Journal of biological chemistry*, 274(5):2953–62, Jan. 1999. ISSN 0021-9258. URL http://www.ncbi.nlm.nih.gov/pubmed/9915833.

Beeckman, D. S. A. and Vanrompay, D. C. G. Zoonotic Chlamydophila psittaci infections from a clinical perspective. *Clinical microbiology and infection : the official publication of the European Society of Clinical Microbiology and Infectious Diseases*, 15(1):11–7, Jan. 2009. ISSN 1469-0691. doi: 10.1111/j.1469-0691.2008.02669.x. URL http://www.ncbi.nlm.nih.gov/pubmed/19220335.

Betts, H. J., Wolf, K., and Fields, K. A. Effector protein modulation of host cells: examples in the Chlamydia spp. arsenal. *Current opinion in microbiology*, 12(1):81–7, Feb. 2009. ISSN 1879-0364. doi: 10.1016/j.mib.2008.11.009. URL http://dx.doi.org/10.1016/j.mib.2008.11.009.

Binet, R. and Maurelli, A. T. Transformation and isolation of allelic exchange mutants of Chlamydia psittaci using recombinant DNA introduced by electroporation. *Proceedings of the National Academy of Sciences of the United States of America*, 106(1):292–7, Jan. 2009. ISSN 1091-6490. doi: 10.1073/pnas.0806768106. URL http://www.pubmedcentral.nih.gov/articlerender.fcgi?artid=2629194&tool=pmcentrez&rendertype=abstract.

Bisel, B., Wang, Y., Wei, J.-H., Xiang, Y., Tang, D., Miron-Mendoza, M., Yoshimura, S.-i., Nakamura, N., and Seemann, J. ERK regulates Golgi and centrosome orientation towards the leading edge through GRASP65. *The Journal of cell biology*, 182(5):837–43, Sept. 2008. ISSN 1540-8140. doi: 10.1083/jcb.200805045. URL http://www.ncbi.nlm.nih.gov/pubmed/18762583.

Boddicker, J. D. and Jones, B. D. Lon protease activity causes down-regulation of Salmonella pathogenicity island 1 invasion gene expression after infection of epithelial cells. *Infection and immunity*, 72(4):2002–13, Apr. 2004. ISSN 0019-9567. URL http://www.pubmedcentral.nih.gov/articlerender.fcgi?artid=375200&tool=pmcentrez&rendertype=abstract.

Bordeleau, F., Galarneau, L., Gilbert, S., Loranger, A., and Marceau, N. Keratin 8/18 modulation of protein kinase C-mediated integrin-dependent adhesion and migration of liver epithelial cells. *Molecular biology of the cell*, 21(10):1698–713, May 2010. ISSN 1939-4586. doi: 10.1091/mbc.E09-05-0373. URL http://www.pubmedcentral.nih.gov/articlerender.fcgi?artid=2869376&tool=pmcentrez&rendertype=abstract.

Burton, M. J. Trachoma: an overview. *British medical bulletin*, 84:99–116, Jan. 2007. ISSN 0007-1420. doi: 10.1093/bmb/ldm034. URL http://www.ncbi.nlm.nih.gov/pubmed/18175788.

Bush, R. M. and Everett, K. D. Molecular evolution of the Chlamydiaceae. *International journal of systematic and evolutionary microbiology*, 51(Pt 1):203–20, Jan. 2001. ISSN 1466-5026. URL http://www.ncbi.nlm.nih.gov/pubmed/11211261.

Capmany, A., Leiva, N., and Damiani, M. T. Golgi-associated Rab14, a new regulator for Chlamydia trachomatis infection outcome. *Communicative & integrative biology*, 4(5):590–3, Sept. 2011. ISSN 1942-0889. doi: 10.4161/cib.4.5.16594. URL http://www.ncbi.nlm.nih.gov/pubmed/22046472.

Carabeo, R. A., Grieshaber, S. S., Hasenkrug, A., Dooley, C., and Hackstadt, T. Requirement for the Rac GTPase in Chlamydia trachomatis invasion of non-phagocytic cells. *Traffic (Copenhagen, Denmark)*, 5(6):418–25, June 2004. ISSN 1398-9219. doi: 10.1111/j.1398-9219.2004.00184.x. URL http://www.ncbi.nlm.nih.gov/pubmed/15117316.

Chen, D., Lei, L., Flores, R., Huang, Z., Wu, Z., Chai, J., and Zhong, G. Autoprocessing and self-activation of the secreted protease CPAF in Chlamydia-infected cells. *Microbial*

pathogenesis, 49(4):164–73, May 2010a. ISSN 1096-1208. doi: 10.1016/j.micpath.2010.05.008. URL http://www.ncbi.nlm.nih.gov/pubmed/20510344.

Chen, D., Lei, L., Lu, C., Flores, R., DeLisa, M. P., Roberts, T. C., Romesberg, F. E., and Zhong, G. Secretion of the chlamydial virulence factor CPAF requires the Sec-dependent pathway. *Microbiology (Reading, England)*, 156 (Pt 10):3031–40, Oct. 2010b. ISSN 1465-2080. doi: 10.1099/mic.0.040527-0. URL http://www.pubmedcentral.nih.gov/articlerender.fcgi?artid=3068695&tool=pmcentrez&rendertype=abstract.

Cheng, C. and Sharp, P. A. Regulation of CD44 alternative splicing by SRm160 and its potential role in tumor cell invasion. *Molecular and cellular biology*, 26 (1):362–70, Jan. 2006. ISSN 0270-7306. doi: 10.1128/MCB.26.1.362-370.2006. URL http://www.pubmedcentral.nih.gov/articlerender.fcgi?artid=1317625&tool=pmcentrez&rendertype=abstract.

Cheng, W., Shivshankar, P., Li, Z., Chen, L., Yeh, I.-T., and Zhong, G. Caspase-1 contributes to Chlamydia trachomatis-induced upper urogenital tract inflammatory pathologies without affecting the course of infection. *Infection and immunity*, 76(2):515–22, Feb. 2008. ISSN 1098-5522. doi: 10.1128/IAI.01064-07. URL http://iai.asm.org/cgi/content/abstract/76/2/515.

Cheung, H. C., Hai, T., Zhu, W., Baggerly, K. a., Tsavachidis, S., Krahe, R., and Cote, G. J. Splicing factors PTBP1 and PTBP2 promote proliferation and migration of glioma cell lines. *Brain : a journal of neurology*, 132(Pt 8):2277–88, Aug. 2009. ISSN 1460-2156. doi: 10.1093/brain/awp153. URL http://www.ncbi.nlm.nih.gov/pubmed/19506066.

Chiu, R., Novikov, L., Mukherjee, S., and Shields, D. A caspase cleavage fragment of p115 induces fragmentation of the Golgi apparatus and apoptosis. *The Journal of cell biology*, 159(4):637–48, Nov. 2002. ISSN 0021-9525. doi: 10.1083/jcb.200208013. URL http://www.pubmedcentral.nih.gov/articlerender.fcgi?artid=2173109&tool=pmcentrez&rendertype=abstract.

Christian, J., Vier, J., Paschen, S. A., and Häcker, G. Cleavage of the NF-{kappa}B family protein p65/RelA by the chlamydial protease-like activity factor (CPAF) impairs proinflammatory signaling in cells infected with Chlamydiae. *The Journal of biological chemistry*, 285(53):41320–7, Dec. 2010. ISSN 1083-351X. doi: 10.1074/jbc.M110.152280. URL http://www.pubmedcentral.nih.gov/articlerender.fcgi?artid=3009857&tool=pmcentrez&rendertype=abstract.

Christian, J. G., Heymann, J., Paschen, S. A., Vier, J., Schauenburg, L., Rupp, J., Meyer, T. F., Häcker, G., and Heuer, D. Targeting of a Chlamydial Protease Impedes Intracellular Bacterial Growth. *PLoS Pathogens*, 7(9):e1002283, Sept. 2011. ISSN 1553-7374. doi: 10.1371/journal.ppat.1002283. URL http://dx.plos.org/10.1371/journal.ppat.1002283.

Churin, Y., Kardalinou, E., Meyer, T. F., and Naumann, M. Pathogenicity island-dependent activation of Rho GTPases Rac1 and Cdc42 in Helicobacter pylori infection. *Molecular Microbiology*, 40(4):815–823, May 2001. ISSN 0950-382X. doi: 10.1046/j.1365-2958.2001.02443.x. URL http://doi.wiley.com/10.1046/j.1365-2958.2001.02443.x.

Clausen, J. D., Christiansen, G., Holst, H. U., and Birkelund, S. Chlamydia trachomatis utilizes the host cell microtubule network during early events of infection. *Molecular Microbiology*, 25(03):441–449, Aug. 1997. ISSN 0950382X. doi: 10.1046/j.1365-2958.1997.4591832.x. URL http://doi.wiley.com/10.1046/j.1365-2958.1997.4591832.x.

Clausen, T., Southan, C., and Ehrmann, M. The HtrA family of proteases: implications for protein composition and cell fate. *Molecular cell*, 10(3):443–55, Sept. 2002. ISSN 1097-2765. URL http://www.ncbi.nlm.nih.gov/pubmed/12408815.

Clifton, D. R., Fields, K. A., Grieshaber, S. S., Dooley, C. A., Fischer, E. R., Mead, D. J., Carabeo, R. A., and Hackstadt, T. A chlamydial type III translocated protein is tyrosine-phosphorylated at the site of entry and associated with recruitment of actin. *Proceedings of the National Academy of Sciences of the United States of America*, 101(27):10166–71, July 2004. ISSN 0027-8424. doi: 10.1073/pnas.0402829101. URL http://www.pubmedcentral.nih.gov/articlerender.fcgi?artid=454183&tool=pmcentrez&rendertype=abstract.

Coates, T. D., Watts, R. G., Hartman, R., and Howard, T. H. Relationship of F-actin distribution to development of polar shape in human polymorphonuclear neutrophils. *The Journal of cell biology*, 117(4):765–74, May 1992. ISSN 0021-9525. URL http://www.pubmedcentral.nih.gov/articlerender.fcgi?artid=2289466&tool=pmcentrez&rendertype=abstract.

Colanzi, A., Sutterlin, C., and Malhotra, V. RAF1-activated MEK1 is found on the Golgi apparatus in late prophase and is required for Golgi complex fragmentation in mitosis. *The Journal of cell biology*, 161(1):27–32, Apr. 2003. ISSN 0021-9525. doi: 10.1083/jcb.200208099. URL http://www.pubmedcentral.nih.gov/articlerender.fcgi?artid=2172875&tool=pmcentrez&rendertype=abstract.

Collingro, A., Tischler, P., Weinmaier, T., Penz, T., Heinz, E., Brunham, R. C., Read, T. D., Bavoil, P. M., Sachse, K., Kahane, S., Friedman, M. G., Rattei, T., Myers, G. S. A., and Horn, M. Unity in Variety - the Pan-Genome of the Chlamydiae. *Molecular biology and evolution*, 28(11):1–47, June 2011. ISSN 1537-1719. doi: 10.1093/molbev/msr161. URL http://www.ncbi.nlm.nih.gov/pubmed/21690563.

Condeelis, J. Life at the leading edge: the formation of cell protrusions. *Annual review of cell biology*, 9:411–44, Jan. 1993. ISSN 0743-4634. doi: 10.1146/annurev.cb.09.110193.002211. URL http://www.ncbi.nlm.nih.gov/pubmed/8280467.

Coyle, J. H., Guzik, B. W., Bor, Y.-C., Jin, L., Eisner-Smerage, L., Taylor, S. J., Rekosh, D., and Hammarskjöld, M.-L. Sam68 enhances the cytoplasmic utilization of intron-containing RNA and is functionally regulated by the nuclear kinase Sik/BRK. *Molecular and cellular biology*, 23(1):92–103, Jan. 2003. ISSN 0270-7306. URL http://www.pubmedcentral.nih.gov/articlerender.fcgi?artid=140664&tool=pmcentrez&rendertype=abstract.

Dautry-Varsat, A., Subtil, A., and Hackstadt, T. Recent insights into the mechanisms of Chlamydia entry. *Cellular microbiology*, 7(12):1714–22, Dec. 2005. ISSN 1462-5814. doi: 10.1111/j.1462-5822.2005.00627.x. URL http://www.ncbi.nlm.nih.gov/pubmed/16309458.

de Hoog, C. L., Foster, L. J., and Mann, M. RNA and RNA binding proteins participate in early stages of cell spreading through spreading initiation centers. *Cell*, 117(5):649–62, May 2004. ISSN 0092-8674. URL http://www.ncbi.nlm.nih.gov/pubmed/15163412.

Del Nery, E., Miserey-Lenkei, S., Falguières, T., Nizak, C., Johannes, L., Perez, F., and Goud, B. Rab6A and Rab6A' GTPases play non-overlapping roles in membrane trafficking. *Traffic (Copenhagen, Denmark)*, 7(4):394–407, Apr. 2006. ISSN 1398-9219. doi: 10.1111/j.1600-0854.2006.00395.x. URL http://www.ncbi.nlm.nih.gov/pubmed/16536738.

del Pozo, M. A., Price, L. S., Alderson, N. B., Ren, X. D., and Schwartz, M. A. Adhesion to the extracellular matrix regulates the coupling of the small GTPase Rac to its effector PAK. *The EMBO journal*, 19(9):2008–14, May 2000. ISSN 0261-4189. doi: 10.1093/emboj/19.9.2008. URL http://www.pubmedcentral.nih.gov/articlerender.fcgi?artid=305684&tool=pmcentrez&rendertype=abstract.

Delevoye, C., Nilges, M., Dehoux, P., Paumet, F., Perrinet, S., Dautry-Varsat, A., and Subtil, A. SNARE protein mimicry by an intracellular bacterium. *PLoS pathogens*,

4(3):e1000022, Mar. 2008. ISSN 1553-7374. doi: 10.1371/journal.ppat.1000022. URL http://www.pubmedcentral.nih.gov/articlerender.fcgi?artid=2265411&tool=pmcentrez&rendertype=abstract.

Dellacasa-Lindberg, I., Fuks, J. M., Arrighi, R. B. G., Lambert, H., Wallin, R. P. A., Chambers, B. J., and Barragan, A. Migratory activation of primary cortical microglia upon infection with Toxoplasma gondii. *Infection and immunity*, 79(8):3046–52, Aug. 2011. ISSN 1098-5522. doi: 10.1128/IAI.01042-10. URL http://www.pubmedcentral.nih.gov/articlerender.fcgi?artid=3147544&tool=pmcentrez&rendertype=abstract.

Derré, I., Swiss, R., and Agaisse, H. The Lipid Transfer Protein CERT Interacts with the Chlamydia Inclusion Protein IncD and Participates to ER-Chlamydia Inclusion Membrane Contact Sites. *PLoS Pathogens*, 7(6):e1002092, June 2011. ISSN 1553-7374. doi: 10.1371/journal.ppat.1002092. URL http://www.pubmedcentral.nih.gov/articlerender.fcgi?artid=3121800&tool=pmcentrez&rendertype=abstract.

Devreotes, P. and Janetopoulos, C. Eukaryotic chemotaxis: distinctions between directional sensing and polarization. *The Journal of biological chemistry*, 278(23):20445–8, June 2003. ISSN 0021-9258. doi: 10.1074/jbc.R300010200. URL http://www.ncbi.nlm.nih.gov/pubmed/12672811.

Diao, A., Rahman, D., Pappin, D. J. C., Lucocq, J., and Lowe, M. The coiled-coil membrane protein golgin-84 is a novel rab effector required for Golgi ribbon formation. *The Journal of cell biology*, 160(2):201–12, Jan. 2003. ISSN 0021-9525. doi: 10.1083/jcb.200207045. URL http://www.pubmedcentral.nih.gov/articlerender.fcgi?artid=2172652&tool=pmcentrez&rendertype=abstract.

Dong, F., Su, H., Huang, Y., Zhong, Y., and Zhong, G. Cleavage of host keratin 8 by a Chlamydia-secreted protease. *Infection and immunity*, 72(7):3863–8, July 2004. ISSN 0019-9567. doi: 10.1128/IAI.72.7.3863-3868.2004. URL http://www.pubmedcentral.nih.gov/articlerender.fcgi?artid=427399&tool=pmcentrez&rendertype=abstract.

Drechsel, D. A Conserved Binding Motif Defines Numerous Candidate Target Proteins for Both Cdc42 and Rac GTPases. *Journal of Biological Chemistry*, 270(49):29071–29074, Dec. 1995. ISSN 00219258. doi: 10.1074/jbc.270.

49.29071. URL http://www.jbc.org/cgi/content/abstract/270/49/29071http://www.jbc.org/cgi/doi/10.1074/jbc.270.49.29071.

Duclos, S. and Desjardins, M. Subversion of a young phagosome: the survival strategies of intracellular pathogens. Microreview. *Cellular Microbiology*, 2(5):365–377, Oct. 2000. ISSN 1462-5814. doi: 10.1046/j.1462-5822.2000.00066.x. URL http://doi.wiley.com/10.1046/j.1462-5822.2000.00066.x.

Ebers, G. *Papyros Ebers - Das hermetische Buch über die Arzneimittel der alten Ägypter in hieratischer Schrift, 2 Bd.* Universität Leipzig, 1875 (1987). URL http://papyri.uni-leipzig.de/receive/UBLPapyri_schrift_00035080.

Eden, S., Rohatgi, R., Podtelejnikov, A. V., Mann, M., and Kirschner, M. W. Mechanism of regulation of WAVE1-induced actin nucleation by Rac1 and Nck. *Nature*, 418(6899):790–3, Aug. 2002. ISSN 0028-0836. doi: 10.1038/nature00859. URL http://www.ncbi.nlm.nih.gov/pubmed/12181570.

Emsley, J., Knight, C. G., Farndale, R. W., Barnes, M. J., and Liddington, R. C. Structural basis of collagen recognition by integrin alpha2beta1. *Cell*, 101(1):47–56, Mar. 2000. ISSN 0092-8674. doi: 10.1016/S0092-8674(00)80622-4. URL http://www.ncbi.nlm.nih.gov/pubmed/10778855.

Erickson, J. W., Cerione, R. A., and Hart, M. J. Identification of an actin cytoskeletal complex that includes IQGAP and the Cdc42 GTPase. *The Journal of biological chemistry*, 272 (39):24443–7, Sept. 1997. ISSN 0021-9258. URL http://www.ncbi.nlm.nih.gov/pubmed/9305904.

Etienne-Manneville, S. Cdc42–the centre of polarity. *Journal of cell science*, 117(Pt 8):1291–300, Mar. 2004. ISSN 0021-9533. doi: 10.1242/jcs.01115. URL http://www.ncbi.nlm.nih.gov/pubmed/15020669.

Etienne-Manneville, S. and Hall, a. Integrin-mediated activation of Cdc42 controls cell polarity in migrating astrocytes through PKCzeta. *Cell*, 106(4):489–98, Aug. 2001. ISSN 0092-8674. URL http://www.ncbi.nlm.nih.gov/pubmed/11525734.

Etienne-Manneville, S. and Hall, A. Rho GTPases in cell biology. *Nature*, 420(6916):629–35, Dec. 2002. ISSN 0028-0836. doi: 10.1038/nature01148. URL http://www.ncbi.nlm.nih.gov/pubmed/12478284.

Etienne-Manneville, S., Manneville, J.-B., Nicholls, S., Ferenczi, M. A., and Hall, A. Cdc42 and Par6-PKCzeta regulate the spatially localized association of Dlg1

and APC to control cell polarization. *The Journal of cell biology*, 170(6): 895–901, Sept. 2005. ISSN 0021-9525. doi: 10.1083/jcb.200412172. URL http://www.pubmedcentral.nih.gov/articlerender.fcgi?artid=2171429&tool=pmcentrez&rendertype=abstract.

Everett, K. D., Kahane, S., Bush, R. M., and Friedman, M. G. An unspliced group I intron in 23S rRNA links Chlamydiales, chloroplasts, and mitochondria. *Journal of bacteriology*, 181(16):4734–40, Aug. 1999. ISSN 0021-9193. URL http://www.pubmedcentral.nih.gov/articlerender.fcgi?artid=93955&tool=pmcentrez&rendertype=abstract.

Evers, E. E., Zondag, G. C., Malliri, A., Price, L. S., ten Klooster, J. P., van Der Kammen, R. A., and Collard, J. G. Rho family proteins in cell adhesion and cell migration. *European journal of cancer (Oxford, England : 1990)*, 36(10):1269–74, June 2000. ISSN 0959-8049. URL http://www.ncbi.nlm.nih.gov/pubmed/10882865.

Fackler, O. T. and Grosse, R. Cell motility through plasma membrane blebbing. *The Journal of cell biology*, 181(6):879–84, June 2008. ISSN 1540-8140. doi: 10.1083/jcb.200802081. URL http://www.pubmedcentral.nih.gov/articlerender.fcgi?artid=2426937&tool=pmcentrez&rendertype=abstract.

Faro, S. Chlamydia trachomatis infection in women. *The Journal of reproductive medicine*, 30(3 Suppl):273–8, Mar. 1985. ISSN 0024-7758. URL http://www.ncbi.nlm.nih.gov/pubmed/4020784.

Finlay, B. B. Exploitation of Mammalian Host Cell Functions by Bacterial Pathogens. *Science*, 276(5313):718–725, May 1997. ISSN 00368075. doi: 10.1126/science.276.5313.718. URL http://www.sciencemag.org/content/276/5313/718.abstract.

Finlay, B. B. and Falkow, S. Common themes in microbial pathogenicity revisited. *Microbiology and molecular biology reviews : MMBR*, 61(2):136–69, June 1997. ISSN 1092-2172. URL http://www.pubmedcentral.nih.gov/articlerender.fcgi?artid=232605&tool=pmcentrez&rendertype=abstract.

Franco, S. J. and Huttenlocher, A. Regulating cell migration: calpains make the cut. *Journal of cell science*, 118(Pt 17):3829–38, Sept. 2005. ISSN 0021-9533. doi: 10.1242/jcs.02562. URL http://www.ncbi.nlm.nih.gov/pubmed/16129881.

Friedl, P. and Gilmour, D. Collective cell migration in morphogenesis, regeneration and cancer. *Nature reviews. Molecular cell biology*, 10(7):445–57, July 2009. ISSN 1471-0080. doi: 10.1038/nrm2720. URL http://www.ncbi.nlm.nih.gov/pubmed/19546857.

Fukata, M., Watanabe, T., Noritake, J., Nakagawa, M., Yamaga, M., Kuroda, S., Matsuura, Y., Iwamatsu, A., Perez, F., and Kaibuchi, K. Rac1 and Cdc42 capture microtubules through IQGAP1 and CLIP-170. *Cell*, 109(7):873–85, June 2002. ISSN 0092-8674. URL http://www.ncbi.nlm.nih.gov/pubmed/12110184.

Gaggioli, C., Hooper, S., Hidalgo-Carcedo, C., Grosse, R., Marshall, J. F., Harrington, K., and Sahai, E. Fibroblast-led collective invasion of carcinoma cells with differing roles for RhoGTPases in leading and following cells. *Nature cell biology*, 9(12):1392–400, Dec. 2007. ISSN 1465-7392. doi: 10.1038/ncb1658. URL http://www.ncbi.nlm.nih.gov/pubmed/18037882.

Gambhir, M., Basáñez, M.-G., Turner, F., Kumaresan, J., and Grassly, N. C. Trachoma: transmission, infection, and control. *The Lancet infectious diseases*, 7(6):420–7, June 2007. ISSN 1473-3099. doi: 10.1016/S1473-3099(07)70137-8. URL http://www.ncbi.nlm.nih.gov/pubmed/17521595.

Garcia-Calvo, M., Peterson, E. P., Leiting, B., Ruel, R., Nicholson, D. W., and Thornberry, N. A. Inhibition of human caspases by peptide-based and macromolecular inhibitors. *The Journal of biological chemistry*, 273(49):32608–13, Dec. 1998. ISSN 0021-9258. URL http://www.ncbi.nlm.nih.gov/pubmed/9829999.

Geiger, B., Bershadsky, A., Pankov, R., and Yamada, K. M. Transmembrane crosstalk between the extracellular matrix–cytoskeleton crosstalk. *Nature reviews. Molecular cell biology*, 2 (11):793–805, Nov. 2001. ISSN 1471-0072. doi: 10.1038/35099066. URL http://www.ncbi.nlm.nih.gov/pubmed/11715046.

Giles, D. K., Whittimore, J. D., LaRue, R. W., Raulston, J. E., and Wyrick, P. B. Ultrastructural analysis of chlamydial antigen-containing vesicles everting from the Chlamydia trachomatis inclusion. *Microbes and infection / Institut Pasteur*, 8(6):1579–91, May 2006. ISSN 1286-4579. doi: 10.1016/j.micinf.2006.01.018. URL http://www.ncbi.nlm.nih.gov/pubmed/16698305.

Girod, A., Storrie, B., Simpson, J. C., Johannes, L., Goud, B., Roberts, L. M., Lord, J. M., Nilsson, T., and Pepperkok, R. Evidence for a COP-I-independent transport route from the Golgi complex to the endoplasmic reticulum. *Nature cell biology*, 1(7):423–30, Nov. 1999. ISSN 1465-7392. doi: 10.1038/15658. URL http://www.ncbi.nlm.nih.gov/pubmed/10559986.

Gomes, E. R., Jani, S., and Gundersen, G. G. Nuclear movement regulated by Cdc42, MRCK, myosin, and actin flow establishes MTOC polarization in migrating cells. *Cell*, 121(3):451–

63, May 2005. ISSN 0092-8674. doi: 10.1016/j.cell.2005.02.022. URL http://www.ncbi.nlm.nih.gov/pubmed/15882626.

Gonatas, N. K., Stieber, A., and Gonatas, J. O. Fragmentation of the Golgi apparatus in neurodegenerative diseases and cell death. *Journal of the neurological sciences*, 246(1-2):21–30, July 2006. ISSN 0022-510X. doi: 10.1016/j.jns.2006.01.019. URL http://dx.doi.org/10.1016/j.jns.2006.01.019.

Griffiths, E., Ventresca, M. S., and Gupta, R. S. BLAST screening of chlamydial genomes to identify signature proteins that are unique for the Chlamydiales, Chlamydiaceae, Chlamydophila and Chlamydia groups of species. *BMC genomics*, 7:14, Jan. 2006. ISSN 1471-2164. doi: 10.1186/1471-2164-7-14. URL http://www.pubmedcentral.nih.gov/articlerender.fcgi?artid=1403754&tool=pmcentrez&rendertype=abstract.

Grifoni, S. C., McKey, S. E., and Drummond, H. A. Hsc70 regulates cell surface ASIC2 expression and vascular smooth muscle cell migration. *American journal of physiology. Heart and circulatory physiology*, 294(5):H2022–30, May 2008. ISSN 0363-6135. doi: 10.1152/ajpheart.01271.2007. URL http://www.ncbi.nlm.nih.gov/pubmed/18310515.

Grigoriev, I., Splinter, D., Keijzer, N., Wulf, P. S., Demmers, J., Ohtsuka, T., Modesti, M., Maly, I. V., Grosveld, F., Hoogenraad, C. C., and Akhmanova, A. Rab6 regulates transport and targeting of exocytotic carriers. *Developmental cell*, 13(2):305–14, Aug. 2007. ISSN 1534-5807. doi: 10.1016/j.devcel.2007.06.010. URL http://www.ncbi.nlm.nih.gov/pubmed/17681140.

Gurtner, G. C., Werner, S., Barrandon, Y., and Longaker, M. T. Wound repair and regeneration. *Nature*, 453(7193):314–21, May 2008. ISSN 1476-4687. doi: 10.1038/nature07039. URL http://www.ncbi.nlm.nih.gov/pubmed/18480812.

Gurumurthy, R. K., Mäurer, A. P., Machuy, N., Hess, S., Pleissner, K. P., Schuchhardt, J., Rudel, T., and Meyer, T. F. A loss-of-function screen reveals Ras- and Raf-independent MEK-ERK signaling during Chlamydia trachomatis infection. *Science signaling*, 3(113):ra21, Jan. 2010. ISSN 1937-9145. doi: 10.1126/scisignal.2000651. URL http://www.ncbi.nlm.nih.gov/pubmed/20234004.

Hackstadt, T., Rockey, D. D., Heinzen, R. A., and Scidmore, M. A. Chlamydia trachomatis interrupts an exocytic pathway to acquire endogenously synthesized sphingomyelin in transit from the Golgi apparatus to the plasma membrane. *The EMBO journal*, 15(5):964–77, Mar. 1996. ISSN 0261-4189. URL

http://www.pubmedcentral.nih.gov/articlerender.fcgi?artid=449991&tool=pmcentrez&rendertype=abstract.

Halberstaedter, L. and von Prowazek, S. Über zelleinschlüsse parasitärer natur beim trachom. *Arbeiten aus dem Kaiserlichen Gesundheitsamte*, 26:44–47, 1907.

Hanada, K., Kumagai, K., Tomishige, N., and Yamaji, T. CERT-mediated trafficking of ceramide. *Biochimica et biophysica acta*, 1791(7):684–91, July 2009. ISSN 0006-3002. doi: 10.1016/j.bbalip.2009.01.006. URL http://dx.doi.org/10.1016/j.bbalip.2009.01.006.

Harada, M. Proteasome inhibition induces inclusion bodies associated with intermediate filaments and fragmentation of the Golgi apparatus. *Experimental Cell Research*, 288(1):60–69, Aug. 2003. ISSN 00144827. doi: 10.1016/S0014-4827(03)00162-9. URL http://dx.doi.org/10.1016/S0014-4827(03)00162-9.

Hatch, G. M. and McClarty, G. Phospholipid composition of purified Chlamydia trachomatis mimics that of the eucaryotic host cell. *Infection and immunity*, 66(8):3727–35, Aug. 1998. ISSN 0019-9567. URL http://www.pubmedcentral.nih.gov/articlerender.fcgi?artid=108408&tool=pmcentrez&rendertype=abstract.

Hehnly, H., Xu, W., Chen, J.-L., and Stamnes, M. Cdc42 regulates microtubule-dependent Golgi positioning. *Traffic (Copenhagen, Denmark)*, 11(8):1067–78, Aug. 2010. ISSN 1600-0854. doi: 10.1111/j.1600-0854.2010.01082.x. URL http://www.pubmedcentral.nih.gov/articlerender.fcgi?artid=2904418&tool=pmcentrez&rendertype=abstract.

Heuer, D., Brinkmann, V., Meyer, T. F., and Szczepek, A. J. Expression and translocation of chlamydial protease during acute and persistent infection of the epithelial HEp-2 cells with Chlamydophila (Chlamydia) pneumoniae. *Cellular Microbiology*, 5(5):315–322, May 2003. ISSN 1462-5814. doi: 10.1046/j.1462-5822.2003.00278.x. URL http://doi.wiley.com/10.1046/j.1462-5822.2003.00278.x.

Heuer, D., Kneip, C., Mäurer, A. P., and Meyer, T. F. Tackling the intractable - approaching the genetics of Chlamydiales. *International journal of medical microbiology : IJMM*, 297 (7-8):569–76, Nov. 2007. ISSN 1438-4221. doi: 10.1016/j.ijmm.2007.03.011. URL http://dx.doi.org/10.1016/j.ijmm.2007.03.011.

Heuer, D., Rejman Lipinski, A., Machuy, N., Karlas, A., Wehrens, A., Siedler, F., Brinkmann, V., and Meyer, T. F. Chlamydia causes fragmentation of the Golgi compartment to ensure reproduction. *Nature*, 457(7230):731–5, Feb. 2009. ISSN 1476-4687. doi: 10.1038/nature07578. URL http://www.ncbi.nlm.nih.gov/pubmed/19060882.

Honda, T., Shimizu, K., Kawakatsu, T., Fukuhara, A., Irie, K., Nakamura, T., Matsuda, M., and Takai, Y. Cdc42 and Rac small G proteins activated by trans-interactions of nectins are involved in activation of c-Jun N-terminal kinase, but not in association of nectins and cadherin to form adherens junctions, in fibroblasts. *Genes to cells : devoted to molecular & cellular mechanisms*, 8(5):481–91, May 2003. ISSN 1356-9597. URL http://www.ncbi.nlm.nih.gov/pubmed/12694536.

Hoogenraad, C. C., Akhmanova, A., Howell, S. A., Dortland, B. R., De Zeeuw, C. I., Willemsen, R., Visser, P., Grosveld, F., and Galjart, N. Mammalian Golgi-associated Bicaudal-D2 functions in the dynein-dynactin pathway by interacting with these complexes. *The EMBO journal*, 20(15):4041–54, Aug. 2001. ISSN 0261-4189. doi: 10.1093/emboj/20.15.4041. URL http://www.pubmedcentral.nih.gov/articlerender.fcgi?artid=149157&tool=pmcentrez&rendertype=abstract.

Hsia, R. C., Pannekoek, Y., Ingerowski, E., and Bavoil, P. M. Type III secretion genes identify a putative virulence locus of Chlamydia. *Molecular microbiology*, 25(2):351–9, July 1997. ISSN 0950-382X. URL http://www.ncbi.nlm.nih.gov/pubmed/9282747.

Huang, Z., Feng, Y., Chen, D., Wu, X., Huang, S., Wang, X., Xiao, X., Li, W., Huang, N., Gu, L., Zhong, G., and Chai, J. Structural basis for activation and inhibition of the secreted chlamydia protease CPAF. *Cell host & microbe*, 4(6):529–42, Dec. 2008. ISSN 1934-6069. doi: 10.1016/j.chom.2008.10.005. URL http://www.ncbi.nlm.nih.gov/pubmed/19064254.

Huot, M.-E., Brown, C. M., Lamarche-Vane, N., and Richard, S. An adaptor role for cytoplasmic Sam68 in modulating Src activity during cell polarization. *Molecular and cellular biology*, 29(7):1933–43, Apr. 2009. ISSN 1098-5549. doi: 10.1128/MCB.01707-08. URL http://www.pubmedcentral.nih.gov/articlerender.fcgi?artid=2655613&tool=pmcentrez&rendertype=abstract.

Hurtado, L., Caballero, C., Gavilan, M. P., Cardenas, J., Bornens, M., and Rios, R. M. Disconnecting the Golgi ribbon from the centrosome prevents directional cell migration and ciliogenesis. *The Journal of cell biology*, 193(5):917–33, May 2011. ISSN 1540-8140. doi: 10.1083/

jcb.201011014. URL http://www.pubmedcentral.nih.gov/articlerender.fcgi?artid=3105543&tool=pmcentrez&rendertype=abstract.

Huston, W. M. Bacterial proteases from the intracellular vacuole niche; protease conservation and adaptation for pathogenic advantage. *FEMS immunology and medical microbiology*, 59 (1):1–10, June 2010. ISSN 1574-695X. doi: 10.1111/j.1574-695X.2010.00672.x. URL http://www.ncbi.nlm.nih.gov/pubmed/20402770.

Hybiske, K. and Stephens, R. S. Mechanisms of host cell exit by the intracellular bacterium Chlamydia. *Proceedings of the National Academy of Sciences of the United States of America*, 104(27):11430–5, July 2007. ISSN 0027-8424. doi: 10.1073/pnas.0703218104. URL http://www.pubmedcentral.nih.gov/articlerender.fcgi?artid=2040915&tool=pmcentrez&rendertype=abstract.

Itoh, R. E., Kurokawa, K., Ohba, Y., Yoshizaki, H., Mochizuki, N., and Matsuda, M. Activation of rac and cdc42 video imaged by fluorescent resonance energy transfer-based single-molecule probes in the membrane of living cells. *Molecular and cellular biology*, 22(18):6582–91, Sept. 2002. ISSN 0270-7306. URL http://www.pubmedcentral.nih.gov/articlerender.fcgi?artid=135619&tool=pmcentrez&rendertype=abstract.

Jackson, C. L. Mechanisms of transport through the Golgi complex. *Journal of cell science*, 122(Pt 4):443–52, Feb. 2009. ISSN 0021-9533. doi: 10.1242/jcs.032581. URL http://www.ncbi.nlm.nih.gov/pubmed/19193869.

Jewett, T. J., Miller, N. J., Dooley, C. A., and Hackstadt, T. The conserved Tarp actin binding domain is important for chlamydial invasion. *PLoS pathogens*, 6 (7):e1000997, Jan. 2010. ISSN 1553-7374. doi: 10.1371/journal.ppat.1000997. URL http://www.pubmedcentral.nih.gov/articlerender.fcgi?artid=2904776&tool=pmcentrez&rendertype=abstract.

Jorgensen, I. and Valdivia, R. H. Pmp-like proteins Pls1 and Pls2 are secreted into the lumen of the Chlamydia trachomatis inclusion. *Infection and immunity*, 76(9):3940–50, Sept. 2008. ISSN 1098-5522. doi: 10.1128/IAI.00632-08. URL http://www.pubmedcentral.nih.gov/articlerender.fcgi?artid=2519427&tool=pmcentrez&rendertype=abstract.

Jorgensen, I., Bednar, M. M., Amin, V., Davis, B. K., Ting, J. P. Y., McCafferty, D. G., and Valdivia, R. H. The Chlamydia Protease CPAF Regulates Host and Bacterial Proteins to

Maintain Pathogen Vacuole Integrity and Promote Virulence. *Cell host & microbe*, 10(1):21–32, July 2011. ISSN 1934-6069. doi: 10.1016/j.chom.2011.06.008. URL http://www.ncbi.nlm.nih.gov/pubmed/21767809.

Kanazawa, S., Fujiwara, T., Matsuzaki, S., Shingaki, K., Taniguchi, M., Miyata, S., Tohyama, M., Sakai, Y., Yano, K., Hosokawa, K., and Kubo, T. bFGF regulates PI3-kinase-Rac1-JNK pathway and promotes fibroblast migration in wound healing. *PloS one*, 5(8):e12228, Jan. 2010. ISSN 1932-6203. doi: 10.1371/journal.pone.0012228. URL http://www.pubmedcentral.nih.gov/articlerender.fcgi?artid=2923192&tool=pmcentrez&rendertype=abstract.

Kaplan, K. B., Bibbins, K. B., Swedlow, J. R., Arnaud, M., Morgan, D. O., and Varmus, H. E. Association of the amino-terminal half of c-Src with focal adhesions alters their properties and is regulated by phosphorylation of tyrosine 527. *The EMBO journal*, 13(20):4745–56, Oct. 1994. ISSN 0261-4189. URL http://www.pubmedcentral.nih.gov/articlerender.fcgi?artid=395413&tool=pmcentrez&rendertype=abstract.

Kari, L., Goheen, M. M., Randall, L. B., Taylor, L. D., Carlson, J. H., Whitmire, W. M., Virok, D., Rajaram, K., Endresz, V., McClarty, G., Nelson, D. E., and Caldwell, H. D. Generation of targeted Chlamydia trachomatis null mutants. *Proceedings of the National Academy of Sciences of the United States of America*, 108(17):7189–93, Apr. 2011. ISSN 1091-6490. doi: 10.1073/pnas.1102229108. URL http://www.pubmedcentral.nih.gov/articlerender.fcgi?artid=3084044&tool=pmcentrez&rendertype=abstract.

Kawakatsu, T., Shimizu, K., Honda, T., Fukuhara, T., Hoshino, T., and Takai, Y. Trans-interactions of nectins induce formation of filopodia and Lamellipodia through the respective activation of Cdc42 and Rac small G proteins. *The Journal of biological chemistry*, 277(52):50749–55, Dec. 2002. ISSN 0021-9258. doi: 10.1074/jbc.M209846200. URL http://www.ncbi.nlm.nih.gov/pubmed/12379640.

Kawakatsu, T., Ogita, H., Fukuhara, T., Fukuyama, T., Minami, Y., Shimizu, K., and Takai, Y. Vav2 as a Rac-GDP/GTP exchange factor responsible for the nectin-induced, c-Src- and Cdc42-mediated activation of Rac. *The Journal of biological chemistry*, 280(6):4940–7, Feb. 2005. ISSN 0021-9258. doi: 10.1074/jbc.M408710200. URL http://www.ncbi.nlm.nih.gov/pubmed/15485841.

Kawana, K., Quayle, A. J., Ficarra, M., Ibana, J. A., Shen, L., Kawana, Y., Yang, H., Marrero, L.,

Yavagal, S., Greene, S. J., Zhang, Y.-X., Pyles, R. B., Blumberg, R. S., and Schust, D. J. CD1d degradation in Chlamydia trachomatis-infected epithelial cells is the result of both cellular and chlamydial proteasomal activity. *The Journal of biological chemistry*, 282(10):7368–75, Mar. 2007. ISSN 0021-9258. doi: 10.1074/jbc.M610754200. URL http://www.ncbi.nlm.nih.gov/pubmed/17215251.

Kawauchi, T., Sekine, K., Shikanai, M., Chihama, K., Tomita, K., Kubo, K.-i., Nakajima, K., Nabeshima, Y.-I., and Hoshino, M. Rab GTPases-dependent endocytic pathways regulate neuronal migration and maturation through N-cadherin trafficking. *Neuron*, 67(4):588–602, Aug. 2010. ISSN 1097-4199. doi: 10.1016/j.neuron.2010.07.007. URL http://www.ncbi.nlm.nih.gov/pubmed/20797536.

Keller, B. O., Sui, J., Young, A. B., and Whittal, R. M. Interferences and contaminants encountered in modern mass spectrometry. *Analytica chimica acta*, 627(1):71–81, Oct. 2008. ISSN 1873-4324. doi: 10.1016/j.aca.2008.04.043. URL http://www.ncbi.nlm.nih.gov/pubmed/18790129.

Kiosses, W. B., Shattil, S. J., Pampori, N., and Schwartz, M. A. Rac recruits high-affinity integrin alphavbeta3 to lamellipodia in endothelial cell migration. *Nature cell biology*, 3(3):316–20, Mar. 2001. ISSN 1465-7392. doi: 10.1038/35060120. URL http://www.ncbi.nlm.nih.gov/pubmed/11231584.

Kolega, J. Asymmetric distribution of myosin IIB in migrating endothelial cells is regulated by a rho-dependent kinase and contributes to tail retraction. *Molecular biology of the cell*, 14(12):4745–57, Dec. 2003. ISSN 1059-1524. doi: 10.1091/mbc.E03-04-0205. URL http://www.pubmedcentral.nih.gov/articlerender.fcgi?artid=284780&tool=pmcentrez&rendertype=abstract.

Kroboth, K., Newton, I. P., Kita, K., Dikovskaya, D., Zumbrunn, J., Waterman-Storer, C. M., and Näthke, I. S. Lack of adenomatous polyposis coli protein correlates with a decrease in cell migration and overall changes in microtubule stability. *Molecular biology of the cell*, 18(3):910–8, Mar. 2007. ISSN 1059-1524. doi: 10.1091/mbc.E06-03-0179. URL http://www.pubmedcentral.nih.gov/articlerender.fcgi?artid=1805109&tool=pmcentrez&rendertype=abstract.

Kumar, Y. and Valdivia, R. Actin and intermediate filaments stabilize the Chlamydia trachomatis vacuole by forming dynamic structural scaffolds. *Cell host & microbe*, 4(2):159–169, Aug. 2008a. ISSN 1931-3128. doi: 10.1016/j.chom.2008.05.018. URL http://linkinghub.elsevier.com/retrieve/pii/S1931312808001923.

Kumar, Y. and Valdivia, R. Reorganization of the host cytoskeleton by the intracellular pathogen Chlamydia trachomatis. *Communicative & Integrative Biology*, 1(2):175, Jan. 2008b. ISSN 1942-0889. doi: 10.1016/j.chom.2008.05.018.www.landesbioscience.com. URL http://www.ncbi.nlm.nih.gov/pmc/articles/PMC2686014/.

Kumar, Y., Cocchiaro, J., and Valdivia, R. H. The obligate intracellular pathogen Chlamydia trachomatis targets host lipid droplets. *Current biology : CB*, 16(16):1646–51, Aug. 2006. ISSN 0960-9822. doi: 10.1016/j.cub.2006.06.060. URL http://www.ncbi.nlm.nih.gov/pubmed/16920627.

Kupfer, A., Louvard, D., and Singer, S. J. Polarization of the Golgi apparatus and the microtubule-organizing center in cultured fibroblasts at the edge of an experimental wound. *Proceedings of the National Academy of Sciences of the United States of America*, 79(8):2603–7, Apr. 1982. ISSN 0027-8424. URL http://www.pubmedcentral.nih.gov/articlerender.fcgi?artid=346248&tool=pmcentrez&rendertype=abstract.

Lad, S. P., Li, J., da Silva Correia, J., Pan, Q., Gadwal, S., Ulevitch, R. J., and Li, E. Cleavage of p65/RelA of the NF-kappaB pathway by Chlamydia. *Proceedings of the National Academy of Sciences of the United States of America*, 104(8):2933–8, Feb. 2007a. ISSN 0027-8424. doi: 10.1073/pnas.0608393104. URL http://www.pubmedcentral.nih.gov/articlerender.fcgi?artid=1815284&tool=pmcentrez&rendertype=abstract.

Lad, S. P., Yang, G., Scott, D. A., Wang, G., Nair, P., Mathison, J., Reddy, V. S., and Li, E. Chlamydial CT441 is a PDZ domain-containing tail-specific protease that interferes with the NF-kappaB pathway of immune response. *Journal of bacteriology*, 189(18):6619–25, Sept. 2007b. ISSN 0021-9193. doi: 10.1128/JB.00429-07. URL http://www.pubmedcentral.nih.gov/articlerender.fcgi?artid=2045167&tool=pmcentrez&rendertype=abstract.

Lambert, H., Hitziger, N., Dellacasa, I., Svensson, M., and Barragan, A. Induction of dendritic cell migration upon Toxoplasma gondii infection potentiates parasite dissemination. *Cellular microbiology*, 8(10):1611–23, Oct. 2006. ISSN 1462-5814. doi: 10.1111/j.1462-5822.2006.00735.x. URL http://www.ncbi.nlm.nih.gov/pubmed/16984416.

Lane, B. J., Mutchler, C., Al Khodor, S., Grieshaber, S. S., and Carabeo, R. A. Chlamydial entry involves TARP binding of guanine nucleotide exchange factors. *PLoS pathogens*, 4(3):e1000014, Mar. 2008. ISSN 1553-7374. URL

http://www.pubmedcentral.nih.gov/articlerender.fcgi?artid=2279300&tool=pmcentrez&rendertype=abstract.

Lane, J. D., Lucocq, J., Pryde, J., Barr, F. A., Woodman, P. G., Allan, V. J., and Lowe, M. Caspase-mediated cleavage of the stacking protein GRASP65 is required for Golgi fragmentation during apoptosis. *The Journal of cell biology*, 156(3):495–509, Feb. 2002. ISSN 0021-9525. doi: 10.1083/jcb.200110007. URL http://www.pubmedcentral.nih.gov/articlerender.fcgi?artid=2173349&tool=pmcentrez&rendertype=abstract.

Lauffenburger, D. and Horwitz, A. Cell migration: a physically integrated molecular process. *Cell*, 84(3):359–370, 1996. ISSN 0092-8674. URL http://www.cell.com/structure/redirectUrl/biophysj/abstract/S0006-3495(94)80502-8.

Le Clainche, C., Schlaepfer, D., Ferrari, A., Klingauf, M., Grohmanova, K., Veligodskiy, A., Didry, D., Le, D., Egile, C., Carlier, M.-F., and Kroschewski, R. IQGAP1 stimulates actin assembly through the N-WASP-Arp2/3 pathway. *The Journal of biological chemistry*, 282 (1):426–35, Jan. 2007. ISSN 0021-9258. doi: 10.1074/jbc.M607711200. URL http://www.ncbi.nlm.nih.gov/pubmed/17085436.

Liang, C.-C., Park, A. Y., and Guan, J.-L. In vitro scratch assay: a convenient and inexpensive method for analysis of cell migration in vitro. *Nature protocols*, 2(2):329–33, Jan. 2007. ISSN 1750-2799. doi: 10.1038/nprot.2007.30. URL http://www.ncbi.nlm.nih.gov/pubmed/17406593.

Lowe, D. C., Savidge, T. C., Pickard, D., Eckmann, L., Kagnoff, M. F., Dougan, G., and Chatfield, S. N. Characterization of candidate live oral Salmonella typhi vaccine strains harboring defined mutations in aroA, aroC, and htrA. *Infection and immunity*, 67(2): 700–7, Feb. 1999. ISSN 0019-9567. URL http://www.pubmedcentral.nih.gov/articlerender.fcgi?artid=96376&tool=pmcentrez&rendertype=abstract.

Lowe, M. Structural organization of the Golgi apparatus. *Current opinion in cell biology*, 23(1):85–93, Feb. 2011. ISSN 1879-0410. doi: 10.1016/j.ceb.2010.10.004. URL http://www.ncbi.nlm.nih.gov/pubmed/21071196.

Lowe, M., Rabouille, C., Nakamura, N., Watson, R., Jackman, M., Jämsä, E., Rahman, D., Pappin, D. J., and Warren, G. Cdc2 kinase directly phosphorylates the cis-Golgi matrix protein GM130 and is required for Golgi fragmentation in mitosis. *Cell*, 94(6):783–93, Sept. 1998. ISSN 0092-8674. URL http://www.ncbi.nlm.nih.gov/pubmed/9753325.

Lukong, K. E. and Richard, S. Sam68, the KH domain-containing superSTAR. *Biochimica et Biophysica Acta (BBA) - Reviews on Cancer*, 1653(2):73–86, Dec. 2003. ISSN 0304419X. doi: 10.1016/j.bbcan.2003.09.001. URL http://dx.doi.org/10.1016/j.bbcan.2003.09.001.

Machacek, M., Hodgson, L., Welch, C., Elliott, H., Pertz, O., Nalbant, P., Abell, A., Johnson, G. L., Hahn, K. M., and Danuser, G. Coordination of Rho GTPase activities during cell protrusion. *Nature*, 461(7260):99–103, Sept. 2009. ISSN 1476-4687. doi: 10.1038/nature08242. URL http://www.pubmedcentral.nih.gov/articlerender.fcgi?artid=2885353&tool=pmcentrez&rendertype=abstract.

Mancini, M., Machamer, C. E., Roy, S., Nicholson, D. W., Thornberry, N. a., Casciola-Rosen, L. a., and Rosen, a. Caspase-2 is localized at the Golgi complex and cleaves golgin-160 during apoptosis. *The Journal of cell biology*, 149(3):603–12, May 2000. ISSN 0021-9525. URL http://www.pubmedcentral.nih.gov/articlerender.fcgi?artid=2174848&tool=pmcentrez&rendertype=abstract.

Martinez, O., Schmidt, a., Salaméro, J., Hoflack, B., Roa, M., and Goud, B. The small GTP-binding protein rab6 functions in intra-Golgi transport. *The Journal of cell biology*, 127(6 Pt 1):1575–88, Dec. 1994. ISSN 0021-9525. URL http://www.pubmedcentral.nih.gov/articlerender.fcgi?artid=2120294&tool=pmcentrez&rendertype=abstract.

Martinez, O., Antony, C., Pehau-Arnaudet, G., Berger, E. G., Salamero, J., and Goud, B. GTP-bound forms of rab6 induce the redistribution of Golgi proteins into the endoplasmic reticulum. *Proceedings of the National Academy of Sciences of the United States of America*, 94(5):1828–33, Mar. 1997. ISSN 0027-8424. URL http://www.pubmedcentral.nih.gov/articlerender.fcgi?artid=20002&tool=pmcentrez&rendertype=abstract.

Mataraza, J. Identification and characterization of the Cdc42-binding site of IQGAP1,. *Biochemical and Biophysical Research Communications*, 305(2):315–321, May 2003. ISSN 0006291X. doi: 10.1016/S0006-291X(03)00759-9. URL http://linkinghub.elsevier.com/retrieve/pii/S0006291X03007599.

McClarty, G. and Fan, H. Purine metabolism by intracellular Chlamydia psittaci. *Journal of bacteriology*, 175(15):4662–9, Aug. 1993. ISSN 0021-9193. URL http://www.pubmedcentral.nih.gov/articlerender.fcgi?artid=204917&tool=pmcentrez&rendertype=abstract.

McClarty, G. and Qin, B. Pyrimidine metabolism by intracellular Chlamydia psittaci. *Journal of bacteriology*, 175(15):4652–61, Aug. 1993. ISSN 0021-9193. URL http://www.pubmedcentral.nih.gov/articlerender.fcgi?artid=204916&tool=pmcentrez&rendertype=abstract.

McLaughlin, L. M., Govoni, G. R., Gerke, C., Gopinath, S., Peng, K., Laidlaw, G., Chien, Y.-H., Jeong, H.-W., Li, Z., Brown, M. D., Sacks, D. B., and Monack, D. The Salmonella SPI2 effector SseI mediates long-term systemic infection by modulating host cell migration. *PLoS pathogens*, 5(11):e1000671, Nov. 2009. ISSN 1553-7374. doi: 10.1371/journal.ppat.1000671. URL http://www.pubmedcentral.nih.gov/articlerender.fcgi?artid=2777311&tool=pmcentrez&rendertype=abstract.

Meng, W., Numazaki, M., Takeuchi, K., Uchibori, Y., Ando-Akatsuka, Y., Tominaga, M., and Tominaga, T. DIP (mDia interacting protein) is a key molecule regulating Rho and Rac in a Src-dependent manner. *The EMBO journal*, 23 (4):760–71, Feb. 2004. ISSN 0261-4189. doi: 10.1038/sj.emboj.7600095. URL http://www.pubmedcentral.nih.gov/articlerender.fcgi?artid=381003&tool=pmcentrez&rendertype=abstract.

Merlot, S. and Firtel, R. A. Leading the way: Directional sensing through phosphatidylinositol 3-kinase and other signaling pathways. *Journal of cell science*, 116(Pt 17):3471–8, Sept. 2003. ISSN 0021-9533. doi: 10.1242/jcs.00703. URL http://www.ncbi.nlm.nih.gov/pubmed/12893811.

Miller, P., Folkmann, A., Maia, A., Efimova, N., Efimov, A., and Kaverina, I. Golgi-derived CLASP-dependent microtubules control Golgi organization and polarized trafficking in motile cells. *Nature cell biology*, 11(9):1069–1080, Sept. 2009. ISSN 1465-7392. doi: 10.1038/ncb1920. URL http://www.nature.com/ncb/journal/v11/n9/abs/ncb1920.html.

Moese, S., Selbach, M., Brinkmann, V., Karlas, A., Haimovich, B., Backert, S., and Meyer, T. F. The Helicobacter pylori CagA protein disrupts matrix adhesion of gastric epithelial cells by dephosphorylation of vinculin. *Cellular microbiology*, 9(5):1148–61, May 2007. ISSN 1462-5814. doi: 10.1111/j.1462-5822.2006.00856.x. URL http://www.ncbi.nlm.nih.gov/pubmed/17217431.

Moffat, J. F., Edelstein, P. H., Regula, D. P., Cirillo, J. D., and Tompkins, L. S. Effects of an isogenic Zn-metalloprotease-deficient mutant of Legionella pneumophila in a guinea-pig

pneumonia model. *Molecular microbiology*, 12(5):693–705, June 1994. ISSN 0950-382X. URL http://www.ncbi.nlm.nih.gov/pubmed/8052122.

Mogensen, M. M., Tucker, J. B., Mackie, J. B., Prescott, A. R., and Näthke, I. S. The adenomatous polyposis coli protein unambiguously localizes to microtubule plus ends and is involved in establishing parallel arrays of microtubule bundles in highly polarized epithelial cells. *The Journal of cell biology*, 157(6):1041–8, June 2002. ISSN 0021-9525. doi: 10.1083/jcb.200203001. URL http://www.pubmedcentral.nih.gov/articlerender.fcgi?artid=2174057&tool=pmcentrez&rendertype=abstract.

Morishita, E. C., Murayama, K., Kato-Murayama, M., Ishizuka-Katsura, Y., Tomabechi, Y., Hayashi, T., Terada, T., Handa, N., Shirouzu, M., Akiyama, T., and Yokoyama, S. Crystal structures of the armadillo repeat domain of adenomatous polyposis coli and its complex with the tyrosine-rich domain of sam68. *Structure (London, England : 1993)*, 19(10):1496–508, Oct. 2011. ISSN 1878-4186. doi: 10.1016/j.str.2011.07.013. URL http://www.ncbi.nlm.nih.gov/pubmed/22000517.

Moulder, J. W. Interaction of chlamydiae and host cells in vitro. *Microbiological reviews*, 55(1):143–90, Mar. 1991. ISSN 0146-0749. URL http://mmbr.asm.org/cgi/content/abstract/55/1/143http://www.pubmedcentral.nih.gov/articlerender.fcgi?artid=372804&tool=pmcentrez&rendertype=abstract.

Murthy, A. K., Li, W., Guentzel, M. N., Zhong, G., and Arulanandam, B. P. Vaccination with the defined chlamydial secreted protein CPAF induces robust protection against female infertility following repeated genital chlamydial challenge. *Vaccine*, 29(14):2519–22, Mar. 2011. ISSN 1873-2518. doi: 10.1016/j.vaccine.2011.01.074. URL http://www.ncbi.nlm.nih.gov/pubmed/21300093.

Nakamura, N., Lowe, M., Levine, T. P., Rabouille, C., and Warren, G. The vesicle docking protein p115 binds GM130, a cis-Golgi matrix protein, in a mitotically regulated manner. *Cell*, 89(3):445–55, May 1997. ISSN 0092-8674. URL http://www.ncbi.nlm.nih.gov/pubmed/9150144.

Näthke, I. S., Adams, C. L., Polakis, P., Sellin, J. H., and Nelson, W. J. The adenomatous polyposis coli tumor suppressor protein localizes to plasma membrane sites involved in active cell migration. *The Journal of cell biology*, 134(1):165–79, July 1996. ISSN 0021-9525. URL http://www.pubmedcentral.nih.gov/articlerender.fcgi?artid=2120913&tool=pmcentrez&rendertype=abstract.

Nobes, C. D. and Hall, A. Rho, rac, and cdc42 GTPases regulate the assembly of multimolecular focal complexes associated with actin stress fibers, lamellipodia, and filopodia. *Cell*, 81(1):53–62, Apr. 1995. ISSN 0092-8674. URL http://www.ncbi.nlm.nih.gov/pubmed/7536630.

Nobes, C. D. and Hall, a. Rho GTPases control polarity, protrusion, and adhesion during cell movement. *The Journal of cell biology*, 144(6):1235–44, Mar. 1999. ISSN 0021-9525. URL http://www.pubmedcentral.nih.gov/articlerender.fcgi?artid=2150589&tool=pmcentrez&rendertype=abstract.

Noritake, J., Watanabe, T., Sato, K., Wang, S., and Kaibuchi, K. IQGAP1: a key regulator of adhesion and migration. *Journal of cell science*, 118(Pt 10):2085–92, May 2005. ISSN 0021-9533. doi: 10.1242/jcs.02379. URL http://www.ncbi.nlm.nih.gov/pubmed/15890984.

Osmani, N., Peglion, F., Chavrier, P., and Etienne-Manneville, S. Cdc42 localization and cell polarity depend on membrane traffic. *The Journal of cell biology*, 191(7):1261–9, Dec. 2010. ISSN 1540-8140. doi: 10.1083/jcb.201003091. URL http://www.pubmedcentral.nih.gov/articlerender.fcgi?artid=3010071&tool=pmcentrez&rendertype=abstract.

Palazzo, A. F., Joseph, H. L., Chen, Y. J., Dujardin, D. L., Alberts, A. S., Pfister, K. K., Vallee, R. B., and Gundersen, G. G. Cdc42, dynein, and dynactin regulate MTOC reorientation independent of Rho-regulated microtubule stabilization. *Current biology : CB*, 11(19):1536–41, Oct. 2001. ISSN 0960-9822. URL http://www.ncbi.nlm.nih.gov/pubmed/11591323.

Paschen, S. A., Christian, J. G., Vier, J., Schmidt, F., Walch, A., Ojcius, D. M., and Häcker, G. Cytopathicity of Chlamydia is largely reproduced by expression of a single chlamydial protease. *The Journal of cell biology*, 182(1):117–27, July 2008. ISSN 1540-8140. doi: 10.1083/jcb.200804023. URL http://www.pubmedcentral.nih.gov/articlerender.fcgi?artid=2447887&tool=pmcentrez&rendertype=abstract.

Paul, F. E., Hosp, F., and Selbach, M. Analyzing protein-protein interactions by quantitative mass spectrometry. *Methods (San Diego, Calif.)*, 54(4):387–395, Mar. 2011. ISSN 1095-9130. doi: 10.1016/j.ymeth.2011.03.001. URL http://www.ncbi.nlm.nih.gov/pubmed/21382495.

Pedersen, L. L., Radulic, M., Doric, M., and Abu Kwaik, Y. HtrA homologue of Legionella pneumophila: an indispensable element for intracellular in-

fection of mammalian but not protozoan cells. *Infection and immunity*, 69(4): 2569–79, Apr. 2001. ISSN 0019-9567. doi: 10.1128/IAI.69.4.2569-2579.2001. URL http://www.pubmedcentral.nih.gov/articlerender.fcgi?artid=98193&tool=pmcentrez&rendertype=abstract.

Petrie, R. J., Doyle, A. D., and Yamada, K. M. Random versus directionally persistent cell migration. *Nature reviews. Molecular cell biology*, 10(8):538–49, Aug. 2009. ISSN 1471-0080. doi: 10.1038/nrm2729. URL http://www.ncbi.nlm.nih.gov/pubmed/19603038.

Pirbhai, M., Dong, F., Zhong, Y., Pan, K. Z., and Zhong, G. The secreted protease factor CPAF is responsible for degrading pro-apoptotic BH3-only proteins in Chlamydia trachomatis-infected cells. *The Journal of biological chemistry*, 281(42):31495–501, Oct. 2006. ISSN 0021-9258. doi: 10.1074/jbc.M602796200. URL http://www.ncbi.nlm.nih.gov/pubmed/16940052.

Plaunt, M. R. and Hatch, T. P. Protein synthesis early in the developmental cycle of Chlamydia psittaci. *Infection and immunity*, 56(12):3021–5, Dec. 1988. ISSN 0019-9567. URL http://www.pubmedcentral.nih.gov/articlerender.fcgi?artid=259694&tool=pmcentrez&rendertype=abstract.

Pollard, T. D. and Borisy, G. G. Cellular motility driven by assembly and disassembly of actin filaments. *Cell*, 112(4):453–65, Feb. 2003. ISSN 0092-8674. URL http://www.ncbi.nlm.nih.gov/pubmed/12600310.

Puthenveedu, M. A., Bachert, C., Puri, S., Lanni, F., and Linstedt, A. D. GM130 and GRASP65-dependent lateral cisternal fusion allows uniform Golgi-enzyme distribution. *Nature cell biology*, 8(3):238–48, Mar. 2006. ISSN 1465-7392. doi: 10.1038/ncb1366. URL http://www.ncbi.nlm.nih.gov/pubmed/16489344.

Ramirez, I. B.-R. and Lowe, M. Golgins and GRASPs: holding the Golgi together. *Seminars in cell & developmental biology*, 20(7):770–9, Sept. 2009. ISSN 1096-3634. doi: 10.1016/j.semcdb.2009.03.011. URL http://www.ncbi.nlm.nih.gov/pubmed/19508854.

Rao, D. D., Senzer, N., Cleary, M. A., and Nemunaitis, J. Comparative assessment of siRNA and shRNA off target effects: what is slowing clinical development. *Cancer gene therapy*, 16 (11):807–9, Nov. 2009. ISSN 1476-5500. doi: 10.1038/cgt.2009.53. URL http://www.ncbi.nlm.nih.gov/pubmed/19713999.

Raulston, J. E. Response of Chlamydia trachomatis serovar E to iron restriction in vitro and evidence for iron-regulated chlamydial proteins. *Infection and immunity*, 65(11):

4539–47, Nov. 1997. ISSN 0019-9567. URL http://www.pubmedcentral.nih.gov/articlerender.fcgi?artid=175652&tool=pmcentrez&rendertype=abstract.

Regen, C. M. and Horwitz, A. F. Dynamics of beta 1 integrin-mediated adhesive contacts in motile fibroblasts. *The Journal of cell biology*, 119(5):1347–59, Dec. 1992. ISSN 0021-9525. URL http://www.pubmedcentral.nih.gov/articlerender.fcgi?artid=2289731&tool=pmcentrez&rendertype=abstract.

Rejman Lipinski, A., Heymann, J., Meissner, C., Karlas, A., Brinkmann, V., Meyer, T. F., and Heuer, D. Rab6 and Rab11 regulate Chlamydia trachomatis development and golgin-84-dependent Golgi fragmentation. *PLoS pathogens*, 5(10): e1000615, Oct. 2009. ISSN 1553-7374. doi: 10.1371/journal.ppat.1000615. URL http://www.pubmedcentral.nih.gov/articlerender.fcgi?artid=2752117&tool=pmcentrez&rendertype=abstract.

Ridley, A. J., Paterson, H. F., Johnston, C. L., Diekmann, D., and Hall, A. The small GTP-binding protein rac regulates growth factor-induced membrane ruffling. *Cell*, 70(3):401–10, Aug. 1992. ISSN 0092-8674. URL http://www.ncbi.nlm.nih.gov/pubmed/1643658.

Ridley, A. J., Schwartz, M. a., Burridge, K., Firtel, R. a., Ginsberg, M. H., Borisy, G., Parsons, J. T., and Horwitz, A. R. Cell migration: integrating signals from front to back. *Science (New York, N.Y.)*, 302(5651):1704–9, Dec. 2003. ISSN 1095-9203. doi: 10.1126/science.1092053. URL http://www.ncbi.nlm.nih.gov/pubmed/14657486.

Rupp, J., Gieffers, J., Klinger, M., van Zandbergen, G., Wrase, R., Maass, M., Solbach, W., Deiwick, J., and Hellwig-Burgel, T. Chlamydia pneumoniae directly interferes with HIF-1alpha stabilization in human host cells. *Cellular microbiology*, 9(9):2181–91, Sept. 2007. ISSN 1462-5814. doi: 10.1111/j.1462-5822.2007.00948.x. URL http://www.ncbi.nlm.nih.gov/pubmed/17490410.

Rzomp, K. A., Scholtes, L. D., Briggs, B. J., Whittaker, G. R., and Scidmore, M. A. Rab GTPases are recruited to chlamydial inclusions in both a species-dependent and species-independent manner. *Infection and immunity*, 71 (10):5855–70, Oct. 2003. ISSN 0019-9567. doi: 10.1128/IAI.71.10.5855. URL http://www.pubmedcentral.nih.gov/articlerender.fcgi?artid=201052&tool=pmcentrez&rendertype=abstract.

Rzomp, K. A., Moorhead, A. R., and Scidmore, M. A. The GTPase Rab4 interacts with Chlamydia trachomatis inclusion membrane protein CT229. *Infection and immunity*, 74(9):5362–73, Sept. 2006. ISSN 0019-9567. doi: 10.1128/IAI.00539-06. URL http://www.pubmedcentral.nih.gov/articlerender.fcgi?artid=1594829&tool=pmcentrez&rendertype=abstract.

Salcedo, S. P. and Holden, D. W. Bacterial interactions with the eukaryotic secretory pathway. *Current opinion in microbiology*, 8(1):92–8, Feb. 2005. ISSN 1369-5274. doi: 10.1016/j.mib.2004.12.007. URL http://www.ncbi.nlm.nih.gov/pubmed/15694862.

Sambrook, J., Fritsch, E., and Maniatis, T. *Molecular Cloning: A Laboratory Manual, Volume 2.* Cold Spring Harbor Laboratory Press, New York, 1989.

Savijoki, K., Alvesalo, J., Vuorela, P., Leinonen, M., and Kalkkinen, N. Proteomic analysis of Chlamydia pneumoniae-infected HL cells reveals extensive degradation of cytoskeletal proteins. *FEMS immunology and medical microbiology*, 54(3):375–84, Dec. 2008. ISSN 0928-8244. doi: 10.1111/j.1574-695X.2008.00488.x. URL http://www.ncbi.nlm.nih.gov/pubmed/19049650.

Schachter, J., Stephens, R. S., Timms, P., Kuo, C., Bavoil, P. M., Birkelund, S., Boman, J., Caldwell, H., Campbell, L. A., Chernesky, M., Christiansen, G., Clarke, I. N., Gaydos, C., Grayston, J. T., Hackstadt, T., Hsia, R., Kaltenboeck, B., Leinonnen, M., Ojcius, D., Ocjius, D., McClarty, G., Orfila, J., Peeling, R., Puolakkainen, M., Quinn, T. C., Rank, R. G., Raulston, J., Ridgeway, G. L., Saikku, P., Stamm, W. E., Taylor-Robinson, D. T., Wang, S. P., and Wyrick, P. B. Radical changes to chlamydial taxonomy are not necessary just yet. *International journal of systematic and evolutionary microbiology*, 51(Pt 1):249; author reply 251–3, Jan. 2001. ISSN 1466-5026. URL http://www.ncbi.nlm.nih.gov/pubmed/11211265.

Schaller, M. D., Hildebrand, J. D., Shannon, J. D., Fox, J. W., Vines, R. R., and Parsons, J. T. Autophosphorylation of the focal adhesion kinase, pp125FAK, directs SH2-dependent binding of pp60src. *Molecular and cellular biology*, 14(3):1680–8, Mar. 1994. ISSN 0270-7306. URL http://www.pubmedcentral.nih.gov/articlerender.fcgi?artid=358526&tool=pmcentrez&rendertype=abstract.

Schlessinger, K., McManus, E. J., and Hall, A. Cdc42 and noncanonical Wnt signal transduction pathways cooperate to promote cell polarity. *The Journal of cell biology*, 178(3):355–61, July 2007. ISSN 0021-9525. doi: 10.1083/jcb.200701083. URL http://www.ncbi.nlm.nih.gov/pubmed/17646398.

Scidmore, M. A., Fischer, E. R., and Hackstadt, T. Restricted fusion of Chlamydia trachomatis vesicles with endocytic compartments during the initial stages of infection. *Infection and immunity*, 71(2):973–84, Feb. 2003. ISSN 0019-9567. URL http://www.pubmedcentral.nih.gov/articlerender.fcgi?artid=145390&tool=pmcentrez&rendertype=abstract.

Sharma, M. and Rudel, T. Apoptosis resistance in Chlamydia-infected cells: a fate worse than death? *FEMS immunology and medical microbiology*, 55(2):154–61, Mar. 2009. ISSN 1574-695X. doi: 10.1111/j.1574-695X.2008.00515.x. URL http://www.ncbi.nlm.nih.gov/pubmed/19281566.

Short, B., Haas, A., and Barr, F. a. Golgins and GTPases, giving identity and structure to the Golgi apparatus. *Biochimica et biophysica acta*, 1744(3):383–95, July 2005. ISSN 0006-3002. doi: 10.1016/j.bbamcr.2005.02.001. URL http://www.ncbi.nlm.nih.gov/pubmed/15979508.

Shorter, J., Beard, M. B., Seemann, J., Dirac-Svejstrup, A. B., and Warren, G. Sequential tethering of Golgins and catalysis of SNAREpin assembly by the vesicle-tethering protein p115. *The Journal of cell biology*, 157(1):45–62, Apr. 2002. ISSN 0021-9525. doi: 10.1083/jcb.200112127. URL http://www.pubmedcentral.nih.gov/articlerender.fcgi?artid=2173270&tool=pmcentrez&rendertype=abstract.

Singh, S., Narang, A. S., and Mahato, R. I. Subcellular Fate and Off-Target Effects of siRNA, shRNA, and miRNA. *Pharmaceutical research*, pages 1–20, Oct. 2011. ISSN 1573-904X. doi: 10.1007/s11095-011-0608-1. URL http://www.ncbi.nlm.nih.gov/pubmed/22033880.

Solomon, S., Xu, Y., Wang, B., David, M. D., Schubert, P., Kennedy, D., and Schrader, J. W. Distinct structural features of caprin-1 mediate its interaction with G3BP-1 and its induction of phosphorylation of eukaryotic translation initiation factor 2alpha, entry to cytoplasmic stress granules, and selective interaction with a subset of mRNAs. *Molecular and cellular biology*, 27(6):2324–42, Mar. 2007. ISSN 0270-7306. doi: 10.1128/MCB.02300-06. URL http://www.pubmedcentral.nih.gov/articlerender.fcgi?artid=1820512&tool=pmcentrez&rendertype=abstract.

Sönnichsen, B., Lowe, M., Levine, T., Jämsä, E., Dirac-Svejstrup, B., and Warren, G. A role for giantin in docking COPI vesicles to Golgi membranes. *The Journal of cell biology*, 140(5):1013–21, Mar. 1998. ISSN 0021-9525.

URL http://www.pubmedcentral.nih.gov/articlerender.fcgi?artid=2132694&tool=pmcentrez&rendertype=abstract.

Spiering, D. and Hodgson, L. Dynamics of the Rho-family small GTPases in actin regulation and motility. *Cell adhesion & migration*, 5(2):170–80, 2011. ISSN 1933-6926. URL http://www.pubmedcentral.nih.gov/articlerender.fcgi?artid=3084983&tool=pmcentrez&rendertype=abstract.

Stephens, R. S., Myers, G., Eppinger, M., and Bavoil, P. M. Divergence without difference: phylogenetics and taxonomy of Chlamydia resolved. *FEMS immunology and medical microbiology*, 55(2):115–9, Mar. 2009. ISSN 1574-695X. doi: 10.1111/j.1574-695X.2008.00516.x. URL http://www.ncbi.nlm.nih.gov/pubmed/19281563.

Stieber, A., Gonatas, J. O., Moore, J. S., Bantly, A., Yim, H.-S., Yim, M. B., and Gonatas, N. K. Disruption of the structure of the Golgi apparatus and the function of the secretory pathway by mutants G93A and G85R of Cu, Zn superoxide dismutase (SOD1) of familial amyotrophic lateral sclerosis. *Journal of the neurological sciences*, 219(1-2):45–53, Apr. 2004. ISSN 0022-510X. doi: 10.1016/j.jns.2003.12.004. URL http://www.ncbi.nlm.nih.gov/pubmed/15050437.

Subtil, A., Wyplosz, B., Balañá, M. E., and Dautry-Varsat, A. Analysis of Chlamydia caviae entry sites and involvement of Cdc42 and Rac activity. *Journal of cell science*, 117(Pt 17): 3923–33, Aug. 2004. ISSN 0021-9533. doi: 10.1242/jcs.01247. URL http://www.ncbi.nlm.nih.gov/pubmed/15265988.

Subtil, A., Delevoye, C., Balañá, M.-E., Tastevin, L., Perrinet, S., and Dautry-Varsat, A. A directed screen for chlamydial proteins secreted by a type III mechanism identifies a translocated protein and numerous other new candidates. *Molecular microbiology*, 56(6): 1636–47, June 2005. ISSN 0950-382X. doi: 10.1111/j.1365-2958.2005.04647.x. URL http://www.ncbi.nlm.nih.gov/pubmed/15916612.

Sun, J. and Schoborg, R. V. The host adherens junction molecule nectin-1 is degraded by chlamydial protease-like activity factor (CPAF) in Chlamydia trachomatis-infected genital epithelial cells. *Microbes and infection / Institut Pasteur*, 11(1):12–9, Jan. 2009. ISSN 1286-4579. doi: 10.1016/j.micinf.2008.10.001. URL http://www.ncbi.nlm.nih.gov/pubmed/18983929.

Sütterlin, C. and Colanzi, A. The Golgi and the centrosome: building a functional partnership. *The Journal of cell biology*, 188(5):621–8, Mar. 2010. ISSN 1540-8140. doi: 10.1083/jcb.200910001. URL http://www.ncbi.nlm.nih.gov/pubmed/20212314.

Sütterlin, C., Hsu, P., Mallabiabarrena, A., and Malhotra, V. Fragmentation and dispersal of the pericentriolar Golgi complex is required for entry into mitosis in mammalian cells. *Cell*, 109 (3):359–69, May 2002. ISSN 0092-8674. URL http://www.ncbi.nlm.nih.gov/pubmed/12015985.

Takai, Y., Irie, K., Shimizu, K., Sakisaka, T., and Ikeda, W. Nectins and nectin-like molecules: roles in cell adhesion, migration, and polarization. *Cancer science*, 94(8):655–67, Aug. 2003. ISSN 1347-9032. URL http://www.ncbi.nlm.nih.gov/pubmed/12901789.

Tam, J. E., Davis, C. H., and Wyrick, P. B. Expression of recombinant DNA introduced into Chlamydia trachomatis by electroporation. *Canadian journal of microbiology*, 40(7):583–91, July 1994. ISSN 0008-4166. URL http://www.ncbi.nlm.nih.gov/pubmed/8076253.

Taylor, S. J. and Shalloway, D. An RNA-binding protein associated with Src through its SH2 and SH3 domains in mitosis. *Nature*, 368(6474):867–71, Apr. 1994. ISSN 0028-0836. doi: 10.1038/368867a0. URL http://dx.doi.org/10.1038/368867a0.

Thornberry, N. a. Caspases: key mediators of apoptosis. *Chemistry & biology*, 5(5):R97–103, May 1998. ISSN 1074-5521. URL http://www.ncbi.nlm.nih.gov/pubmed/9578633.

Tipples, G. and McClarty, G. The obligate intracellular bacterium Chlamydia trachomatis is auxotrophic for three of the four ribonucleoside triphosphates. *Molecular microbiology*, 8 (6):1105–14, June 1993. ISSN 0950-382X. URL http://www.ncbi.nlm.nih.gov/pubmed/8361355.

Ullrich, O., Reinsch, S., Urbé, S., Zerial, M., and Parton, R. G. Rab11 regulates recycling through the pericentriolar recycling endosome. *The Journal of cell biology*, 135(4):913–24, Nov. 1996. ISSN 0021-9525. doi: 10.1083/jcb.135.4.913. URL http://www.jcb.org/cgi/doi/10.1083/jcb.135.4.913http://www.pubmedcentral.nih.gov/articlerender.fcgi?artid=2133374&tool=pmcentrez&rendertype=abstract.

Valdivia, R. H. Chlamydia effector proteins and new insights into chlamydial cellular microbiology. *Current opinion in microbiology*, 11(1):53–9, Feb. 2008. ISSN 1369-5274. doi: 10.1016/j.mib.2008.01.003. URL http://www.ncbi.nlm.nih.gov/pubmed/18299248.

Van Voorhis, W. C., Barrett, L. K., Sweeney, Y. T., Kuo, C. C., and Patton, D. L. Repeated Chlamydia trachomatis infection of Macaca nemestrina fallop-

ian tubes produces a Th1-like cytokine response associated with fibrosis and scarring. *Infection and immunity*, 65(6):2175–82, June 1997. ISSN 0019-9567. URL http://www.pubmedcentral.nih.gov/articlerender.fcgi?artid=175300&tool=pmcentrez&rendertype=abstract.

Vinogradova, T., Miller, P. M., and Kaverina, I. Microtubule network asymmetry in motile cells: role of Golgi-derived array. *Cell cycle (Georgetown, Tex.)*, 8(14):2168–74, July 2009. ISSN 1551-4005. URL http://www.pubmedcentral.nih.gov/articlerender.fcgi?artid=3163838&tool=pmcentrez&rendertype=abstract.

Walsh, N. P., Alba, B. M., Bose, B., Gross, C. A., and Sauer, R. T. OMP peptide signals initiate the envelope-stress response by activating DegS protease via relief of inhibition mediated by its PDZ domain. *Cell*, 113(1):61–71, Apr. 2003. ISSN 0092-8674. URL http://www.ncbi.nlm.nih.gov/pubmed/12679035.

Wang, Y. Etiology of trachoma: a great success in isolating and cultivating Chlamydia trachomatis. *Chinese medical journal*, 112(10):938–41, Oct. 1999. ISSN 0366-6999. URL http://www.ncbi.nlm.nih.gov/pubmed/11717981.

Wang, Y., Seemann, J., Pypaert, M., Shorter, J., and Warren, G. A direct role for GRASP65 as a mitotically regulated Golgi stacking factor. *The EMBO journal*, 22(13):3279–90, July 2003. ISSN 0261-4189. doi: 10.1093/emboj/cdg317. URL http://www.pubmedcentral.nih.gov/articlerender.fcgi?artid=165642&tool=pmcentrez&rendertype=abstract.

Wang, Y., Weiss, L. M., and Orlofsky, A. Coordinate control of host centrosome position, organelle distribution, and migratory response by Toxoplasma gondii via host mTORC2. *The Journal of biological chemistry*, 285(20):15611–8, May 2010. ISSN 1083-351X. doi: 10.1074/jbc.M109.095778. URL http://www.pubmedcentral.nih.gov/articlerender.fcgi?artid=2865287&tool=pmcentrez&rendertype=abstract.

Wang, Y., Kahane, S., Cutcliffe, L. T., Skilton, R. J., Lambden, P. R., and Clarke, I. N. Development of a Transformation System for Chlamydia trachomatis: Restoration of Glycogen Biosynthesis by Acquisition of a Plasmid Shuttle Vector. *PLoS Pathogens*, 7(9):e1002258, Sept. 2011. ISSN 1553-7374. doi: 10.1371/journal.ppat.1002258. URL http://www.pubmedcentral.nih.gov/articlerender.fcgi?artid=3178582&tool=pmcentrez&rendertype=abstract.

Watanabe, T., Wang, S., Noritake, J., Sato, K., Fukata, M., Takefuji, M., Nakagawa, M., Izumi, N., Akiyama, T., and Kaibuchi, K. Interaction with IQGAP1 links APC to Rac1, Cdc42, and actin filaments during cell polarization and migration. *Developmental cell*, 7(6):871–83, Dec. 2004. ISSN 1534-5807. doi: 10.1016/j.devcel.2004.10.017. URL http://www.ncbi.nlm.nih.gov/pubmed/15572129.

Wehrl, W., Brinkmann, V., Jungblut, P. R., Meyer, T. F., and Szczepek, A. J. From the inside out–processing of the Chlamydial autotransporter PmpD and its role in bacterial adhesion and activation of human host cells. *Molecular microbiology*, 51(2):319–34, Jan. 2004. ISSN 0950-382X. doi: 10.1046/j.1365-2958.2003.03838.x. URL http://www.ncbi.nlm.nih.gov/pubmed/14756775.

Wei, J.-H. and Seemann, J. Unraveling the Golgi ribbon. *Traffic (Copenhagen, Denmark)*, 11 (11):1391–400, Nov. 2010. ISSN 1600-0854. doi: 10.1111/j.1600-0854.2010.01114.x. URL http://www.ncbi.nlm.nih.gov/pubmed/21040294.

Welch, H. C. E., Coadwell, W. J., Stephens, L. R., and Hawkins, P. T. Phosphoinositide 3-kinase-dependent activation of Rac. *FEBS letters*, 546(1):93–7, July 2003. ISSN 0014-5793. URL http://www.ncbi.nlm.nih.gov/pubmed/12829242.

White, J., Johannes, L., Mallard, F., Girod, A., Grill, S., Reinsch, S., Keller, P., Tzschaschel, B., Echard, A., Goud, B., and Stelzer, E. H. Rab6 coordinates a novel Golgi to ER retrograde transport pathway in live cells. *The Journal of cell biology*, 147(4):743–60, Nov. 1999. ISSN 0021-9525. URL http://www.ncbi.nlm.nih.gov/pubmed/20833257http://www.pubmedcentral.nih.gov/articlerender.fcgi?artid=2156170&tool=pmcentrez&rendertype=abstract.

WHO. Global prevalence and incidence of selected curable sexually transmitted infections: overview and estimates. *World Health Organization, Geneva*, 2001.

Wilcke, M., Johannes, L., Galli, T., Mayau, V., Goud, B., and Salamero, J. Rab11 regulates the compartmentalization of early endosomes required for efficient transport from early endosomes to the trans-golgi network. *The Journal of cell biology*, 151(6):1207–20, Dec. 2000. ISSN 0021-9525. URL http://www.pubmedcentral.nih.gov/articlerender.fcgi?artid=2190589&tool=pmcentrez&rendertype=abstract.

Worthylake, R. A., Lemoine, S., Watson, J. M., and Burridge, K. RhoA is required for monocyte tail retraction during transendothelial migration. *The*

Journal of cell biology, 154(1):147–60, July 2001. ISSN 0021-9525. URL http://www.pubmedcentral.nih.gov/articlerender.fcgi?artid=2196864&tool=pmcentrez&rendertype=abstract.

Wreghitt, T. Chlamydial infection of the respiratory tract. *Communicable disease report. CDR review*, 3(9):R119–24, Aug. 1993. ISSN 1350-9349. URL http://www.ncbi.nlm.nih.gov/pubmed/7693170.

Wylie, J. L., Hatch, G. M., and McClarty, G. Host cell phospholipids are trafficked to and then modified by Chlamydia trachomatis. *Journal of bacteriology*, 179(23):7233–42, Dec. 1997. ISSN 0021-9193. URL http://www.pubmedcentral.nih.gov/articlerender.fcgi?artid=179671&tool=pmcentrez&rendertype=abstract.

Wyrick, P. B. Chlamydia trachomatis persistence in vitro: an overview. *The Journal of infectious diseases*, 201 Suppl:S88–95, June 2010. ISSN 1537-6613. doi: 10.1086/652394. URL http://www.pubmedcentral.nih.gov/articlerender.fcgi?artid=2878585&tool=pmcentrez&rendertype=abstract.

Yadav, S., Puri, S., and Linstedt, A. D. A primary role for Golgi positioning in directed secretion, cell polarity, and wound healing. *Molecular biology of the cell*, 20(6):1728–36, Mar. 2009. ISSN 1939-4586. doi: 10.1091/mbc.E08-10-1077. URL http://www.pubmedcentral.nih.gov/articlerender.fcgi?artid=2655245&tool=pmcentrez&rendertype=abstract.

Yu, H., Schwarzer, K., Förster, M., Kniemeyer, O., Forsbach-Birk, V., Straube, E., and Rödel, J. Role of high-mobility group box 1 protein and poly(ADP-ribose) polymerase 1 degradation in Chlamydia trachomatis-induced cytopathicity. *Infection and immunity*, 78(7):3288–97, July 2010. ISSN 1098-5522. doi: 10.1128/IAI.01404-09. URL http://www.pubmedcentral.nih.gov/articlerender.fcgi?artid=2897395&tool=pmcentrez&rendertype=abstract.

Zaidel-Bar, R., Ballestrem, C., Kam, Z., and Geiger, B. Early molecular events in the assembly of matrix adhesions at the leading edge of migrating cells. *Journal of cell science*, 116(Pt 22):4605–13, Nov. 2003. ISSN 0021-9533. doi: 10.1242/jcs.00792. URL http://jcs.biologists.org/cgi/content/abstract/116/22/4605.

Zerial, M. and McBride, H. Rab proteins as membrane organizers. *Nature reviews. Molecular cell biology*, 2(2):107–17, Feb. 2001. ISSN 1471-0072. doi: 10.1038/35052055. URL http://www.ncbi.nlm.nih.gov/pubmed/11252952.

Zhang, C.-j. Mammalian Cdc42 Is a Brefeldin A-sensitive Component of the Golgi Apparatus. *Journal of Biological Chemistry*, 271(43):26850–26854, Oct. 1996. ISSN 00219258. doi: 10.1074/jbc.271.43.26850. URL http://www.jbc.org/cgi/content/abstract/271/43/26850.

Zhang, J. P. and Stephens, R. S. Mechanism of C. trachomatis attachment to eukaryotic host cells. *Cell*, 69(5):861–869, May 1992. ISSN 00928674. doi: 10.1016/0092-8674(92)90296-O. URL http://dx.doi.org/10.1016/0092-8674(92)90296-O.

Zhong, D., Zhang, J., Yang, S., Soh, U. J. K., Buschdorf, J. P., Zhou, Y. T., Yang, D., and Low, B. C. The SAM domain of the RhoGAP DLC1 binds EF1A1 to regulate cell migration. *Journal of cell science*, 122(Pt 3):414–24, Feb. 2009. ISSN 0021-9533. doi: 10.1242/jcs.027482. URL http://www.ncbi.nlm.nih.gov/pubmed/19158340.

Zhong, G. Killing me softly: chlamydial use of proteolysis for evading host defenses. *Trends in microbiology*, 17(10):467–74, Oct. 2009. ISSN 1878-4380. doi: 10.1016/j.tim.2009.07.007. URL http://www.pubmedcentral.nih.gov/articlerender.fcgi?artid=2755597&tool=pmcentrez&rendertype=abstract.

Zhong, G. Chlamydia trachomatis secretion of proteases for manipulating host signaling pathways. *Frontiers in microbiology*, 2:14, Jan. 2011. ISSN 1664-302X. doi: 10.3389/fmicb.2011.00014. URL http://www.pubmedcentral.nih.gov/articlerender.fcgi?artid=3109274&tool=pmcentrez&rendertype=abstract.

Zhong, G., Fan, P., Ji, H., Dong, F., and Huang, Y. Identification of a chlamydial protease-like activity factor responsible for the degradation of host transcription factors. *The Journal of experimental medicine*, 193(8):935–42, Apr. 2001. ISSN 0022-1007. URL http://www.pubmedcentral.nih.gov/articlerender.fcgi?artid=2193410&tool=pmcentrez&rendertype=abstract.

Zilberman, Y., Alieva, N. O., Miserey-Lenkei, S., Lichtenstein, A., Kam, Z., Sabanay, H., and Bershadsky, A. Involvement of the Rho-mDia1 pathway in the regulation of Golgi complex architecture and dynamics. *Molecular biology of the cell*, 22(16):2900–11, Aug. 2011. ISSN 1939-4586. doi: 10.1091/mbc.E11-01-0007. URL http://www.pubmedcentral.nih.gov/articlerender.fcgi?artid=3154885&tool=pmcentrez&rendertype=abstract.

List of Figures

List of Tables

Publications

Articles

Rab6 and Rab11 Regulate *Chlamydia trachomatis* Development and Golgin-84-Dependent Golgi Fragmentation
Anette Rejman Lipinski, Julia Heymann, Charlotte Meissner, Alexander Karlas, Volker Brinkmann, Thomas F. Meyer and Dagmar Heuer
PLoS Pathogens, 2009 October; 5(10)

Targeting of a chlamydial protease impedes intracellular bacterial growth
Jan G. Christian* and Julia Heymann*, Stefan A. Paschen, Juliane Vier, Linda Schauenburg, Jan Rupp, Thomas F. Meyer, Georg Häcker and Dagmar Heuer
PLoS Pathogens, 2011 September; 7(9)
* equal contribution

***Chlamydia trachomatis* infection prevents re-orientation of the Golgi apparatus in migrating cells**
Julia Heymann, Anette Rejman Lipinski, Bianca Bauer, Lesley A. Ogilvie, Thomas F. Meyer and Dagmar Heuer
Cellular Microbiology, submitted

A shRNA screen identifies Dynamin and cPLA2 as essential factors for *Chlamydia trachomatis* induced Golgi fragmentation
Rajendra K. Gurumurthy, Alexander Karlas, Cindrilla Chumduri, Sonja Kimmig, Julia Heymann, Erik Gonzales, Nikolaus Machuy, Thomas Rudel, and Thomas F. Meyer
Cell Host & Microbes, in preparation

Poster Presentations

***Chlamydia* Infection and host cell Golgi complex: Investigating Golgin-84**
Julia Heymann, Dagmar Heuer, Charlotte Meißner, Anette Rejman Lipinski and Thomas F. Meyer
Summerschool "host-pathogen-interplay"
Interdisziplinäres Zentrum für Infektionsbiologie und Immunität der Humboldt-Universität zu Berlin (ZIBI), Potsdam 2008

***Chlamydia trachomatis* Inhibits Cell Migration by Fragmentation of the Golgi Apparatus**
Julia Heymann, Anette Rejman Lipinski, Bianca Bauer, Thomas F. Meyer and Dagmar Heuer
Young Scientists Meeting "Imaging Cell Migration"
Deutsche Gesellschaft für Zellbiologie (DGZ), Martinsried 2009

***Chlamydia* Infection Inhibits Host Cell Motility**
Julia Heymann, Anette Rejman Lipinski, Bianca Bauer, Thomas F. Meyer and Dagmar Heuer
Fachgruppentagung "mikrobielle Pathogenität"
Deutsche Gesellschaft für Hygiene und Mikrobiologie (DGHM), Bad Urach 2010

***Chlamydia* Infection Inhibits Host Cell Motility**
Julia Heymann, Florian E. Paul, Anette Rejman Lipinski, Bianca Bauer, Thomas F. Meyer and Dagmar Heuer
7^{th} Annual EIMID Meeting
European Initiative for basic research In Microbiology and Infectious Diseases (EIMID), Stockholm 2010

Berlin, August 2, 2012 Julia Heymann

Acknowledgments

I owe thanks to the following people who helped during the creation of this thesis:

Prof. Dr. Thomas F. Meyer for the unique opportunity to work in a fantastic lab on an exciting project and for help and advice during my PhD work.

Dr. Dagmar Heuer for being the best supervisor and motivator of all times.

Jan Christian and **Prof. Dr. Georg Häcker** at Uniklinik Freiburg for realizing the CPAF project and paper together with us.

Florian Paul and **Prof. Dr. Matthias Selbach** at MDC Berlin for the mass spectrometry measurements of the interaction proteomics approach and important discussions.

Dr. Anette Rejman Lipinski and **Dr. Bianca Bauer** for their help, ideas, discussions and a fabulous time in and outside of the lab.

Anja Greiser, **Jörg Angermann** and **Dagmar Frahm** for excellent technical support.

Vicci Dyer for very helpful language corrections.

Meinen Eltern für ihre Unterstützung und ihr Vertrauen.

Christian für alles. Für immer.

Selbständigkeitserklärung

Ich erkläre, dass ich die vorliegende Arbeit selbständig und nur unter Verwendung der angegebenen Literatur und Hilfsmittel angefertigt habe. Wurden Ergebnisse in Kooperation produziert, ist dies entsprechend angegeben.

Berlin, den 2. August 2012 Julia Heymann